

1
2
3
4
5 EASTSIDE TIMBER
6 HABITAT EVALUATION
7 PROJECT (ETHEP)
8

9 EVALUATION OF FRAMEWORKS FOR APPLYING RIPARIAN HARVEST
10 RULES ALONG TYPE S AND TYPE F STREAMS IN EASTERN WASHINGTON
11 BASED ON FPHCP OBJECTIVES AND PERFORMANCE TARGETS: FINAL
12 REPORT

13
14
15
16
17
18 *Prepared by:*

19 Benjamin Spei¹, Mark Teply¹, Rachel Rubin², Mark Kimsey¹, Charles Goebel¹

20 ¹College of Natural Resources, Department of Forest, Rangeland and Fire Sciences, University
21 of Idaho, 875 Perimeter Drive MS 1133 Moscow, Idaho.

22 ²Washington Department of Natural Resources, 1111 Washington St. SE, Olympia, Washington
23 98504

24
25 **October 2025**

26	Table of Contents	
27	List of Figures	2
28	List of Tables	4
29	Executive Summary	6
30	Introduction.....	8
31	Background.....	8
32	Purpose.....	9
33	Objectives	10
34	Study area.....	11
35	Phase I.....	14
36	Step 1: Appraisal of Available Datasets.....	14
37	Available Datasets	14
38	Data Suitability	16
39	Step 2: Framework Development.....	22
40	Procedural Overview	22
41	Data Extraction	22
42	Field Reconnaissance	24
43	Boosted Regression Tree (BRT).....	25
44	Conclusions	30
45	Step 3: Framework Refinement with Simulation Modeling using Existing Field Data.....	30
46	Phase II.....	32
47	Step 1: Field Data Collection	32
48	Site Selection Methods	32
49	Field Methods	33
50	Results	34
51	Step 2: Validation and Refinement	37
52	Procedural Overview	37
53	Accuracy Assessment	37
54	Modeling Riparian Function (Shade and Large Wood Recruitment).....	41
55	Refinement.....	45
56	Discussion	46
57	References:.....	50

58	Appendix I Supplemental Figures and Tables	55
59	Appendix II Maps	62
60	Appendix III Confusion matrices.....	68
61	Appendix IV: Single-factor frameworks	71
62		

63 List of Figures

64	Figure 1. Diagrammatic representation of habitat type and topography relationships on a	
65	southern facing slope of the Palouse Range in Eastern Washington. Taken from Daubenmire	
66	1980. The vegetation groups listed in order from top to bottom: Thuja plicata/Clintonia uniflora,	
67	Abies grandis/Clintonia uniflora, Pseudotsuga/Physocarpus malvaceus, Pinus	
68	ponderosa/Symphoricarpos albus, Fastuca idahoensis/symphoricarpos.....	9
69	Figure 2. Flow chart representation of each Phase and Step of the proposed study design from	
70	Spei et al. 2023.....	11
71	Figure 3. Study Area. Study sites were selected from lands subject to the Washington State	
72	Forest Practices Rules defined by the FPHCP; FPA includes riparian forest stands along Type S	
73	and Type F streams (fish-bearing) in eastern Washington (east of the Cascade Crest) that have	
74	the potential to be harvested under WAC-222-30-022. Sampling sites, shown in blue, were	
75	selected from Bailey’s Ecoregions: East Cascades, Okanogan, Canadian Rocky Mountains,	
76	Columbia Plateau, and Blue Mountains ecoregions. Streams colored in blue represent all mapped	
77	Type F and S streams in eastern Washington. Streams colored orange represent Type F and S	
78	streams within the study area with adjacent forested areas that have the potential to be harvested	
79	under WAC-222-30-022.	13
80	Figure 4. Map of forest types defined by the 20-year Forest Health Plan (6-category) within 120	
81	m of a Type F or Type S (fish-bearing) stream identified by the Washington State Department of	
82	Natural Resources Hydrology Layer. Field sites were identified as Cold, Dry, or Moist based on	
83	observed species composition, stand structure, and estimated fire return intervals (LANDFIRE	
84	dataset) following field-data collection at these points (described in Phase II). The map shows the	
85	Northeastern area of Washington, centered on the Little Pend Oreille National Wildlife Refuge,	
86	to increase visibility of forest type variability.....	23
87	Figure 5. Screenshot of the 10 x 10-meter point grid used to extract vegetation cover data	
88	(20yFHP map), physiographic data (20yFHP map, MSDIM). The point grid was developed	
89	within a 120 m buffer on either side of the WA DNR Hydrography Watercourses shapefile. The	
90	full buffer point grid was used to extract 47,089,718 data points (containing all available	
91	vegetation, physiography, and soil attributes) for the BRT and predictive modeling approach. .	24
92	Figure 6. Zoomed in display of mapped regulatory zones of the THT for side-by-side	
93	comparison with forest type categories (coarse) mapped by the 20yFHP map, and the predictive	
94	forest type category map (coarse) developed during the BRT assessment of the 20yFHP map	
95	forest type categories.	29

96 **Figure 7.** General sample plot layout showing start point, central axis, 24 subplots each 10' x 5',
97 and trees and snags tallied using horizontal line sampling (taken from MB & G, 2006). For
98 purposes of ETHEP the transect was reduced to a maximum length of 160' (~50 m) to describe
99 only vegetation within the designated RMZ. This also resulted in only 16-10 x 5 foot subplots
100 instead of 24..... 33

101 **Figure 8.** Frequency distribution of forest type categories found at 88 field sites across eastern
102 Washington. PP = ponderosa pine, WR = western redcedar, SF = spruce-fir. 34

103 **Figure 9.** Frequency of ownership across 88 field sites. Other state agencies include the
104 Department of Fish and Wildlife and the Washington State Parks and Recreation Commission.
105 Industrial land included owners Inland Empire Paper, Manulife, Stimson, and Bennet Lumber. 35

106 **Figure 10.** Frequency of dominant conifer species across 88 field sites based on basal area per
107 acre. PSME = Douglas-fir, PIPO = ponderosa pine, ABGR = grand fir, PIEN = Englemann
108 spruce, THPL = western redcedar, TSHE = western hemlock, LAOC = western larch..... 35

109 **Figure 11.** Error matrix describing the percent error for each forest type category predicted by
110 the BRT Map when compared to field site forest type category (Observed). 37

111 **Figure 12.** Error matrix describing the percent error for each forest type category predicted by
112 the 20yFHP map when compared to observed field site forest type categories. 37

113 **Figure 13.** NMDS ordination of species basal area/acre for 83 timber sites with final stress =
114 0.1607668, observed with 2 dimensions (k = 2). Post-hoc ellipses encompass full coverage of
115 forest type categories to show the overlap of forest type categories determined from the field
116 data. They show distinct groupings of the ponderosa pine (PP) and SF forest types groups (Table
117 3). Separation of the western redcedar (WR), moist mixed conifer (MOIST MXD), dry mixed
118 conifer (DRY MXD), and dry Douglas-fir (DRY DF) forest type categories is less distinct. The
119 WR forest type category appears to be a specific condition of the MOIST MXD, and the DRY
120 DF type appears to be a specific condition of the DRY MXD forest type category. 39

121 **Figure 14.** NMDS ordination of species basal area/acre for 83 timber sites with final stress =
122 0.1607668, observed with 2 dimensions (k = 2). Post-hoc ellipses encompass full coverage of
123 coarsened forest type categories to show overlap of forest type categories derived from the field
124 data. When the forest type categories derived from the field data are coarsened to three
125 categories (DRY, MOIST, COLD), we see that separations and correlations are more apparent
126 and visible than with the fine categories. 40

127 **Figure 15 (A-D).** Expected change in LW recruitment potential for piece counts per 1000 feet of
128 stream. Piece counts were tallied if they had a >25% (A, B) or >50% (C, D) probability of
129 entering the stream channel after mortality and averaged by forest type categories. 43

130 **Figure 16 (A and B).** Line graph showing the change in mean effective shade on August 1st,
131 2024 – 2074 (50 years) at 10-year timesteps for the fine (A) and coarse (B) forest type
132 categories. 44

134 **List of Tables**

135 **Table 1.** Estimated stream lengths (mi) for each THT category within each of five Bailey’s
136 ecoregions on lands potentially subjected to timber harvest rules defined in the Forest Practices
137 Act (FPA) based on the WA DNR Hydro layer. Stream length was estimated by clipping the WA
138 DNR Hydro layer by Bailey’s ecoregion and then by THT regulatory zone (based on elevation).
139 The resulting length of each section was calculated in ArcGIS Pro. 11

140 **Table 2.** Answers to the four screening questions used to gauge the suitability of each geospatial
141 and stand-level dataset in forest habitat mapping and framework building. Areas highlighted in
142 green indicate that the criteria for inclusion were met. 18

143 **Table 3.** Table of forest type categories developed from pre-existing forest type categories
144 defined in the 20yFHP map and used in the BRT approach as dependent variable. 25

145 **Table 4.** List of independent variables, their source, and description, that were used in ordination
146 and BRT to evaluate their relative contribution in predicting the dependent variable (i.e., forest
147 type categories). 26

148 **Table 5.** List of the top ten independent variables based on their relative importance in predicting
149 the six forest cover type categories used in BRT. The percentage column shows the percentage of
150 the variation in the dependent variable distribution that could be explained by the variable. ILAP
151 zone shows the highest percentage (higher than Bailey’s ecoregion) and was chosen as the first
152 factor for delineation for frameworks #1 and #2. While AET and NDVI also showed relatively
153 high importance, these factors were not appropriate for framework development given their high
154 annual variability and ephemeral nature. We chose temperature, precipitation, and elevation as
155 the factors for framework development. 28

156 **Table 6.** Estimated number of acres of RMZ by ownership across the study area based on a
157 contiguous 75-foot buffer for comparison. We used a 75-foot buffer (the smallest regulatory
158 buffer) to be conservative. 33

159 **Table 7.** Confusion matrix shows the percentage error of the BRT Map predictions when
160 compared to the observed field site categories. The results show an overall slightly better
161 performance than the THT framework. However, the MOIST forest type category was predicted
162 with greater error than the THTs. Also, note the small sample size of the COLD group, the
163 decreased error was only a result of 1 data point. 44

164 **Table 8.** Confusion matrix shows the percentage error of the Timber Habitat Type (THT)
165 framework when compared to the observed field site categories. ⁺The THT categories for
166 Ponderosa Pine, Mixed Conifer, and High Elevation were evaluated as DRY, MOIST, and
167 COLD types, respectively. 44

168 **Table 9.** Confusion matrix shows the percentage error of the 20-year Forest health Plan mapped
169 coarse forest type categories when compared to observed field forest type categories. The
170 20yFHP map outperforms the THT regulatory zones overall and in each category. 45

171

172 **Executive Summary**

173 This report presents results from Phases I and II of the Eastside Timber Habitat Evaluation
174 Project (ETHEP). The purpose of ETHEP was to develop alternative framework(s) to the current
175 Timber Habitat Type (THT) framework for applying riparian harvest rules along Type S (i.e.,
176 shorelines of the state) and Type F (i.e., fish-bearing) streams in eastern Washington based on
177 the five riparian functions defined in the Forest Practices rules ([WAC 222-16-010](#)), along with
178 the functional objectives and performance targets (Schedule L-1, Appendix N) of the Forest
179 Practices Habitat Conservation Plan (FPHCP) (FPHCP, 2005). ETHEP was performed and
180 conducted under the authority and guidance of the Cooperative Monitoring Evaluation and
181 Research (CMER) Committee. ETHEP was accomplished in two Phases. Phase I involved the
182 appraisal of publicly available datasets and then the development of alternative framework(s)
183 based on the best available data. Phase II involved collecting field data to evaluate the
184 performance of the alternative framework(s) developed in Phase I.

185 As a part of Phase I, alternative frameworks were chosen or developed from the best available
186 data. Each alternative framework employed a different method to discriminate forest type
187 categories derived from the Washington State Department of Natural Resources' (WA DNR) 20-
188 year Forest Health Plan (20yFHP map). Some alternative frameworks discriminate forest
189 vegetation cover at a relatively fine resolution (e.g., species and/or species groups), and others
190 aggregate the finer resolutions into broader ecological groupings (e.g., DRY, MOIST, and
191 COLD forest communities). They included:

- 192 1. The 20yFHP map – providing an independent mapped alternative to the THT framework
193 at both the fine (6-category) and coarse (3-category) levels of resolution of forest type
194 categories.
- 195 2. Machine Learning Map (BRTBRT Map) – Fine- and coarse-resolution forest type
196 categories derived from the 20yFHP map and predicted from independent environmental
197 variables.

198
199 In Phase II, each alternative framework was evaluated for its accuracy and usefulness relative to
200 the THT. Accuracy was assessed using error matrices that compared the framework-based
201 classification of forest type categories to classifications based on the collection and analysis of
202 detailed forest cover and site characteristics observed in the field at 88 sites randomly selected
203 along Type S and F streams in eastern Washington, as regulated by Washington Forest Practice
204 Rules. Usefulness was qualitatively assessed based on the framework's relationship between
205 forest type categories and riparian function (evaluated in Step 2 of Phase II). Specifically, the
206 final framework will contain the most parsimonious groupings of forest type categories as they
207 relate to their expected functional relationships.

208
209 The alternative framework showing the greatest improvement over the THT framework was the
210 20yFHP map at the coarse resolution of forest type categories. Three forest type categories were

211 delineated—DRY, MOIST, and COLD—which are comparable to the three THT categories—
212 Ponderosa Pine, Mixed Conifer, and High Elevation, respectively—in terms of their riparian
213 function. The mapping of the distribution of these 20yFHP map coarse forest type categories,
214 however, was substantially improved relative to the THT equivalents.

215 The 20yFHP map showed error percentages of 19%, 22%, and 50% for the DRY, MOIST, and
216 COLD forest type categories, respectively, with an overall error rate of **22%** when evaluated
217 with the observed field site classifications. The BRT Map framework showed error percentages
218 of 21%, 41%, and 50% for the DRY, MOIST, and COLD forest type categories, respectively,
219 and an overall error rate of **30%**. The THT framework yielded error percentages of 34%, 25%,
220 and 75% for the crosswalk 20yFHP map forest type categories, corresponding to DRY =
221 Ponderosa Pine, MOIST = Mixed Conifer, and COLD = High Elevation, respectively, with an
222 overall error rate of **33%** when evaluated against the observed field site classifications.

223 In summary, the alternative framework we developed (BRT Map) performed as well or better
224 than the THT, but did not perform as well as the 20yFHP map, based on our accuracy assessment
225 in Step 2 of Phase II. The BRT Map framework fine variant (6-categories) did not discriminate
226 dry and moist forest type categories very well, and the coarse variant (3-category), while
227 performing better than the THT framework, did not perform as well as the 20yFHP map
228 ([Appendix III Confusion matrices](#)).

229 We identified several pertinent future directions, including improving the BRT Map through
230 additional field data collection and independent verification of the 20yFHP map. The BRT Map
231 was trained on millions of data points, using the 20yFHP map as the dependent variable and
232 environmental variables as independent variables. Although we attempted to calibrate the BRT
233 Map with collected field data, the relatively small sample size compared to the much larger
234 training sample did not improve the map's accuracy. We considered supplementing our field data
235 with a pre-existing, publicly available dataset of stand-level field data from the Eastern
236 Washington Riparian Assessment Project (EWRAP). However, the site locations were not
237 evenly distributed throughout the conditions we identified as important factors for predicting
238 forest type categories. Further, the methods used for data collection in EWRAP (e.g., 240 ft
239 transects) meant the transects crossed multiple conditions at several locations. Finally, the field
240 protocols of EWRAP collected site factors (e.g., slope, aspect, elevation) at a coarser resolution
241 than what was used for our field protocols. Thus, we ultimately decided that the EWRAP data
242 had a limited scope of inference for our assessment analysis. Thus, the BRT Map framework has
243 the potential for improvement with the collection of more field data. Furthermore, to the best of
244 our knowledge, WA DNR has not conducted an accuracy assessment of the mapped 20yFHP
245 map forest type categories. Since this analysis treated the 20yFHP mapped forest types as the
246 dependent variable, we recommend a more robust evaluation of its accuracy.

247

248 **Introduction**

249 This report presents results from Phases I and II of the Eastside Timber Habitat Evaluation
250 Project (ETHEP). ETHEP is seeking to develop framework(s) for applying riparian harvest rules
251 along Type S (i.e., fish-bearing streams that are also classified as shorelines of the state) and
252 Type F (fish-bearing) streams in eastern Washington that are based on the Forest Practices
253 Habitat Conservation Plan (FPHCP 2005) objectives and performance targets. The project was
254 conducted under the authority and guidance of the Scientific Advisory Group Eastside (SAGE), a
255 subgroup of the Cooperative Monitoring, Evaluation, and Research (CMER) Committee, and it
256 addresses Eastside Type F Riparian Rule Tool Program research needs presented in the 2025-
257 2027 Biennium CMER Work Plan. This report describes the implementation of the [*Study Design
258 to Evaluate Frameworks for Applying Riparian Harvest Rules Along Type S and Type F Streams
259 in Eastern Washington Based on FPHCP Objectives and Performance Targets*](#) (Spei et al. 2023).

260 **Background**

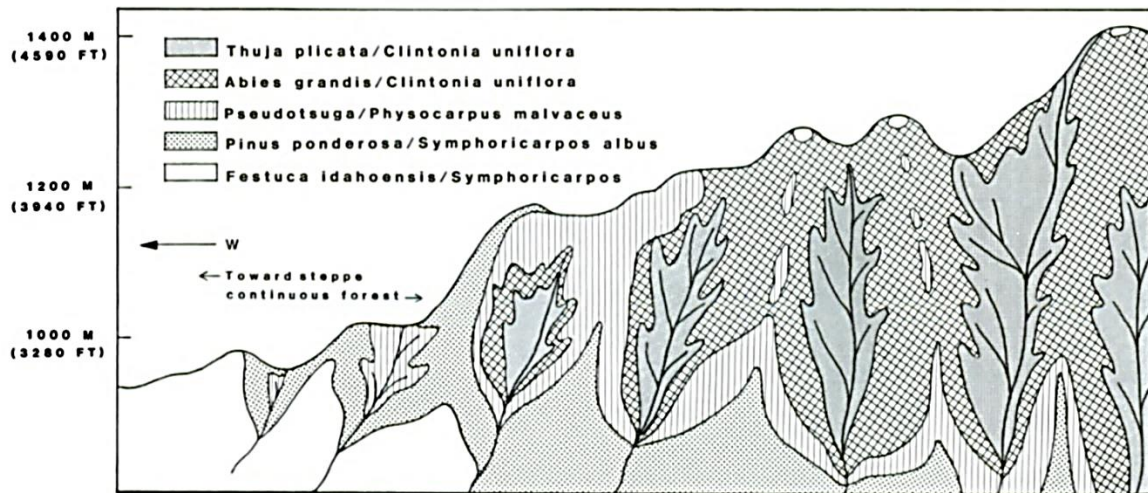
261 Washington’s current Forest Practices Rules in eastern Washington use a Timber Habitat Type
262 (THT) system to determine the application of riparian rule prescriptions along Type S and Type
263 F streams ([WAC 222-30-022](#)). This system defines THTs according to three elevation zones:
264 <2500 feet (nominally, “Ponderosa Pine”), 2500-5000 feet (“Mixed Conifer”), and >5000 feet
265 (“High Elevation”). The riparian harvest rules specify different leave tree requirements for each
266 THT. For instance, thinning of the riparian management zone within Mixed Conifer (2500 –
267 5000 feet) habitat type requires a higher minimum basal area (70 – 110 square feet per acre,
268 depending on site index) compared to the Ponderosa Pine (< 2500 feet; 60 square feet per acre
269 regardless of site index) habitat type. Other rules for preferred species and tree distributions are
270 further described in the WAC 222-30-022. Though developed prior to the FPHCP, the THT
271 system reflects that potential riparian function—a metric by which to gauge restoration and
272 maintenance of riparian habitat (and FPHCP objective)—differs among forest stands as
273 represented by these nominal forest type categories.

274 While the current application of THTs relies on elevation alone to reflect the dominant riparian
275 forest vegetation, a previous CMER study indicated that elevation zones alone do not fully
276 identify differences in riparian forest vegetation. Phase II of the Eastern Washington Riparian
277 Assessment Project (EWRAP; Schuett-Hames, 2015) determined the reclassification of potential
278 late successional or climax species for 103 riparian sites in eastern Washington using the
279 classification criteria established by Cooper et al. (1991) and Kovalchik and Clausnitzer (2004).
280 They found that the distribution of riparian forest vegetation does not necessarily align with the
281 predominant species suggested by the THTs. Ceder et al. (2020) evaluated the effectiveness of
282 the Forest Practice Rules using the same EWRAP data set. They found there was considerable
283 overlap in riparian vegetation conditions among THTs, which also supports the premise that
284 elevation is likely not a reliable surrogate in determining dominant forest vegetation, and thus in
285 determining the silvicultural prescriptions necessary to support riparian functions.

286 The shortcoming of using elevation alone is acknowledged elsewhere in the literature. Franklin
287 and Dyrness (1973) cautioned that the use of a zonal classification scheme (e.g., THTs) should
288 consider several caveats regarding riparian zones:

289 “Zones may occur as sequential belts on mountain slopes, but more often they interfinger,
290 with each attaining its lower elevational limits in valleys and its highest limits on ridges;
291 as a consequence, the zones along the slopes of a narrow valley can be reversed from
292 their otherwise altitudinal relationship.”

293 Similarly, in an analysis of landscapes of northern Idaho and eastern Washington, Daubenmire
294 (1980) concluded that microclimates controlled by topographic features allow vegetation
295 characteristic of subalpine environments to descend locally to very low altitudes, and vice versa
296 (Figure 1). Overall, though it seems reasonable to identify three coarse vegetation types—
297 Ponderosa Pine, Mixed Conifer, and High Elevation—among which riparian functions would
298 reasonably be expected to differ, the use of elevation alone does not entirely describe the
299 differences in riparian vegetation found across eastern Washington.



301 **Figure 1.** Diagrammatic representation of habitat type and topography relationships on a
302 southern facing slope of the Palouse Range in Eastern Washington. Taken from Daubenmire
303 1980. The vegetation groups listed in order from top to bottom: *Thuja plicata/Clintonia uniflora*,
304 *Abies grandis/Clintonia uniflora*, *Pseudotsuga/Physocarpus malvaceus*, *Pinus*
305 *ponderosa/Symphoricarpos albus*, *Festuca idahoensis/symphoricarpos*.

306 Purpose

307 The purpose of ETHEP was to develop alternative frameworks (to the THT system) for applying
308 riparian harvest rules along Type S and Type F streams in eastern Washington based on the
309 functional objectives and performance targets (Schedule L-1, Appendix N) of the Forest
310 Practices Habitat Conservation Plan (FPHCP, 2005). The five “key” riparian forest functions
311 specified in the FPHCP include “large woody debris recruitment, sediment filtration, stream
312 bank stability, shade, litterfall and nutrients, in addition to other processes important to riparian

313 and aquatic systems.” For this study, a framework is generally defined as a system that can be
314 used to inform and guide management prescriptions that support the goals and objectives of the
315 FPHCP (the current THT system is one example). Such alternative framework(s) could improve
316 on the current THT system.

317 Objectives

318 ETHEP was guided by a [scoping document](#) approved by SAGE, CMER, and the Timber Fish
319 and Wildlife Policy Committee (Policy) (2021). The scoping document identified two objectives:

- 320 1. Develop a framework for applying riparian harvest rules in eastern Washington based on the
321 FPHCP functional objectives and performance targets (Schedule L-1, Appendix N).
322
- 323 2. Test the framework(s) for characterizing eastside riparian forests using data collected in the
324 field.

325 From these objectives, ETHEP sought to answer four critical questions, also outlined in the
326 scoping document:

327 Objective 1:

- 328 1. What type and quality of data are needed to accurately characterize and differentiate
329 riparian stands, their development in eastern Washington, and their associated riparian
330 functions?
331
- 332 2. Do existing datasets (alone or in combination) provide the necessary information to
333 accurately characterize and differentiate riparian stands, their development, and
334 associated riparian functions?
335
- 336 3. If existing datasets do not provide the necessary information to differentiate riparian
337 stands, their development, and associated riparian functions, how can this additional
338 information be acquired and utilized?

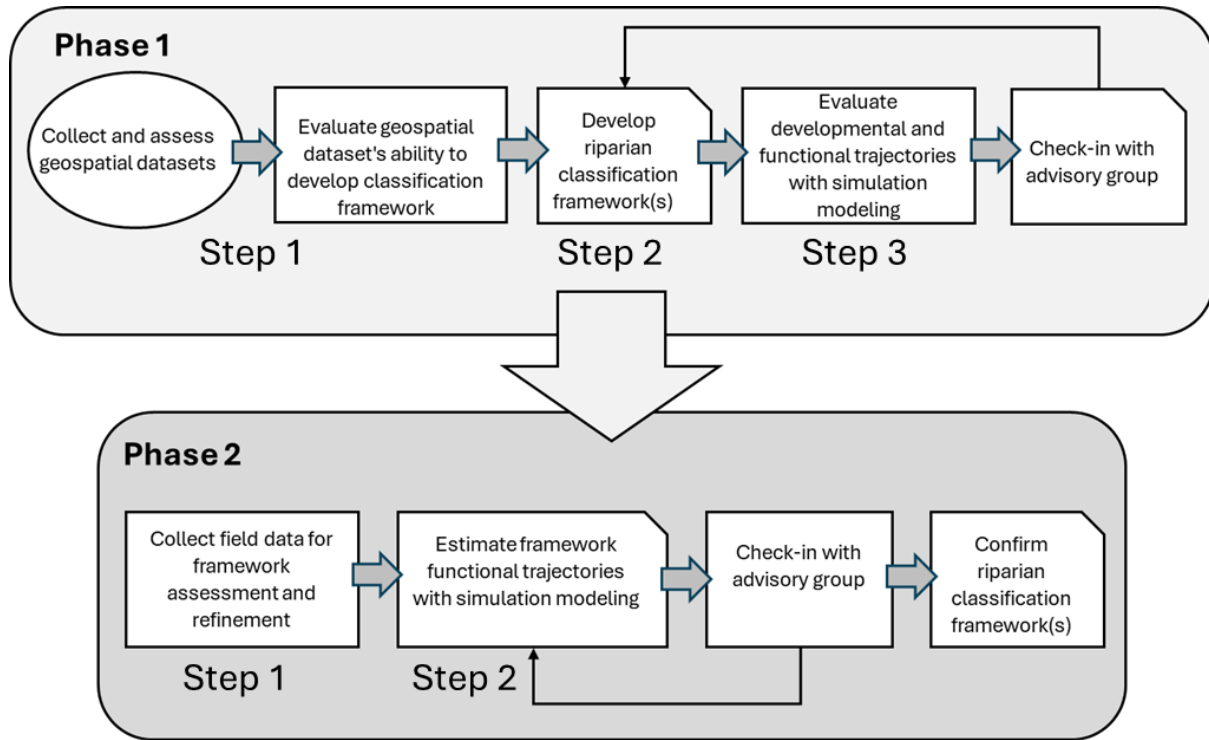
339 Objective 2:

- 340 4. Does the framework accurately characterize riparian forests in the field based on
341 characteristics important for meeting FPHCP functional objectives and performance
342 targets?

343 The study design (Spei et al. 2023) laid out procedures and methods for addressing these
344 questions in two phases (Figure 2). Phase I addressed Objective 1 and involved three steps that
345 provided information for answering the first three critical questions. Phase II addressed
346 Objective 2 and involved two steps that provided information for answering the fourth critical
347 question.

348 Step 1 of Phase I entailed a desktop analysis of publicly available datasets that evaluated their
349 ability to characterize site, vegetation, and landscape features. Step 2 of Phase I involved the

350 development of alternative classification frameworks, based on data deemed useful in Step 1,
 351 using multiple classification methods. Step 3 of Phase I sought to assess and refine alternative
 352 classification frameworks using simulation modeling. Step 1 of Phase II entailed field data
 353 collection to assess alternative classification frameworks developed in Phase I and to fill data
 354 gaps (e.g., data to support simulation modeling). Step 2 of Phase II entailed validating the
 355 frameworks developed in Phase I and refining those alternative classification frameworks.



356
 357 **Figure 2.** Flow chart representation of each Phase and Step of the proposed study design from
 358 Spei et al. 2023.

359 **Study area**

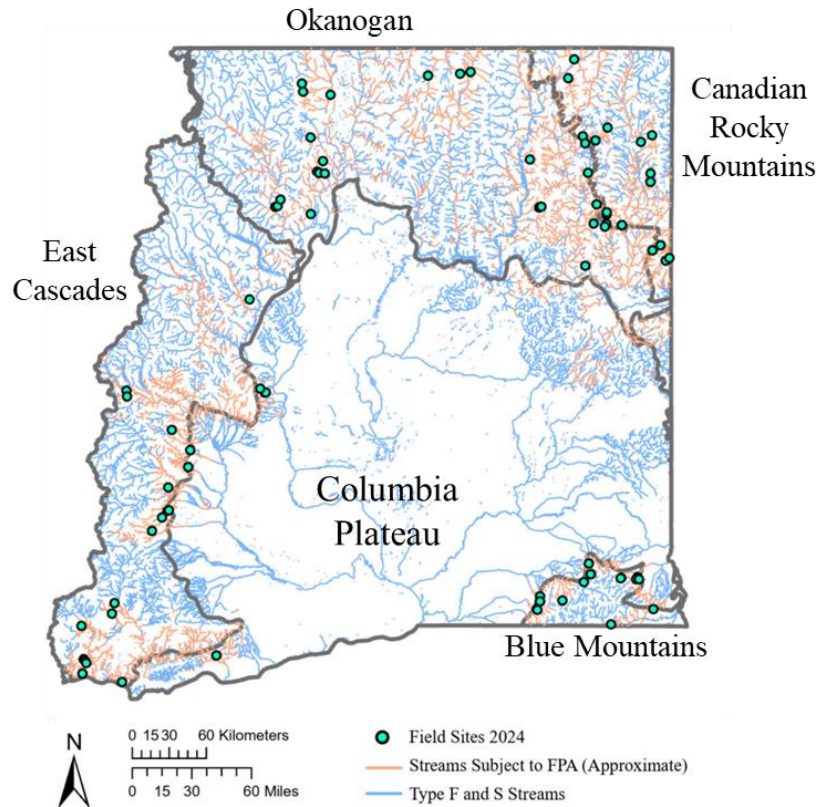
360 Existing data sets were used to derive a geospatial data layer representing riparian areas along
 361 streams classified as Type F or Type S by the WA DNR Hydrography Watercourses Forest
 362 Practices Regulation stream layer (hereafter referred to as the WA DNR Hydro layer). This
 363 includes both Private Lands and State Lands that are subject to the WA DNR Forest Practice
 364 Application Process. Type F and Type S streams were extracted from the publicly available WA
 365 DNR Hydro layer. The extracted streams were clipped to exclude reaches within federal and
 366 tribal lands as mapped in the parcel ownership data layer retrieved from the WA DNR website.
 367 Finally, the layer was further clipped to include only reaches along forested landscapes as
 368 mapped in the LANDFIRE, LEMMA, and 20-year Forest Health Plan datasets (described in
 369 Phase I, Step 1). The LANDFIRE, LEMMA, and 20-year Forest Health Plan datasets contain
 370 predictive maps with expected vegetation types (LANDFIRE), modeled individual tree species
 371 coverage (LEMMA), and expected forest types (20- year Forest Health Plan datasets).

372 The resulting study area covers approximately 4,500 miles of Type F and Type S stream length
 373 across Bailey’s five ecoregions (Table 1; Figure 3). Over three-fifths of the study area occurs in
 374 the Okanogan Highlands and East Cascades; the Columbia Plateau and the Canadian Rockies
 375 each contain about 15%; and less than 5% occurs in the Blue Mountains. Nearly all the study
 376 areas occur within the Ponderosa Pine and Mixed Conifer THTs, split about 60/40 between the
 377 two types, respectively. The High Elevation category contains only approximately 0.01% of FPA
 378 managed stream length.

379 **Table 1.** Estimated stream lengths (mi) for each THT category within each of the five Bailey’s
 380 ecoregions on lands potentially subjected to timber harvest rules defined in the Forest Practices
 381 Act (FPA) based on the WA DNR Hydro layer. Stream length was estimated by clipping the WA
 382 DNR Hydro layer by Bailey’s ecoregion and then by THT regulatory zone (based on elevation).
 383 The resulting length of each section was calculated in ArcGIS Pro.

Timber Habitat Type (THT)	Okanogan	East Cascades	Columbia Plateau	Canadian Rockies	Blue Mountains	Total
Ponderosa Pine	913	641	574	317	66	2,511
Mixed Conifer	619	571	224	383	145	1,942
High Elevation	34	17	0	1	0	51
Total	1,566	1,228	798	701	211	4,504

384



385

386 **Figure 3.** Study Area. Study sites were selected from lands subject to the Washington State
 387 Forest Practices Rules defined by the FPHCP; FPA includes riparian forest stands along Type S
 388 and Type F streams (fish-bearing) in eastern Washington (east of the Cascade Crest) that have
 389 the potential to be harvested under WAC-222-30-022. Sampling sites, shown in blue, were
 390 selected from Bailey’s Ecoregions: East Cascades, Okanogan, Canadian Rocky Mountains,
 391 Columbia Plateau, and Blue Mountains ecoregions. Streams colored in blue represent all mapped
 392 Type F and S streams in eastern Washington. Streams colored orange represent Type F and S
 393 streams within the study area with adjacent forested areas that have the potential to be harvested
 394 under WAC-222-30-022.

395 Phase I

396 Step 1: Appraisal of Available Datasets

397 Available Datasets

398 We evaluated 12 geospatial datasets that contained tree species and/or productivity information:

- 399 • [Forest Inventory and Analysis BIGMAP Tree Species Aboveground Forest Biomass \(FIA](#)
400 [BIGMAP](#)). FIA’s cloud-based national scale modeling, mapping, and analysis
401 environment for US forests produced by the USDA Forest Service. FIA uses an
402 annualized sample of over 350,000 plots distributed across the United States to provide
403 information on the status and trends of the Nation’s forest resources. (Last updated 2019,
404 Datasets not listed in the ETHEP study design)

- 405 • [Ecological Classification of Native Wetland and Riparian Vegetation of Washington](#)
406 (ECNW). (Rocchio and Crawford, Washington Natural Heritage Program, *in progress*).
407 Developed by NatureServe to provide a mid-scale ecological classification for uplands
408 and wetlands, which is useful for conservation and environmental planning. Ecological
409 Systems represent recurring groups of terrestrial plant communities found in similar
410 climatic and physical environments and are influenced by similar dynamic ecological
411 processes, such as fire or flooding, share similar substrates, and/or environmental
412 gradients. (Last updated 2024)

- 413 • [Ecological Systems of Washington](#) (ESW) Produced by NatureServe and the Washington
414 Natural Heritage Program (Rocchio and Crawford 2015). Terrestrial ecological systems
415 concepts form the basis for three map products from the inter-agency Landfire effort: 1)
416 Existing Vegetation Type (EVT); i.e., the current location of vegetative components of
417 each terrestrial ecological system is mapped in that layer. 2) Environmental Site Potential
418 (ESP) is a spatial model of environments that constrain the possible locations where a
419 given ecological system could occur, without including natural disturbance regime as a
420 factor. 3) Biophysical Settings (BpS) provides another spatial model depicting the
421 probable location of each ecological system type, assuming the inclusion of natural
422 disturbance regimes as a factor. (Last updated 2019)

- 423 • [Forest Biomass geospatial dataset](#) (USDA Forest Service). A spatially explicit dataset of
424 aboveground live forest biomass made from ground measured inventory plots for the
425 conterminous U.S., Alaska and Puerto Rico. The plot data are from the USDA Forest
426 Service Forest Inventory and Analysis (FIA) program. To scale these plot data to maps,
427 models were developed relating field-measured response variables to plot attributes
428 serving as the predictor variables. Among the predictor layers used were digital elevation
429 models (DEM) and DEM derivatives; Moderate Resolution Spectroradiometer (MODIS)
430 multi-date composites, vegetation indices and vegetation continuous fields; class
431 summaries from the 1992 National Land Cover Dataset (NLCD); various ecologic zones;
432 and summarized Parameter-elevation Regressions on Independent Slopes Model
433 (PRISM) climate data. (Last updated 2018)

- 434 • [Individual Tree Species Parameter Maps](#) (ITSP) (USDA Forest Service). The Individual
435 Tree Species Parameter Maps were developed to support the [National Insect and Disease](#)
436 [Risk Map](#) (NIDRM). Basal area and stand density index are mapped for each individual

- 437 tree species. The parameter products are based on 30-meter Landsat satellite data,
438 climate, terrain, and soil predictor layers and ground samples from the USFS Forest
439 Inventory and Analysis plot data. (Last update 2012)
- 440 • [Landscape Ecology, Modeling, Mapping, and Analysis \(LEMMA\) dataset](#) produced by
441 the USDA Forest Service, Pacific Northwest Research Station, and the Department of
442 Forest Ecosystems and Society at Oregon State University (OSU) (e.g., Ohmann and
443 Spies 1998, Ohmann et al. 2011). The gradient nearest neighbor (GNN) was used to
444 develop quantitative maps of forest vegetation based on imputations of numerous
445 attributes (e.g., species, density, basal area, canopy cover, height, diameter) collected by
446 the Forest Inventory and Analysis data program. (Last updated 2017)
 - 447 • [Maps of Specific Forest Plant Species and Climate Profile Predictions \(MSFP\)](#) (USDA
448 Forest Service). Contains three generations of climate surface models developed using
449 1961 to 1990 climate normals—access to ancillary datasets used in modeling. Models
450 contain predictions for species range changes based on multiple emission scenarios. (Last
451 updated 2024)
 - 452 • [Maximum Stand Density Index models](#) (MSDIM) developed by the University of Idaho
453 (UofI) Intermountain Forestry Cooperative (Kimsey et al. 2019). In these models, the
454 maximum stand density index was fit with stochastic frontier regression using stand
455 density (trees per hectare) as the dependent variable, quadratic mean diameter (QMD) as
456 the independent variable, and site factors (e.g., soil, topography, climate) as covariates.
457 Provides access to multiple climate, soil, and topographic variables. (Last updated 2025)
 - 458 • [Modeled Potential Vegetation Zones \(MPVZ\) of Washington and Oregon](#) and [Modeled
459 Plant Association Groups \(MPAG\) of Washington and Oregon](#) were produced by the
460 USDA Forest Service and hosted by [Ecoshare](#), the Interagency Clearinghouse for
461 Ecological Information. The site includes analytical tools, publications, data sets, code
462 sets, GIS data/maps, digital imagery, and educational opportunities and materials. (Last
463 updated 2010)
 - 464 • [Public data for the 20-year Forest Health Strategic Plan \(20yFHP\): Eastern Washington](#)
465 (Washington Department of Natural Resources); <https://bit.ly/ForestHealthData>.
466 Landscape evaluations conducted for priority planning areas across central and eastern
467 Washington. Access to 1) Key information for each planning area, including landscape
468 evaluation summaries, presentation slides, and datasets. 2) Maps and spatial data
469 covering eastern Washington. 3) Data documentation and methods. 4) Reports and
470 documents related to each planning area and the 20-year plan. (Last updated 2023)
 - 471 • [Site Potential Tree Height Public \(MapServer\) \(wa.gov\)](#) Statewide riparian site potential
472 tree height map produced for priority habitats and species by the Washington State
473 Department of Fish and Wildlife (WDFW). (Date of last update unknown)
 - 474 • [TreeMap, a tree-level model of conterminous US forests circa 2014 produced by
475 imputation of FIA plot data | Scientific Data \(nature.com\)](#). Continuous raster of tree cover
476 produced by the USDA Forest Service. The values associated with the raster contain
477 unique identifiers of Forest Inventory Analysis (FIA) plots. Plots are identified in a

478 supplemental table containing codes for individual tree species within each plot. (Last
479 updated 2014)

480 Acronyms listed in parentheses define the source of each dataset. Oregon State University
481 (OSU), United States Department of Agriculture (USDA), University of Idaho (UofI), United
482 States Forest Service (USFS).

483 Of these geospatial datasets, we asked three questions:

- 484 1. Does the dataset differentiate between riparian and upland forest types?
- 485 2. Does the data set cover lands managed under FPA (Forest Practice Act)?
- 486 3. Does the data set offer adequate resolution (i.e., mapped pixel resolution 40 m or finer,
487 size distinguishes a regulatory buffer zone)?

488 In the study design, we also proposed using available stand-level data in simulation modeling
489 (e.g., FVS, SHADE.xls). This involves evaluating not only distinctions in dominant riparian
490 forest vegetation but also evaluating distinctions in associated riparian function (e.g., shade, large
491 wood recruitment). These data were appraised for their potential to be used in Step 3 of Phase I:
492 the refinement of the preliminary classification frameworks (developed in Step 2, Phase I), using
493 simulation modeling. We evaluated five stand-level datasets for this purpose:

- 494 • PacFish/InFish Biological Opinion Monitoring Program (PIBO MP; USFS)
- 495 • Forest Inventory and Analysis (FIA)
- 496 • Landscape Fire and Resource Management Planning Tools (LANDFIRE) (USDA)
- 497 • Eastern Washington Riparian Assessment Project (EWRAP) Phase 1 (Bonoff et al. 2008)
- 498 • Forest Resource Information System (FRIS; WA DNR)*

499 *Datasets not originally listed in the experimental design.

500 On these, we considered four questions:

- 501 1. Does the dataset differentiate between riparian and upland forest stands?
- 502 2. Does the data set cover lands managed under FPA?
- 503 3. Does the data set offer adequate resolution (i.e., define characteristics at a scale within
504 the regulatory zone: 75-130 feet)?
- 505 4. Does the dataset support use in simulators (e.g., Forest Vegetation Simulator, Shade.xls)?

506 These questions are derived from the first two Critical Questions—briefly, what type of data are
507 needed to characterize riparian stands, and do existing datasets fulfill this need? These questions
508 were developed explicitly from the attributes identified in the study plan as important for
509 classification development (Spei et al., 2023). They include coverage, scale/resolution, and types
510 of data needed (e.g., topography, climate, soil characteristics, and vegetation descriptions).

511 Data Suitability

512 Of the 12 geospatial vegetation datasets we evaluated, only one—the 20-year Forest Health
513 Strategic Plan: Eastern Washington (20yFHP map) dataset from the Washington State
514 Department of Natural Resources (WA DNR) answered in the affirmative for all three questions
515 (Table 2). The other datasets fell short for various reasons. Several datasets—LEMMA,

516 TreeMap, and ITSP—provided detailed depictions of stocking by species at the pixel level from
517 which we considered the possibility of deriving forest type categories; however, they provided
518 either limited coverage of the study area or were too coarse (i.e., >40 m resolution) for our
519 application. Nevertheless, they show general agreement among each other where coverage
520 within the study area overlapped (Table 2). ESW, MPVZ, and BigMap mapped forest types, but
521 classifications were not specific enough to be of practical use; ECNW and LANDFIRE mapped
522 riparian areas only generally; MSFP mapped forest types but provided no coverage at all within
523 the study area; and the remaining datasets provided ancillary data for classification. The MSDIM
524 dataset did not contain useful vegetation cover.

525 We chose to move forward with the 20yFHP map not only as an alternative framework itself but
526 also to use to explore additional alternative framework development (Phase I, Step 2). The
527 20yFHP map was the only dataset that contained delineated forest types at multiple scales,
528 complete coverage of the study area, and was mapped at a resolution within which riparian areas
529 could be distinguished (30 m x 30 m). The 20yFHP map vegetation type layers were constructed
530 using two versions of Potential Vegetation Type (PVT) data from the Integrated Landscape
531 Assessment Project (ILAP) for forested areas (Burcsu et al. 2014). The current version of the
532 20yFHP map PVTs includes an update of different plant association groups from Henderson
533 (“Henderson’s update”; WA DNR 2020). Especially relevant to our objectives, this map includes
534 an updated forest mask that identifies forested areas and their vegetation types in FPA managed
535 areas identified as “non-forest” or “no data” in the federal datasets we appraised and investigated
536 (Table 2). Further, while riparian forests are not specifically delineated or designated as “riparian
537 forests,” the 30 m x 30 m resolution is a fine enough resolution that shows expected riparian
538 forest types (e.g., western redcedar). Indeed, the mapped forest categories show variation that
539 follows riparian areas with differences and transitions into different forest types with increasing
540 distance from the stream (see Figure S6).

541
542 The specific methods used for generating forest type predictions (i.e., PVTs), delineations, and
543 groupings in the 20yFHP are, however, unclear. The methods are described in Burcsu et al.
544 (2014) as “dynamic”, utilizing a combination of modeling systems as well as “expert opinion”
545 where data were lacking. We were also unable to find any formal evaluations or accuracy
546 assessments of the 20yFHP map. Thus, framework development from the 20yFHP data will first
547 require investigation into how these groups distribute across the study area and their relationship
548 to predictor variables (e.g., physiographic data). We explore these relationships further in Step 2
549 (Framework Development).

550 Of the stand-level datasets, none answered in the affirmative for all four questions (Table 2).
551 Three of the five datasets provided some coverage of FPA-managed lands—EWRAP, FRIS, and
552 FIA (Table 2). Each provides detailed tree information that could be used to discern forest type
553 categories and to inform simulators. However, none provided comprehensive coverage of FPA-
554 managed lands. Because of the limited sample size, EWRAP did not cover the range of
555 elevation, moisture, and temperature regimes encountered on FPA-managed lands. Similarly, the
556 FRIS dataset, though of similar data quality, where it was collected, only covered DNR lands and
557 did not cover all riparian conditions covered by the Step 2 frameworks. And, though the FIA
558 dataset was of similar quality as EWRAP and FRIS, exact plot locations are not publicly

559 available, and we could not discern plots in riparian areas nor FPA management. The remaining
560 stand datasets—LANDFIRE and PIBO—were located on federal lands and, therefore, are
561 unrepresentative.

Table 2. Answers to the four screening questions used to gauge the suitability of each geospatial and stand-level dataset in forest habitat mapping and framework building. Areas highlighted in green indicate that the criteria for inclusion were met.

Geospatial Datasets

Source	Q1. Forest types mapped	Q2. % Study area covered	Q3. Resolution
20-year Forest Health Strategic Plan Eastern Washington (20yFHP map; version February 2023)	Forest types mapped: Dominant conifer species; species groups; and relative moisture and temperature categories (i.e., DRY, MOIST, COLD). Riparian areas are not explicitly delineated.	100	30 m
BIGMAP	Forest types mapped: Continental species groups. Limited to lands classified as forests by the federal database. Riparian areas not delineated.	50	30 m
Ecological Classification of Native Wetland and Riparian Vegetation of Washington (ECNW)	Forest types are not mapped in the study area.	100	Large polygons
Ecological Systems of Washington (ESW)	Forest types mapped: Plant association groups. Riparian areas are not explicitly delineated	100	30 m
Forest Biomass Geospatial Dataset (Forest Biomass)	Forest types are not mapped. This data set depicts modeled projections of forest biomass	50	250 m
Individual Tree Species Parameter Maps (ITSP)	Forest types are not mapped. However, basal area per acre by tree species is calculated for each pixel permitting forest typing. Riparian areas not explicitly delineated.	100	240 m
Landscape Ecology, Modeling, Mapping, and Analysis (LEMMA)	Forest types mapped: Predominant species/groups; however, basal area per acre by tree species is calculated for each pixel permitting forest typing. Limited to lands classified as forests. Riparian areas are not explicitly delineated	50	30 m

Landscape Fire and Resource Management Planning Tools (LANDFIRE)	Upland forest types mapped: Existing vegetation type; and Biophysical Settings Riparian areas are explicitly classified but only categorized into one broad 'Riparian' class (i.e., riparian forest types not mapped)	100	30 m
Maps of Specific Forest Plant Species and Climate Profile Predictions (MSFP)	Forest types not mapped in the study area	0	1 km
Maximum Stand Density Index Models (MSDIM)	Forest types are not mapped. Instead, this tool is used for mapping maximum stand density index for individual tree and species groups.	100	30 m
Modeled Potential Natural Vegetation Zones of Washington and Oregon (MPVZ)	Forest types mapped: Modeled potential natural vegetation zones. Riparian areas are not explicitly delineated.	100	90 m
Site Potential Tree Height Maps	Forest types are not mapped. This data set depicts modeled expected height of several common tree species at 200 years of growth.	100	Large polygons
TreeMap	Forest types mapped: Predominant species/groups; however, basal area per acre by tree species is calculated for each pixel permitting forest typing. Predominantly limited to federal lands. Riparian areas are not explicitly delineated	50	30 m

Stand Level Datasets

Source	Q1. Stand data collected	Q2. Study area covered	Q3. Resolution	Q4. Ancillary Data
EWRAP	Tree species, size, condition, cover, and location measured along a 240 ft transect perpendicular from the stream bank. Tree lists can inform FVS. Study designed to assess riparian stands, however, transects can include uplands. Breaks interpreted using tree locations and site data.	102 transects	Variable width transect	Yes. Site-specific characteristics (elevation, slope, aspect, topographic position)
FIA	Tree species, size, and condition measured on variable radius plots. Tree lists can inform FVS. Locations degraded so cannot select plots within specified distance of the stream.	Unknown	Variable radius plot	Yes. Site-specific characteristics (elevation, slope, aspect, topographic position)
FRIS	Tree species, size, and condition measured on variable radius plots. Tree lists can inform FVS. GPS locations permit selecting plots within a specified distance of mapped streams.	DNR lands only	Variable radius plot	Yes. Site-specific characteristics (elevation, slope, aspect)
LANDFIRE	Tree species, size, and condition measured on variable radius plots. Tree lists can inform FVS. Locations degraded, so cannot select plots within specified distance of the stream.	Federal lands only	Fixed plots	Yes. PRISSM climate data; SSURGO soils data; POLARIS soils data; Elevation, slope, aspect, Topographic position
PIBO	Cover class of vascular vegetation > 5 pct cover by species in each of two layers--lower and upper	Federal lands only	Strip transect	Yes. Site-specific characteristics (elevation, slope, aspect, topographic position)

562 Step 2: Framework Development

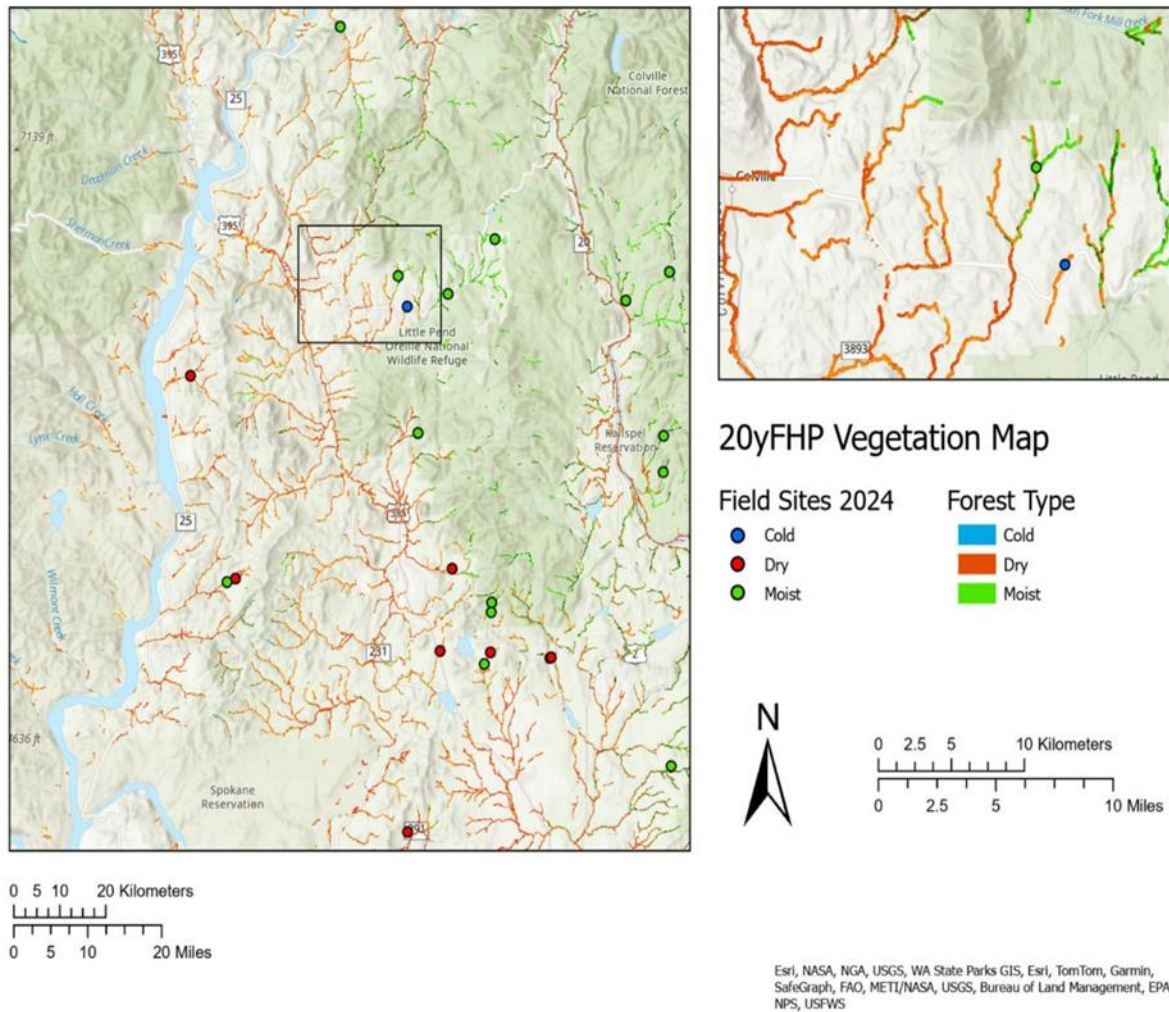
563 Procedural Overview

564 In this step, we attempted to develop an alternative framework, in addition to the 20yFHP map,
565 by developing a predictive model of the distribution of forest type categories in the 20yFHP data
566 set based on environmental factors (e.g., physiography, climate, soil, topography). We used the
567 MSDIM dataset, evaluated in Step 1, to quantify these environmental factors. MSDIM contains
568 several unique data layers (e.g., heatload, solar radiation at the soil layer) useful as independent
569 variables. Heatload is the interaction term of solar radiation x Degree Days between 10-40 °C. In
570 attempting to develop such an alternative framework, we would also be testing the hypothesis
571 that the 20yFHP forest type categories are meaningfully distributed along environmental
572 gradients. Next, we conducted a reconnaissance survey of riparian forest stands across the study
573 area to observe common species assemblages and compared these to the forest types listed in the
574 20yFHP map. Following that, we used Boosted Regression Tree analysis (BRT) to identify the
575 most important factors (e.g., physiography) determining the distribution of forest types along the
576 study area as mapped in the 20yFHP map. From these identified factors, a map was generated of
577 expected forest types (dependent variable) based on the variation and interaction of these factors
578 (independent variables). Variable importance results from BRT were corroborated with non-
579 metric dimensional scaling (NMDS) performed on a subset of the data (methods and results are
580 described in [Appendix I](#)). After identifying the important factors relevant to dominant tree
581 species, including ILAP zone (ecoregion), precipitation, and elevation, we sought to identify
582 thresholds, or break point values, for the important factors above and below which forest types
583 mapped in the 20yFHP map were distributed. With this approach, we developed two alternative
584 frameworks.

585 Data Extraction

586 For data extraction from the 20yFHP map, we first applied a 120 m buffer surrounding either
587 side (240 m total) of the prepared WA DNR Hydrography Watercourses Forest Practices
588 Regulation stream layer clipped to the study area (Figure 4). We chose a 120 m buffer as a sum
589 of 75 m (240 ft), the length of the EWRAP transect sampling design + 12.2 m to account for the
590 national mapping standard inaccuracy + 26 m to account for the greatest discrepancy between
591 lines in the WA DNR stream layer and the USGS hydrography stream layer. This equaled 107.2
592 m, which we rounded up to 120 m to fit 12-10 m pixels (resolution of the digital elevation
593 model; DEM) on either side of the stream (Figure 5). We converted the buffer to a polygon that
594 covered approximately 671.7 sq mi (173,969.5 ha). We then generated a 10 x 10 m point grid
595 over the study area polygon for data extraction. This resulted in 47,089,718 points, which were
596 used for BRT. A subset of these data was also employed in (NMDS) to corroborate these results
597 ([Appendix I](#)).

598



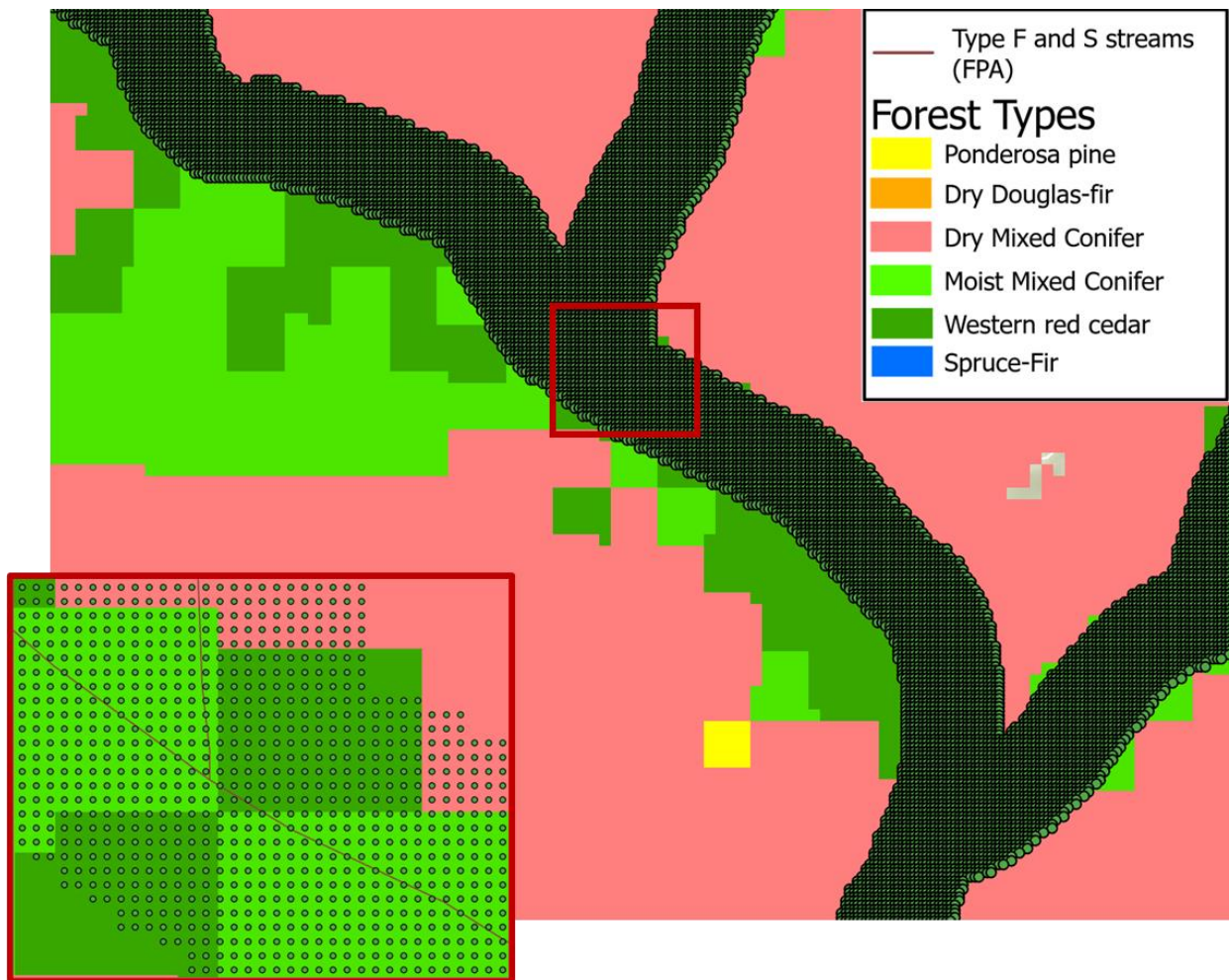
599

600 **Figure 4.** Map of forest types defined by the 20-year Forest Health Plan (6-category) within 120
 601 m of a Type F or Type S (fish-bearing) stream identified by the Washington State Department of
 602 Natural Resources Hydrology Layer. Field sites were identified as Cold, Dry, or Moist based on
 603 observed species composition, stand structure, and estimated fire return intervals (LANDFIRE
 604 dataset) following field-data collection at these points (described in Phase II). The map shows the
 605 Northeastern area of Washington, centered on the Little Pend Oreille National Wildlife Refuge,
 606 to increase visibility of forest type variability.

607

608

609



610

611 **Figure 5.** Screenshot of the 10 x 10-meter point grid used to extract vegetation cover data
612 (20yFHP map), physiographic data (20yFHP map, MSDIM). The point grid was developed
613 within a 120 m buffer on either side of the WA DNR Hydrography Watercourses shapefile. The
614 full buffer point grid was used to extract 47,089,718 data points (containing all available
615 vegetation, physiography, and soil attributes) for the BRT and predictive modeling approach.

616 Field Reconnaissance

617 In June of 2023, we conducted field reconnaissance across the study area as accessible. Field
618 reconnaissance is the first step in the Multi-factor Classification and Habitat Typing Approaches
619 (Layser 1974; Pfister & Arno 1980; Barnes et al. 1982). This step was done to give the
620 researchers an understanding of the variety of communities present in the study area and their
621 relative frequency. Generally, this entails driving along the study area (Forested Type F and S
622 streams on FPA managed lands) and recording areas of continuous vegetation associations that
623 are of a considerable size (e.g., > 1000 m of stream length). The team leader drove along as
624 many reaches as accessible by road, covering as much of the study area as possible. The team

625 leader noted visible transitions of homogenous vegetation communities, topographic, and
626 edaphic features. The team made frequent stops in areas of continuous communities (based on
627 feature homogeneity and vegetation) and collected data on soil, topography, and species
628 composition and coverage. Specifically, areas with distinct and continuous dominant timber
629 species (e.g., Douglas-fir) or forest type communities (e.g., moist forest: western redcedar and
630 western hemlock) that were accompanied by relatively continuous site features (e.g., aspect,
631 slope, soil type). Sites were deemed appropriate for data collection if they 1) had a continuous
632 vegetation association (i.e., not an ecotone or transitional zone of two or more vegetation
633 associations); this criteria is a part of the traditional ecosystem classification approaches (Pfister
634 & Arno 1980; Barnes et al. 1982) in that they identify forest type categories that are of
635 considerable size, are repeatable across the landscape, and will thus, most likely provide similar
636 function throughout, 2) did not show evidence of recent disturbance (e.g., freshly cut stumps,
637 logging roads, recent burn scars); this criteria minimizes the possibility that the stand is in a
638 novel stage of development or is deviated from a “natural” condition, and 3) contained a
639 vegetation structure that reflected a mature forest (e.g., in stem-exclusion phase or older); this
640 criteria is specific too the purpose of our framework which will only be applied to forest stands
641 that have the potential to be harvested for timber. These three criteria were important for
642 grouping forest categories based on our framework objectives (i.e., a framework that categorizes
643 forest types with potential to be harvested for timber and are combined based on their likelihood
644 of having similar functions, such as shade and LW recruitment).

645 From the data collected, potential forest type categories were developed through interpretation of
646 visual ordination (Figure S1). We used these hypothesized groups to cross-reference with the
647 vegetation groups listed in the 20yFHP map: ponderosa pine (PP), dry Douglas-fir (DRY DF),
648 western redcedar (WR), dry mixed conifer (DRY MXD), moist mixed conifer (MOIST MXD),
649 and Engelmann spruce/silver fir (SF). The reconnaissance data was not used.

650 The reconnaissance survey yielded species cover data for 63 sites on a mixture of WA DNR trust
651 lands and industrial timber lands (Inland Empire Paper, Manulife). We attempted to type each
652 site based on species compositions using riparian forest series listed by Kovalchik and
653 Clausnitzer (2004): western redcedar/western hemlock; grand fir/Douglas-fir; Douglas-fir;
654 lodgepole pine/Engelmann spruce. Overall, the reconnaissance survey gave us additional
655 confidence that the six categories listed in the 20YFHP map were appropriately classified and
656 represented commonly found (i.e., repeatable forest type categories of considerable size).
657 Because the reconnaissance data was collected based on ease of accessibility (e.g., accessible by
658 road), it was not used for any tests of statistical significance; it was only used for hypothesis
659 development and cross-referencing with available data.

660 [Boosted Regression Tree \(BRT\)](#)

661 Boosted Regression Tree (BRT) was used to identify the most important input variables (e.g.,
662 physiography) for predicting categorical output variables (i.e., six forest type categories as
663 mapped by the 20yFHP map). Because the methods employed for the construction of the
664 20yFHP map are unclear (see [Data Suitability](#) section), we sought to gain a better understanding
665 of how the listed forest types are distributed across the study area based on their relationships
666 with physiographic variables. We used this analysis as further validation of the 20yFHP forest

667 groups to increase our confidence in the dataset and thus, its use as a potential framework.
668 During this exploration, the BRT also generated a new predictive map that was trained on these
669 data points extracted from the 20yFHP map. These points extracted and used for training fell
670 solely within riparian corridors and adjacent uplands. This newly generated predictive map (BRT
671 map) was a byproduct of our exploration and was also investigated as a potential alternative
672 framework.

673 We used a Gradient Boosting Machine (GBM) algorithm from H2O-3, an open source, in-
674 memory, distributed, fast, and scalable machine learning and predictive analytics platform.
675 Boosted regression trees (BRT) can handle different types of predictors (categorical or
676 continuous data) and accommodate missing data. BRT models are complex, but they can be
677 summarized to give ecological insight and provide a predictive performance that is superior to
678 most traditional modeling approaches (Elith et al., 2008). The BRT is also appropriate for
679 developing predictive maps of species distributions across environmental gradients when
680 applying an auto-logistic modeling approach to account for spatial autocorrelation by calculating
681 the auto-covariates on spatial autocorrelation in residuals (Crane et al., 2012).

682 The BRT was conducted on 36,425,967 unique points derived from the prepared dataset of
683 47,089,718 points. Points with the same values for all dependent and independent variables were
684 removed. We combined categorical ecoregions (aka ILAP zones) and continuous variables
685 (physiographic data) for the BRT exercise to compare their relative strength at predicting
686 riparian forest type. The model was trained on 95% of the points to determine how soil, climate,
687 and topographic factors vary across different forest type categories. Then, it predicted which
688 category each remaining 5% of the original data should be defined in based on the values of
689 these factors. The result of the prediction generates an error matrix to estimate the expected
690 accuracy of the newly produced classification model. Once produced, the model must be
691 validated with field data collected along a gradient of the most important ecological factors
692 identified in the model for predicting riparian forest type (Phase II). After the initial validation of
693 the model with site specific field data, the model was further calibrated by increasing the weight
694 of the field data compared to the modeled data in Phase 2. To align with species assemblages we
695 encountered during our field reconnaissance in the summer of 2023 and determined from
696 ordination ([Appendix I](#)), riparian forest types mapped in the 20yFHP map were collapsed into six
697 forest type categories (Table 3): ponderosa pine (PP), dry Douglas-fir (DRY DF), western
698 redcedar (WR), dry mixed conifer (DRY MXD), moist mixed conifer (MOIST MXD), and
699 spruce-fir (SF).

700 **Table 3.** Table of forest type categories developed from pre-existing forest type categories
 701 defined in the 20yFHP map and used in the BRT approach as the dependent variable.

20yFHP Categories	ML Categories
Dry Douglas-Fir	Dry Douglas-fir (DRY DF)
Dry Mixed Conifer	Dry Mixed Conifer (DRY MXD)
NRM Mixed Conifer*	Dry Mixed Conifer (DRY MXD)
Moist Mixed Conifer	Moist Mixed Conifer (MOIST MXD)
Mountain Hemlock	Moist Mixed Conifer (MOIST MXD)
Pacific Silver Fir	Moist Mixed Conifer (MOIST MXD)
Herbland	Non-Forest (NF)
Shrubland	Non-Forest (NF)
Ponderosa Pine	Ponderosa Pine (PP)
Subalpine - Spruce	Spruce-Fir (SF)
Subalpine Parklands	Spruce-Fir (SF)
Subalpine Fir	Spruce-Fir (SF)
Western Redcedar	Western Redcedar (WR)

702

703 In assessing the most important factors for predicting riparian forest type categories, we used the
 704 ancillary data available in the 20yFHP map (Table 4). We also sourced several unique data layers
 705 (e.g., heatload, solar radiation at the soil layer) from the MSDIM dataset. Finally, we sourced
 706 other ancillary datasets such as the digital elevation model (DEM) from the United States
 707 Geological Survey (USGS).

708 **Table 4.** List of independent variables, their source, and description, that were used in ordination
 709 and BRT to evaluate their relative contribution in predicting the dependent variable (i.e., forest
 710 type categories).

<i>Variables</i>	<i>Source</i>	<i>Description</i>
<i>Actual Evapotranspiration (AET)</i>	20yFHP map	Sourced originally from PRISM. Continuous variable
<i>Ash Prescription</i>	MSDIM	Categorical variables: Soil type and presence of ash (e.g., Sedimentary, Andisol, Ash influence)
<i>Aspect</i>	Calculated from DEM	Continuous variable: converted to Sine(Asspect) and Cosine(Asspect)
<i>Available Water Supply (AWS)</i>	MSDIM	Volume of plant available water that the soil can store in a designated layer based on all map unit components
<i>Depth to Restrictive layer (DEP2RES)</i>	MSDIM	Continuous variable: Soil depth to non-permeable/hydrophobic layer
<i>Digital Elevation Model (DEM)</i>	USGS	Continuous variable: 3DEP DEM 10 m resolution
<i>Heatload</i>	MSDIM	Continuous variable: Calculated from the interaction between solar radiation and degree days between 10 -40 degrees Celsius in ArcGIS Pro

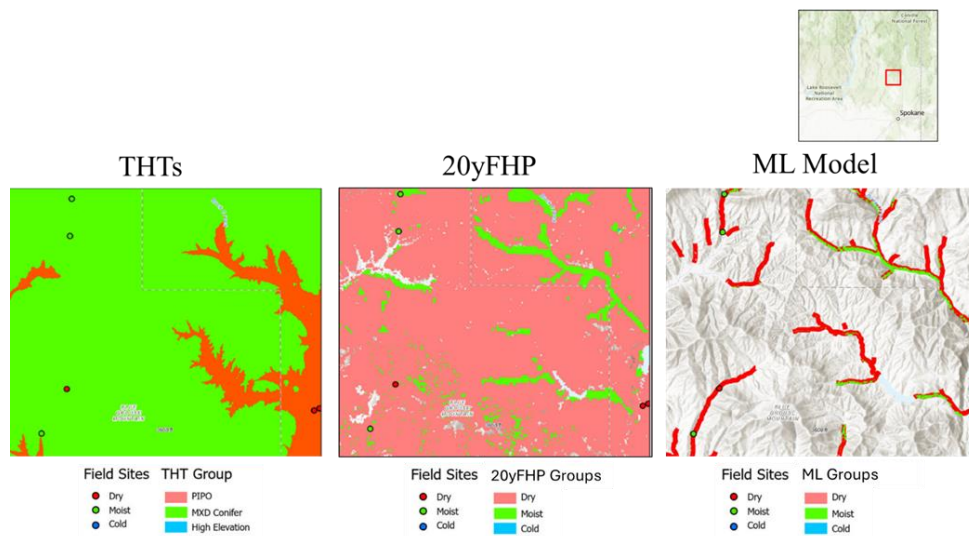
<i>HillShade (HILLS)</i>	Calculated from DEM	Continuous variable: Shade produced by local topography
<i>Latitude</i>	Calculated in ArcGIS Pro	Continuous variable
<i>Mean Annual Precipitation (MAP)</i>	20yFHP map	Sourced originally from PRISM. Continuous variable
<i>Normalized Difference Vegetation Index (NDVI)</i>	USGS	Continuous variable: calculated from USGS Landsat imagery
<i>Slope</i>	Calculated from DEM	Continuous variable
<i>Solar Radiation (Solar)</i>	MSDIM	Continuous variable: calculated in ArcGIS Pro from multiple physiographic variables
<i>Mean Annual Temperature (Tave)</i>	20yFHP map	Sourced originally from PRISM. Continuous variable: From 30-year normals 1980 -2010
<i>Maximum Annual Temperature (Tmax)</i>	20yFHP map	Sourced originally from PRISM. Continuous variable: From 30-year normals 1980 -2011
<i>Maximum Summer temperature (Tmax_sm)</i>	20yFHP map	Sourced originally from PRISM. Continuous variable: From 30-year normals 1980 -2012
<i>Maximum Winter Temperature (Tmax_wt)</i>	20yFHP map	Sourced originally from PRISM. Continuous variable: From 30-year normals 1980 -2013
<i>Minimum Annual Temperature (Tmin)</i>	20yFHP map	Sourced originally from PRISM. Continuous variable: From 30-year normals 1980 -2014
<i>Topographic Position Index (TPI)</i>	Calculated from DEM	Continuous variable: From 30-year normals 1980 -2015
<i>Point Distance to Stream (DTS)</i>	Calculated in ArcGIS Pro	linear distance from a randomly sampled point to the closest stream
<i>Bailey's Ecoregions</i>	USGS	Categorical variable: Delineation of study area by ecoregions defined by Baileys
<i>Integrated Landscape Assessment Project (ILAP) Zone</i>	20yFHP map	Categorical variable: Delineation of study area by ecoregions defined by ILAP and used in the 20yFHP map

711

712 The results of the model showed that nearly 80% of the variation in the 20yFHP map forest type
713 categories could be predicted using the 10 most important independent variables listed in Table
714 5. The model identified that the most important variables in predicting forest cover type
715 categories were those associated with the Integrated Landscape Assessment Project (ILAP) zone
716 (an ecoregion delineation used in the 20yFHP map, modified from Bailey's ecoregions to
717 combine the Okanogan and Canadian Rocky mountains), maximum summer temperature, actual
718 evapotranspiration, Normalized Difference Vegetation Index (NDVI), maximum winter
719 temperature, mean annual precipitation (MAP), and elevation. Using these variables, we
720 generated a map of the study area that predicted what forest type categories would most likely
721 occur under the combination of conditions (Figure 6 below and Figure M3, [Appendix II](#)). We
722 interpreted these results as confirmation that the 20yFHP map forest type distributions follow a

723 temperature and moisture gradient. This increased our confidence in the utility of the 20yFHP
724 map as an alternative framework.

725 The side-by-side comparison of the THT and 20yFHP map (Figure 6) shows how the details of
726 the 20yFHP map forest type categories better reflect not only coarse differences in upland forest
727 type categories but also finer-scale moisture and temperature influences that better represent
728 interfingering of forest type categories as depicted in Figure 1. The BRT Map, developed from
729 machine learning investigation of the 20yFHP map, builds on the 20yFHP map and attempts to
730 refine the classifications based on the input factors (independent variables) used to learn from the
731 20yFHP map forest groups and redefine them based on those predictions. The BRT Map shows
732 an even finer resolution forest type separations along streams (note that aspect appears to
733 influence typing more strongly than in the 20yFHP map). However, because the model learned
734 from the 20yFHP map, the error already associated with the 20yFHP map has been potentially
735 compounded during the modeling process. Thus, we assume that the BRT Map's model
736 predictions may have overpredicted the effect of the leading independent variables on the
737 dependent variable (forest type categories). We attempted to rectify the compounding of error by
738 calibrating with field data, but the relatively small sample size across a large error had little
739 impact (discussed further in Phase II, Step 2).



741 **Figure 6.** Zoomed in display of mapped regulatory zones of the THT for side-by-side
742 comparison with forest type categories (coarse) mapped by the 20yFHP map, and the predictive
743 forest type category map (coarse) developed during the BRT assessment of the 20yFHP map
744 forest type categories.

745 Moving forward, we dropped AET and NDVI for further consideration in our experimental
746 design field validation sampling effort ([Phase II](#)). While AET and NDVI also showed relatively
747 high importance, these factors were not appropriate for framework development given their high
748 annual variability and ephemeral nature (i.e., they are calculated across varying timescales from
749 factors that are themselves variable and thus less stable than other factors considered).

750 Consequently, we chose to move forward with the remaining ILAP zone ecoregions,
 751 temperature, precipitation, and elevation factors for framework assessment.

752 **Table 5.** List of the top ten independent variables based on their relative importance in predicting
 753 the six forest cover type categories used in BRT. The percentage column shows the percentage of
 754 the variation in the dependent variable distribution that could be explained by the variable. ILAP
 755 zone shows the highest percentage (higher than Bailey’s ecoregion) and was chosen as the first
 756 factor for delineation for frameworks #1 and #2. While AET and NDVI also showed relatively
 757 high importance, these factors were not appropriate for framework development given their high
 758 annual variability and ephemeral nature. We chose temperature, precipitation, and elevation as
 759 the factors for single-factor framework development ([Appendix IV](#)).

<i>Variables</i>	<i>Relative Importance</i>	<i>Scaled Importance</i>	<i>Percentage</i>
<i>ILAP Zone</i>	2.02E+06	1	21.70%
<i>Maximum summer temperature</i>	9.37E+05	0.463543	10.06%
<i>Actual Evapotranspiration (AET)</i>	7.38E+05	0.365275	7.93%
<i>Normalized Difference Vegetation Index (NDVI)</i>	6.94E+05	0.343481	7.45%
<i>Bailey’s Ecoregions</i>	6.48E+05	0.320631	6.96%
<i>Maximum Winter Temperature</i>	6.24E+05	0.308966	6.71%
<i>Mean Annual Precipitation</i>	4.22E+05	0.208962	4.53%
<i>Elevation</i>	4.04E+05	0.199903	4.34%
<i>Minimum Annual Temperature</i>	3.96E+05	0.195998	4.25%
<i>Mean Annual Temperature</i>	3.45E+05	0.17065	3.70%

760

761 To corroborate the results of the BRT approach, we also applied an NMDS analysis on a random
 762 subsample of the points extracted from the study area (~15,000) as part of the Multifactor
 763 Classification and Habitat Typing Approaches. The results of NMDS showed agreement with the
 764 BRT that the temperature, precipitation, and elevation factors were most important ([Appendix I](#)).

765 **Conclusions**

766 All modeling efforts and statistical analyses yielded consistent results (detailed in [Appendix I](#)),
 767 indicating that forest type categories derived from the 20yFHP map are consistent and repeatable
 768 components that tend to distribute across the study area based, most commonly, on factors that
 769 quantify temperature and moisture (e.g., actual evapotranspiration, mean annual precipitation,
 770 heatload, seasonal maximum and minimum temperatures). Indeed, the species groups inherently
 771 identify forest type categories that are expected to follow a dry to moist and warm to cold
 772 distribution. Drier forest type categories (e.g., ponderosa pine) tend to associate with lower mean
 773 annual precipitation and/or elevations, and moister (e.g., moist mixed conifer) and colder (e.g.,
 774 spruce-fir) forest type categories at higher precipitation and/or elevation levels. These results
 775 were not surprising and are consistent with the relationships described in Daubenmire (1980) and
 776 Franklin and Dyrness (1973).

777 In Phase 1, as a byproduct of our exploration of the 20yFHP map, the model generated a
 778 predictive map (BRT Map) with an estimated classification error ranging between 5.5% and
 779 19.7%. Considering the evidence that the 20yFHP forest types are distributed based on

780 environmental factors, and the mixture of methods used to construct the 20yFHP, the
781 development of the BRT map was experimental. While it was trained on the existing 20yFHP
782 forest groups, it only used data extracted from the riparian corridors in the study area and
783 immediately adjacent uplands. We saw this as an opportunity to test another potential alternative
784 framework (the BRT map).

785 Step 3: Framework Refinement with Simulation Modeling using Existing Field 786 Data

787 Our study design (Spei et al., 2023) proposed using existing field data to refine and validate,
788 through simulation modeling, the preliminary frameworks developed in Phase I, Step 2, based on
789 the relationships between forest type categories and riparian function (e.g., large wood
790 recruitment, shade). However, our results from Phase I, Step 1 showed that the available field
791 data were insufficient for this analysis. For example, the EWRAP data did not cover all
792 conditions described by the preliminary frameworks (Phase I, Step 2). Similarly, the FRIS
793 dataset did not cover all the riparian conditions defined by the preliminary frameworks.
794 Furthermore, the FRIS dataset only covered DNR trust lands and did not contain important
795 riparian zone characteristics necessary for modeling (e.g., distance to stream for each stem).
796 Thus, we did not initiate Phase I, Step 3, due to a lack of sufficient data. We presented these
797 findings to SAGE on June 11, 2024, and received approval to initiate Phase II of the study.

798 Phase II

799 Step 1: Field Data Collection

800 Field data were collected to assess the alternative classification frameworks developed in Phase
801 I, to refine the frameworks, and to use in modeling riparian function.

802 In eastern Washington, riparian management zones (RMZs) vary in width depending on 1) the
803 width of the stream at bank full width (BFW), and 2) site class, grouped into 5 classes depending
804 on site index, which quantifies a site's timber growing capacity (WAC 222-30-022). Streams
805 with a bank full width (BFW) less than or equal to 15 feet are assigned an RMZ width between
806 75 and 130 feet, depending on site class. Streams with a BFW greater than 15 feet are assigned
807 an RMZ width between 100 and 130 feet, depending on site class. Our proposed frameworks
808 were developed as a tool for applying harvest rules in eastern Washington (objective 1). Thus,
809 our field data used to test these proposed frameworks should be collected at regular intervals,
810 describing features and vegetation within these RMZs at a minimum. However, our available
811 geospatial data lacked the necessary information to determine the expected RMZ width at any
812 given location. Therefore, we chose a sampling design that would cover the maximum possible
813 RMZ width (130 feet) with a 30-foot extension (160 feet total) to compensate for any
814 inaccuracies in the geospatial datasets. The 160-foot sampling distance was applied to the site
815 selection, and field data collection protocols described below.

816 Site Selection Methods

817 Our site selection was implemented along an ecological gradient intended to capture the
818 variation of conditions (independent variables: elevation, precipitation, temperature, and

819 ecoregion) and their relationship to forest type categories (dependent variable). The population
820 of sampling locations was defined as those 36,425,967 unique sampling points used in BRT
821 (Phase I) that fell within 50 m of a Type F or Type S stream identified by the WA DNR
822 Hydrography Watercourses layer. A 50 m buffer width (~164 feet) was chosen to encompass
823 (capture) the maximum width of all possible regulatory riparian buffers in eastern Washington
824 under the current Forest Practices rules, across all water types, plus a 25% “cushion” beyond that
825 to compensate for any potential inaccuracies in identifying the high-water mark. A total of
826 14,888 points were in this sampling population. From this, a total of 90 sites were randomly
827 selected across a range of ecoregions, mean annual precipitation, elevation, and heatload
828 (interaction term of solar radiation x Degree Days between 10-40 °C). We chose heatload
829 because it localizes temperature to the topographic factors of aspect slope, and sun azimuth
830 through the use of solar radiation.

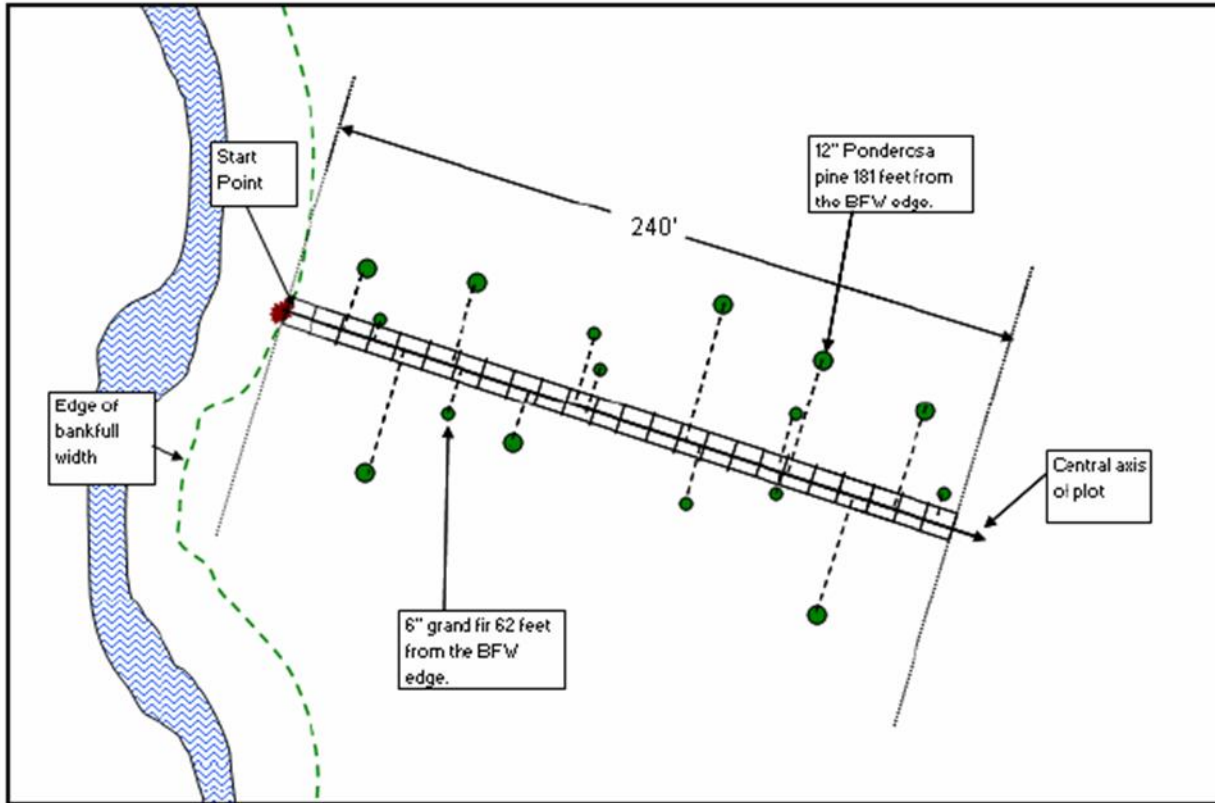
831 The sample population was first stratified by Bailey’s Ecoregions (Bailey 1998), which were also
832 used in the 20yFHP map (Canadian Rocky Mountains, Okanogan, East Cascades, Columbia
833 Plateau, and Blue Mountains). Then, we used an orthogonal sampling approach to select points
834 within each Bailey ecoregion randomly. Orthogonal sampling is an experimental design that
835 ensures representative sampling across multiple dimensions by minimizing correlation between
836 sample points. In each ecoregion, we used an orthogonal sampling matrix consisting of 3 levels
837 each of mean annual precipitation and heatload, across two elevation bands, to randomly select
838 sites for field visits. This resulted in 18 unique combinations within each ecoregion (2 elevation
839 x 3 precipitation x 3 heatload) for a total of 90 site types across the entire study area (18 x 5
840 ecoregions). This method creates 90 unique site types for field-data collection (i.e., no
841 replication). This sampling design captured the range of variability observed across independent
842 variable datasets (site factors) associated with forest type categories (dependent variable) across
843 the study area. This selection process is appropriate for calibration and assessment of the BRT
844 Map and ensures objective coverage of all forest type categories developed for the precipitation-
845 based and elevation-based frameworks. We selected a set of five points within each strata, with
846 the intention of sampling the first point chosen, but with four alternative points of identical
847 conditions. Alternative points were used if, in the field, the first point selected was highly
848 disturbed (e.g., freshly cut stumps or road construction, evidence of recent burning such as fire
849 scars and ash) or inaccessible (e.g., gated roads that passed through privately owned parcels,
850 decommissioned roads not labelled in available maps, roads rendered impassable from recent
851 disturbance such as flooding, fire, or large tree blow-down). This orthogonal sampling design
852 stratified landscapes based on an input variable’s mean and +/- 1 standard deviation, which has
853 been shown to be useful for the development, refinement, and validation of forest type landscape
854 prediction models (Olea, 1980; Hemingway and Kimsey, 2020).

855 **Field Methods**

856 We modified the protocols developed by Mason, Bruce, and Girard (MB&G 2006), which were
857 developed for the EWRAP Study (Schuett-Hames, 2015), to collect data at each sampling
858 location on large and small trees, canopy closure, and in-channel large wood percent cover
859 during the Summer and Fall of 2024. The basic plot configuration used a variable horizontal line
860 sampling transect with a Basal Area Factor (BAF) of 20 for snags (standing dead trees) and live

861 trees ≥ 3.0 " diameter at breast height (DBH), and fixed area subplots (10 x 5 ft) for smaller trees
862 established at each 10-foot mark (i.e. at the 0', 10', 20', ..., 150' marks) along the central axis
863 and extending out perpendicularly on either side by 2.5 feet (i.e. the 10' x 5' plot is centered on
864 the central axis). Sampling transects were oriented perpendicular to the stream bank and
865 extended 160 ft from the estimated bank-full width (BFW) or high-water mark. Sites that showed
866 evidence of recent management (e.g., logging immediately beyond riparian buffer, evidence of
867 dramatic changes in age class, logging road construction) or disturbance (e.g., fire) were avoided,
868 and an alternative site location was sampled. The species, DBH, total height, height to crown,
869 status (live/dead), health (presence of damage agents), and distance to BFW were recorded for all
870 large trees ≥ 3.0 " DBH. Large trees were identified as "in" by a person walking the transect line
871 looking in both directions with a relascope (Spiegel Relaskop^(R)). Small trees (< 3.0 " DBH)
872 were tallied within each 10 x 5 ft fixed area subplot and grouped by species and diameter class.
873 Diameter classes for small trees included four categories (0 = seedlings < 3.5 feet tall, 1 = trees
874 0.1- 1 in DBH, 2 = trees 1.1 – 2 in DBH, and 3 = trees 2.1 – 2.9 in DBH). Site characteristics
875 such as slope, aspect, BFW, Rosgen valley, and stream type (Rosgen 1996) were recorded.
876 Photographs of the stream and site were taken from multiple vantage points. Sketches of the
877 valley shape with notations of natural or anthropogenic disturbance (e.g., abandoned logging
878 roads, cut stumps) or topographic changes (e.g., terracing) and where they were located along the
879 transect were also recorded for each site. Horizontal line sampling has been described by Ducey
880 et al (2002).

881



882
 883 **Figure 7.** General sample plot layout showing start point, central axis, 24 subplots each 10' x 5',
 884 and trees and snags tallied using horizontal line sampling (taken from MB & G, 2006). For
 885 purposes of ETHEP, the transect was reduced to a maximum length of 160' (~50 m) to describe
 886 only vegetation within the designated RMZ. This also resulted in only 16-10 x 5 foot subplots
 887 instead of 24.

888 **Results**

889 We were able to obtain access and successfully sample 88 of the 90 sites. One site in the
 890 Columbia Plateau (lower elevation, highest heatload, highest precipitation), and one site in the
 891 Blue Mountains (higher elevation, highest heatload, and highest precipitation) could not be
 892 sampled because they (primary and alternate sites) were only within the boundaries of small
 893 privately owned land parcels, and owners could not be contacted for access permission. Of the
 894 88 sites sampled, the relative frequencies of the moist mixed conifer (28%), ponderosa pine
 895 (28%), and dry mixed conifer (27%) types were nearly equal (Figure 8). The methods used for
 896 forest typing followed methods described in the 20yFHP (explained in more detail in the
 897 Accuracy Assessment section). The western redcedar (WR; 6%), dry Douglas-fir (5%), and
 898 spruce-fir (5%) occurred much less frequently. Field sites occurred most frequently on WA DNR
 899 trust lands (55%), less frequently on parcels owned and managed by Washington State agencies
 900 (Department of Fish & Wildlife, Department of Parks & Recreation; 24%), and parcels owned
 901 and managed by industrial forestry companies (Inland Empire Paper company, Manulife,
 902 Stimson, Bennet; 22%) (Figure 9). These ownership distributions of random site selection were
 903 commensurate with the distribution of our study area when accounting for the inaccessibility of
 904 privately owned parcels (Table 6). Across all sites, the most common dominant conifers based on

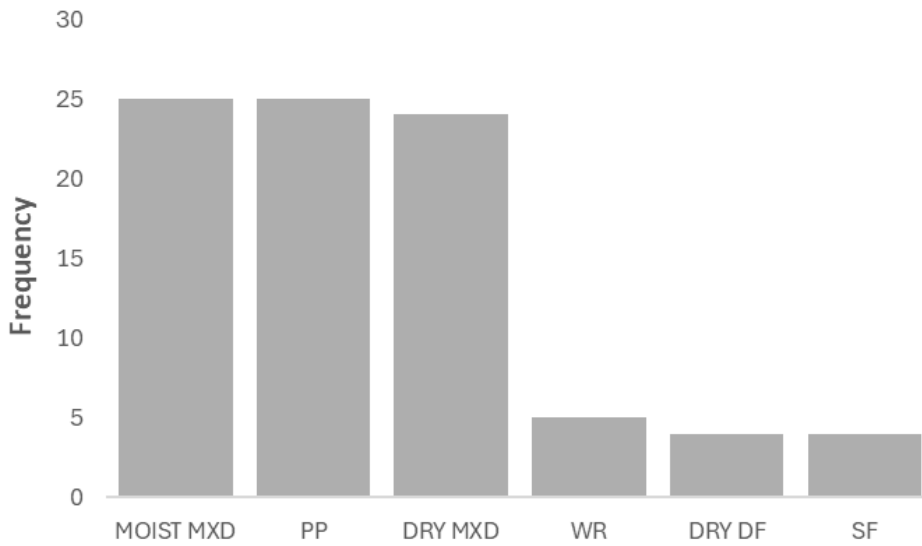
905 basal area per acre were Douglas-fir (43% of sites) and ponderosa pine (28% of sites) (Figure
 906 10).

907 **Table 6.** Estimated number of acres of RMZ by ownership across the study area based on a
 908 contiguous 75-foot buffer for comparison. We used a 75-foot buffer (the smallest regulatory
 909 buffer) to be conservative.

	Industrial	DNR	Other State	Private
Length (miles) of Type F and S streams estimated by the WA DNR Hydro layer	1,288.1	1,463.6	669.7	1082.9

910

911



912

913 **Figure 8.** Frequency distribution of forest type categories found at 88 field sites across eastern
 914 Washington. PP = ponderosa pine, WR = western redcedar, SF = spruce-fir.

915

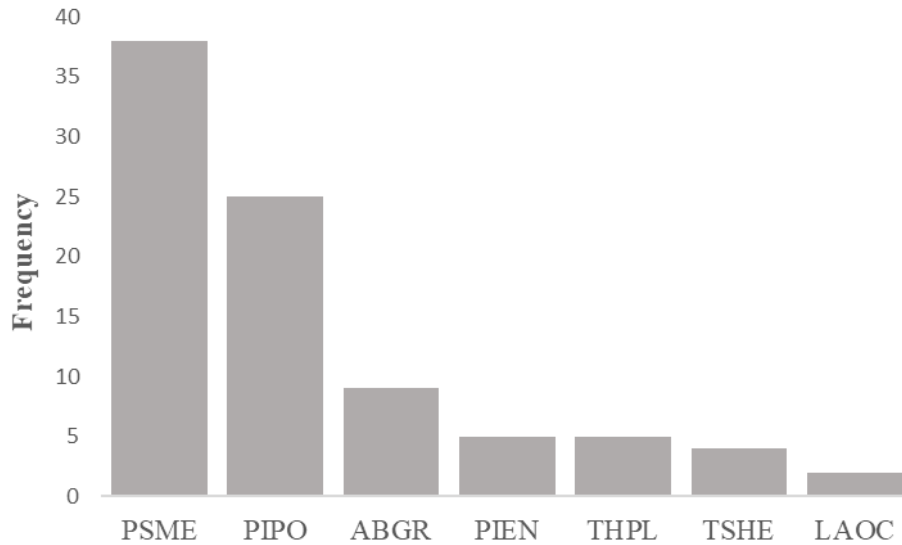


916

917 **Figure 9.** Frequency of ownership across 88 field sites. Other state agencies include the
 918 Department of Fish and Wildlife and the Washington State Parks and Recreation Commission.
 919 Industrial land included owners Inland Empire Paper, Manulife, Stimson, and Bennet Lumber.

920

921



922

923 **Figure 10.** Frequency of dominant conifer species across 88 field sites based on basal area per
 924 acre. PSME = Douglas-fir, PIPO = ponderosa pine, ABGR = grand fir, PIEN = Englemann
 925 spruce, THPL = western redcedar, TSHE = western hemlock, LAOC = western larch.

926

927 Step 2: Validation and Refinement

928 Procedural Overview

929 Field data were used to assess the accuracy of the three alternative classification frameworks
930 developed in Phase I and to model riparian functions of shade and LWD potential. We performed
931 an accuracy assessment by producing error matrices showing the frequency of errors associated
932 with the field classified forest type categories when compared to those mapped by the 20yFHP
933 map itself and those predicted by the BRT Map. We also produced error matrices for the THT
934 classifications to compare the performance of the alternative frameworks. Simulation modeling
935 (FVS) was used to compare estimates for LW recruitment potential and effective shade after 50
936 years of growth, at 10-year time steps, to assess similarities and differences in riparian function
937 among the forest type categories over time. Error matrices and results of modeling were then
938 considered during calibration of the BRT Map and/or to inform the framework refinement.

939 Accuracy Assessment

940 We categorized each field site into one of the framework categories (moist mixed conifer, dry
941 mixed conifer, etc.) using methods employed by the 20yFHP map (WA DNR 2020) and
942 informed by data collected in Step 1. This approach identifies forest type categories based on (1)
943 current dominant species coverage using relative dominance (total basal area of a species/total
944 basal area of all species), (2) interpretation of stand-level data, including physiography (e.g.,
945 aspect, valley morphology), groundcover (e.g., noted presence of indicator species such as
946 *Gymnocarpium dryopteris*, *Alnus spp.*, *Thuja plicata*, *Tsuga heterophylla*), photos, and (3)
947 historical fire return interval and fire severity. Specifically, we used field data to derive species
948 composition and stand structure (e.g., dominance by trees per acre). We supplemented this data
949 with interpretation of stand-level photographs and sketches of valley topography, species
950 groupings, and distribution. Finally, we also cross-referenced this information with fire regime
951 information retrieved from LANDFIRE.

952 We removed five sites from the Blue Mountains ecoregion because they were dominated by non-
953 conifer species (e.g., quaking aspen, cottonwood), and considered non-forest based on a <10%
954 canopy cover. Thus, 83 sites were used for validation and ecological modeling. The results of the
955 BRT Map showed relatively high overall error, with individual forest type category errors
956 ranging from 15-75% (Figures 11 and 12). Because of these high error rates, we considered
957 investigating the effect of distance to stream in forest type category delineation. For example,
958 some sites showed a moist forest type category (e.g., western redcedar dominant) within the first
959 20-50 feet of the stream, which rapidly transitioned to dry forest type categories (e.g., ponderosa
960 pine dominant) beyond 30-50 feet from the stream bank. Thus, we also conducted typing along
961 the core buffer zone (0-30 ft from BFW) and within the outer zone (31-160 ft) from BFW,
962 reflecting regulatory buffer zones. Results are shown in Figures S3, S4, and S5 in [Appendix I](#).

963 To better understand the ability of the 20yFHP map to be used in the machine learning model
964 (BRT Map), we evaluated the accuracy of the BRT Map predictions (Figure 11) as well as the
965 accuracy of forest type categories as mapped by the 20yFHP map dataset (Figure 12). Error rates
966 in the BRT Map predictions ranged from 17-75% depending on the forest type category, with PP
967 having the highest error and DRY MXD having the lowest (Figure 11). Error rates in the

968 20yFHP map vegetation ranged from 21-75% with PP and DRY DF (dry Douglas-fir) having the
 969 highest error, and DRY MXD (dry mixed conifer) having the lowest (Figure 12).

970

		Predicted with BRT						Forest Type	%Error
		PP	DRY MXD	DRY DF	MOIST MXD	WR	SF		
Observed	PP	5	11	0	4	0	0	PP	75%
	DRY MXD	0	20	0	4	0	0	DRY MXD	17%
	DRY DF	1	0	1	2	0	0	DRY DF	75%
	MOIST MXD	0	10	0	10	5	0	MOIST MXD	60%
	WR	0	4	0	0	2	0	WR	67%
	SF	0	1	0	1	0	2	SF	50%
								Overall	52%

971 **Figure 11.** Error matrix describing the percent error for each forest type category predicted by
 972 the BRT Map when compared to field site forest type category (Observed).

973

974

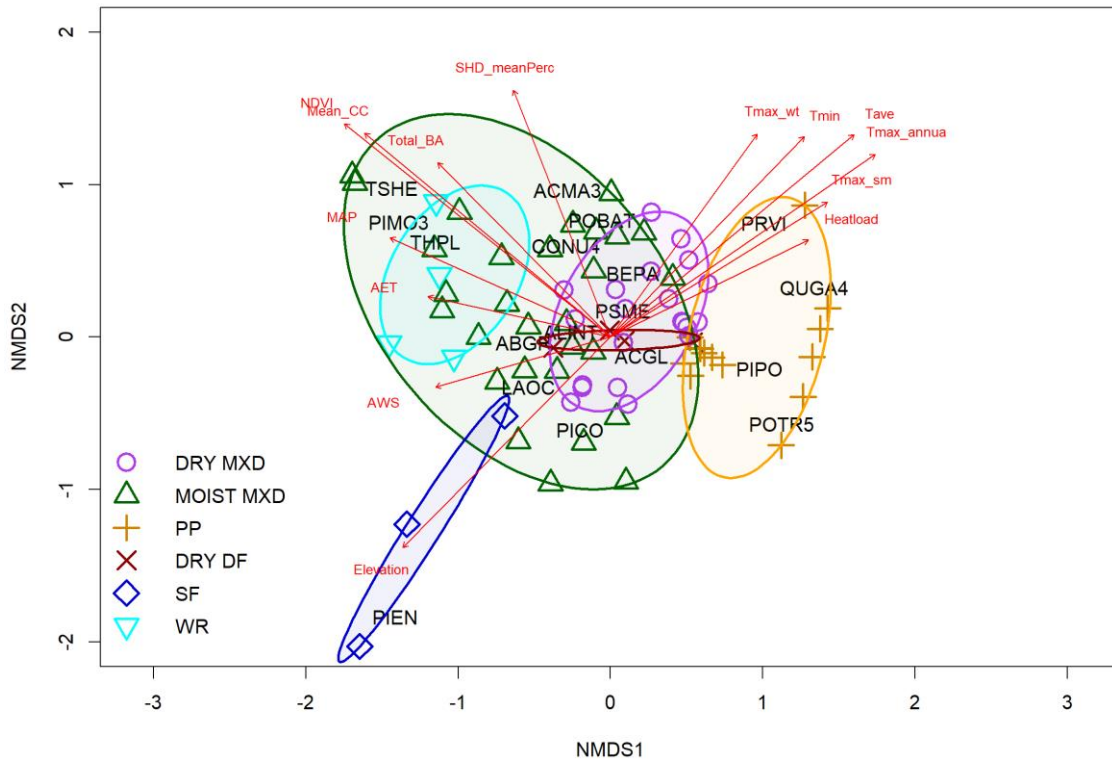
		Predicted by 20yFHP Map						Forest Type	%Error
		PP	DRY MXD	DRY DF	MOIST MXD	WR	SF		
Observed	PP	5	11	0	4	0	0	PP	75%
	DRY MXD	0	19	0	4	0	1	DRY MXD	21%
	DRY DF	2	0	1	1	0	0	DRY DF	75%
	MOIST MXD	0	5	0	14	6	0	MOIST MXD	44%
	WR	0	2	0	1	3	0	WR	50%
	SF	0	1	0	1	0	2	SF	50%
								Overall	47%

975 **Figure 12.** Error matrix describing the percent error for each forest type category predicted by
 976 the 20yFHP map when compared to observed field site forest type categories.

977 We also investigated the relationships between the field-observed forest type categories and
 978 physiographic characteristics. This approach produces evidence of the strength of these
 979 relationships, the relative importance of each factor in driving forest stand development, and the
 980 level of overlap and separation between groups (i.e., forest type categories). To investigate these

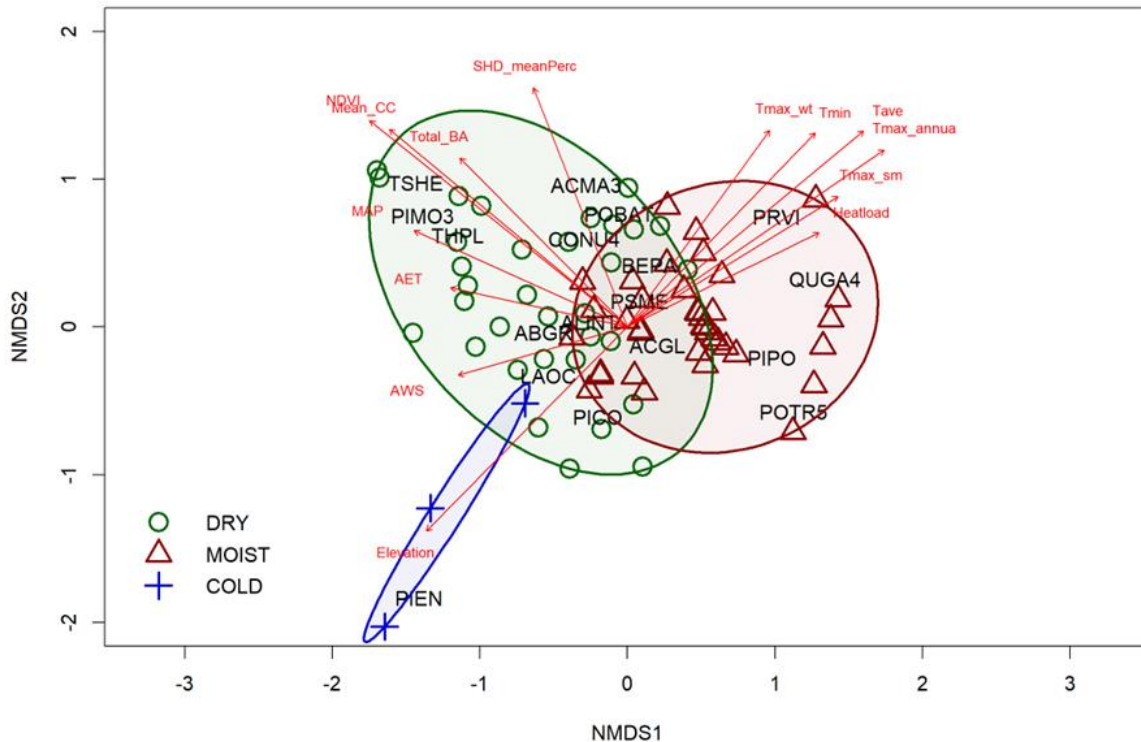
981 relationships and patterns of riparian forest type distribution across the study area, we performed
982 non-metric multidimensional scaling (NMDS) with the 83 field sites using the metaMDS
983 package in R. The species matrix included the basal area by species of all trees present within a
984 site that was relativized to a value between 0 and 1. The dimensionality of the NMDS was
985 determined with a scree plot of stress vs. the number of dimensions and the lowest number of
986 dimensions with stress less than 2.0 (e.g., stress values 0-0.5 = excellent, 0.5-1.0 = fair, 1.0 = 2.0
987 = fair; > 2.0 = poor; as values approach a value of 2 less reliance should be placed on the details
988 of the plot), following criteria suggested by McCune and Grace (2002). The goodness-of-fit of
989 the model with the chosen number of dimensions was cross-referenced with a stress plot of the
990 residuals. We applied a Bray-Curtis dissimilarity to measure ecological distance based on species
991 abundances. We overlaid environmental vectors to visualize their correlations with forest types
992 using the envfit function in R's vegan package. Finally, we used the ordiplot, orditorp, and
993 ordiellipse functions in R's vegan package to visualize patterns of site groupings in ordination
994 space by field identified forest types (e.g., PP, DRY DF, WR, etc.).

995 Results from the NMDS of the 83 field sites with six categories show distinct groupings of the
996 ponderosa pine (PP) and spruce-fir (SF) categories (Figure 13). Separation of the western
997 redcedar (WR), moist mixed conifer (MOIST MXD), dry mixed conifer (DRY MXD), and dry
998 Douglas-fir (DRY DF) is less distinct. The WR category appears to be a specific condition of the
999 MOIST MXD, and the DRY DF category appears to be a specific condition of the DRY MXD
1000 category. While there is much overlap between the DRY MXD and MOIST MXD categories,
1001 they correlate with different factors. The MOIST MXD category ellipsoid shows stretching along
1002 the axes that correlate with all direct and indirect moisture factors, MAP (mean annual
1003 precipitation), AWS (available water supply), AET (actual evapotranspiration), and NDVI
1004 (normalized difference vegetation index). The MOIST MXD group also shows correlations with
1005 site productivity factors such as total basal area (Total_BA), mean canopy cover over the stream
1006 (mean_CC), and the mean percent shade within the riparian area (SHD_meanPerc). The DRY
1007 MXD category stretches along the axes that correlate with all temperature factors and heatload.
1008 The SF category aggregates in the negative x- and y-coordinate values of the ordination plot,
1009 showing occurrence in areas with higher elevation and lower annual and seasonal temperature
1010 means relative to other forest type categories.



1011

1012 **Figure 13.** NMDS ordination of species basal area/acre for 83 timber sites with final stress =
 1013 0.1607668, observed with 2 dimensions ($k = 2$). Post-hoc ellipses encompass full coverage of
 1014 forest type categories to show the overlap of forest type categories determined from the field
 1015 data. They show distinct groupings of the ponderosa pine (PP) and SF forest type groups (Table
 1016 3). Separation of the western redcedar (WR), moist mixed conifer (MOIST MXD), dry mixed
 1017 conifer (DRY MXD), and dry Douglas-fir (DRY DF) forest type categories is less distinct. The
 1018 WR forest type category appears to be a specific condition of the MOIST MXD, and the DRY
 1019 DF type appears to be a specific condition of the DRY MXD forest type category.



1020

1021 **Figure 14.** NMDS ordination of species basal area/acre for 83 timber sites with final stress =
 1022 0.1607668, observed with 2 dimensions ($k = 2$). Post-hoc ellipses encompass full coverage of
 1023 coarsened forest type categories to show overlap of forest type categories derived from the field
 1024 data. When the forest type categories derived from the field data are coarsened to three
 1025 categories (DRY, MOIST, COLD), we see that separations and correlations are more apparent
 1026 and visible than with the fine categories.

1027 These analyses suggested that a more accurate framework could be constructed by coarsening
 1028 the forest type categories into three groupings (DRY, MOIST, COLD) (Figure 14). While there
 1029 is considerable overlap between the MOIST MXD and the DRY MXD groups, the DRY MXD
 1030 group correlates more strongly with the temperature and heatload factors than the MOIST MXD.
 1031 Further, the DRY MXD shows minimal correlation with MAP, AET, AWS, and NDVI,
 1032 indicating they appear in areas of lower moisture availability. The overlap of MOIST MXD and
 1033 DRY MXD types is potentially the result of unaccounted for local site factors (i.e., disturbance
 1034 history) and likely due to a combination of factors, such as an interaction between such factors as
 1035 aspect and slope. The WR group appears to be a group that falls within a narrow range of site
 1036 factors that correlate with the MOIST MXD group (e.g., MAP, AET). Similarly, the DRY DF
 1037 group is completely encompassed by the DRY MXD group, showing it occurs within a narrower
 1038 range of conditions. However, DRY DF's placement near the centroid shows it is itself as a
 1039 group, variable, and not distinctly distributed in correlation with identifying factors. This could
 1040 be due to a limited sample size, but it could also imply that it is not a distinct group and may be
 1041 collapsed into the DRY MXD group altogether. Likewise, this option should be explored with

1042 the WR group, as well as its potential for collapse into the MOIST MXD category. These options
1043 are further explored in the modeling of riparian function sections.

1044 We also considered evaluating forest type categories by regulatory zones (i.e., splitting the
1045 transect into core (≤ 30 ft) and non-core zones > 30 ft). Splitting the transect by regulatory zones
1046 did reduce variability in sites; however, it also caused groups to homogenize (i.e., there was less
1047 separation and distinction between groups), indicating that the variability within sites based on
1048 the full transect was useful for delineation (Figures S4, S5, and S6 in [Appendix I](#))

1049 **Modeling Riparian Function (Shade and Large Wood Recruitment)**

1050 Overall, our results for ecological modeling of effective shade and large wood (LW) recruitment
1051 potential show compelling evidence that the coarser groups (DRY, MOIST, COLD) exhibit
1052 greater separation and lower associated errors than the fine (six-category) forest groups (PP,
1053 DRY DF, DRY MXD, MOIST MXD, WR, SF). Over time, differences among fine forest type
1054 categories in riparian function, as measured by shade and LW, become indistinguishable within
1055 each coarse forest type category. These results corroborate what was observed in the comparison
1056 of groups in the ordination results (Figures 13 and 14), that the coarse forest type categories
1057 based on (DRY, MOIST, COLD) may be more meaningful than the finer forest type categories.

1058 Two riparian functions were modeled: LW recruitment potential and effective shade (ES). We
1059 compared estimates for LW recruitment potential and effective shade after 50 years of growth, at
1060 10-year time steps. We chose a short 50-year timeline with 10-year timesteps because all stands
1061 sampled were mature stands (i.e., not regenerating stands), and the accuracy of stand
1062 development reduces beyond 30 years of growth and shows evidence of overprediction beyond
1063 50 years of simulated growth even when calibrated with sufficient data (Bagdon et al. 2021;
1064 Swann et al. 2025). This step was developed only to compare the estimated riparian forest
1065 function over time by forest type category and is not intended to inform harvest prescriptions
1066 specifically. Stand development over this timeframe was simulated using Forest Vegetation
1067 Simulator (FVS) informed by the field data. Site and tree data were organized into FVS-ready
1068 formats for each specific variant used. Tree data were converted to trees per acre (TPA) using a
1069 modified version of the expansion factor for horizontal line sampling developed by Ducey et al.
1070 (2002) for all trees ≥ 3.0 in DBH. This method uses tree-specific expansion factors based on
1071 DBH, the basal area factor (BAF), and the length of the transect (160 ft). For seedlings (trees
1072 < 3.0 in DBH), we used the subplot area (50 ft^2) to calculate TPA. For seedlings, we used the
1073 midpoint of the diameter class to estimate DBH, and the midpoint of the plot was used to
1074 estimate seedling distance from the stream. Maximum stand density index (Max SDI) was
1075 estimated for each stand using the Forest Site Type Calculator tool developed and operated by
1076 the University of Idaho's Intermountain Forestry Cooperative (Kimsey et al., 2019). Max SDI is
1077 necessary when modeling stand growth and development in FVS. Without specifying the Max
1078 SDI of a stand, the growth rate and eventual plateau would not accurately reflect what would
1079 occur under the specified site conditions. The resulting data tables were developed in FVS-ready
1080 Excel sheets and used as the data source.

1081 FVS variants used were 1) Blue Mountains (Keyser & Dixon, 2008a) for sites in southeastern
1082 Washington; 2) East Cascades (Keyser & Dixon, 2008b) for all sites along the eastern Cascade

1083 Mountains, northcentral and portions of northeastern Washington; and 3) Inland Empire (Keyser,
1084 2008) for all remaining sites in northeast Washington. The **COMPUTE** keyword was used to
1085 calculate the percent canopy cover (PCC). The PCC of each stand was needed to model effective
1086 shade in the Shade.xls model. Keywords used included: **NoTriple** to preserve stem counts, and
1087 **NumCycle** to specify 10-year output periods. We also selected outputs for periodic height and
1088 diameter growth. We ran each simulation with a no-management scenario to estimate stand
1089 development in the absence of anthropogenic disturbance. We chose a no-management scenario
1090 because we were seeking the potential function of forest type categories through undisturbed
1091 development (i.e., “natural conditions”).

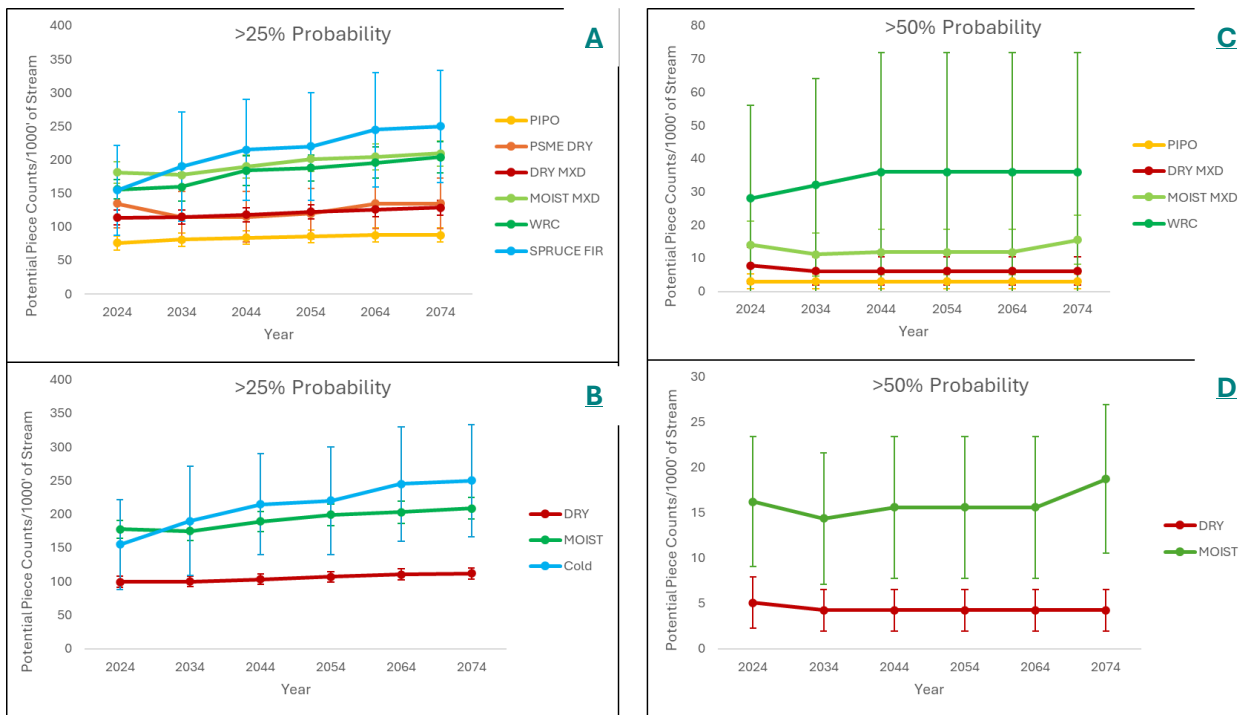
1092 To estimate the LW recruitment potential for each stand, we used tree list outputs from FVS for
1093 each timestep containing data for DBH, total height, and distance to stream for each stem. This
1094 information was used to estimate LW recruitment potential via the equation $P_s = \cos^{-1}(d/Ht)/\pi$,
1095 where P_s is the probability of a stem entering the stream, d = slope distance of stem to stream,
1096 and Ht is the height of the stem (Welty et al., 2002). A bias factor of 1.5 was applied to sites with
1097 a mean slope $>30^\circ$ (Teply et al., 2014). Trees were only included in the equation if they had a
1098 $DBH \geq 5$ in and a height that was at least 10 feet greater than their distance to the channel edge.
1099 This was done to increase the probability that wood entering the channel was of functional size
1100 (i.e., ≥ 4 inches in diameter at the smaller end, and ≥ 10 feet in length). This calculation was used
1101 to compare LW recruitment potential only and is not an estimate of changes in LW load potential
1102 over time. The resulting P_s value for each stem at each site was converted to a percentage. We
1103 counted potential pieces in 2 categories: those with a $>25\%$ potential of entering the stream and
1104 those with a $>50\%$ potential of entering the stream.

1105 To estimate effective shade, we used the percent canopy cover (PCC) for each timestep for each
1106 sampling site. We used this information in Shade.xls (hereafter, SHADE) model (Washington
1107 State Department of Ecology, 2003). SHADE is an Excel/Visual Basic for Applications (VBA)
1108 program that uses topography and riparian vegetation characteristics (e.g., buffer width/height,
1109 PCC). We used the outputs for estimated PCC and tree heights from FVS at 10-year timesteps
1110 over the 50-year period. For buffer height, we used the mean height of the 20 tallest trees within
1111 130 feet of the stream. The 20 tallest trees were used as an estimate of the average height of
1112 mature tree height of the species found at each site. We assigned a 130-foot buffer width in the
1113 model because that is the widest regulatory buffer width assigned in the WAC 222-30-022. We
1114 deactivated the effect of topography and overhang to estimate the shade produced only by the
1115 trees. In the model, sites were grouped by latitude, with all sites in each group being within 1
1116 degree of latitude of each other. The effective shade was estimated from sunrise to sunset for
1117 August 1, 2024, to 2074 in 10-year increments. We chose August 1 as the input date because it is
1118 the day when air temperatures tend to peak regionally and shade becomes most important. We
1119 averaged the overall hourly shade for August 1, for each period and for each forest type category
1120 at the fine (e.g., ponderosa pine, moist mixed conifer, etc.) and coarse (e.g., DRY, MOIST,
1121 COLD) scale.

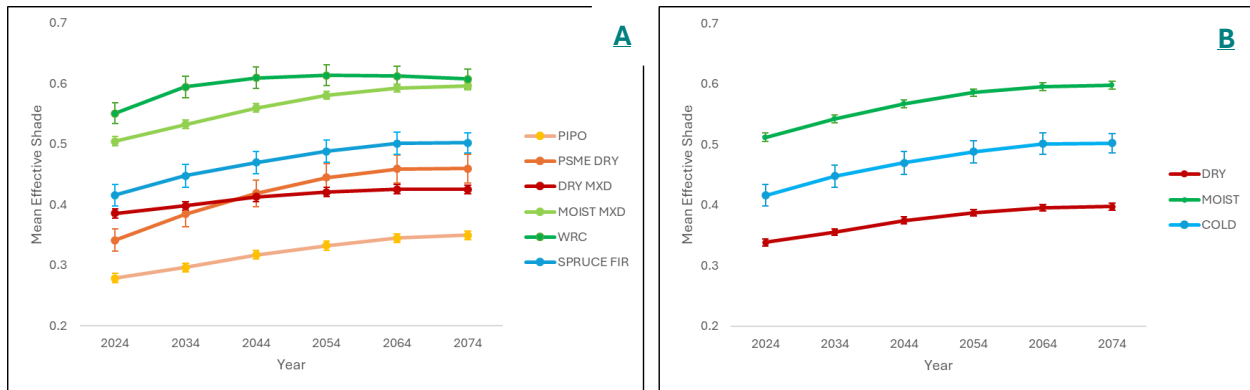
1122 The results of the LW potential recruitment model for pieces with a $>25\%$ probability of entering
1123 the stream show distinct separation of some groups, while others converge to similar values

1124 (Figure 15A). Specifically, the ponderosa pine group (PP), the dry mixed conifer group (DRY
 1125 MXD), the moist mixed conifer group (MOIST MXD), and the SF group all show divergence
 1126 over time, with the PP group having the lowest potential piece count values and the SF group
 1127 having the highest. The dry Douglas-fir group (DRY DF) immediately converges with the DRY
 1128 MXD group after the first time step and maintains similar values throughout the 50-year period.
 1129 The western redcedar (WR) group appears to converge with the MOIST MXD group by the third
 1130 time-step and maintains similar values. For the coarse categories (Figure 15 B), the separations
 1131 are more apparent and consistent, showing evidence of differences in riparian function. The
 1132 COLD group has the highest variability based on the length of the standard error bars. The high
 1133 variability of the COLD group is due to the low sample size (n = 4) compared to the other two
 1134 groups. The low sample size in the COLD group is due to its relatively low frequency of
 1135 occurrence in the study area (Table 1).

1136 The results of the LW potential recruitment model for pieces with a >50% probability of entering
 1137 the stream also show distinct groupings but with much higher variability (i.e., greater standard
 1138 error) due to many sites having no stems meeting the 50% probability threshold (Figure 15 C-
 1139 D). The WR group, for example, shows a mean piece count probability 2-3 times greater than all
 1140 other groups, but with a relatively large standard error. Neither the SF/COLD nor the DRY DF
 1141 group had sites containing stems with a >50% chance of entering the stream.



1142
 1143 **Figure 15 (A-D).** Expected change in LW recruitment potential for piece counts per 1000 feet of
 1144 stream. Piece counts were tallied if they had a >25% (A, B) or >50% (C, D) probability of
 1145 entering the stream channel after mortality and averaged by forest type categories.



1146

1147 **Figure 16 (A and B).** Line graph showing the change in mean effective shade on August 1st,
 1148 2024 – 2074 (50 years) at 10-year timesteps for the fine (A) and coarse (B) forest type
 1149 categories.

1150 The results from the effective shade estimates show similar trends to the LW model. The graph
 1151 shows distinct separation of some groups (Figure 16 A), which is more noticeable in the
 1152 collapsed coarse groups (DRY, MOIST, COLD) (Figure 16 B). The trend for the fine categories
 1153 (PP, DRY DF, etc.) show PP as a distinct group, along with the SF group. The western redcedar
 1154 (WR) group shows convergence with the MOIST MXD group, but only after 50 years of
 1155 simulation. Further, our model does not account for the stochastic nature of mortality nor the
 1156 susceptibility of different forest type categories to disturbances such as windthrow or fire. The
 1157 convergence of the DRY DF group with the DRY MXD group within the first 30 years is likely
 1158 more meaningful when considering function (i.e., while the forest types are different, the
 1159 function provided is likely similar enough to combine for the framework). Taken together, the
 1160 results of the LW model and the SHADE model show that the coarser groups (DRY, MOIST,
 1161 COLD) exhibit greater separation and lower associated errors. This is also observed in the
 1162 comparison of groups in the ordination results (Figures 13 and 14).

1163 **Refinement**

1164 Multiple lines of evidence showed that species distributions and assemblages (i.e., forest groups)
 1165 followed several environmental gradients. From our analysis, we found evidence that the most
 1166 influential factors (i.e., independent variables) in predicting forest type categories (i.e.,
 1167 dependent variable) were those describing temperature (e.g., mean annual temperature) and
 1168 moisture gradients (e.g., mean annual precipitation), as well as elevation, which is negatively
 1169 correlated with temperature (Table 5). We also found that ILAP zone was an important
 1170 categorical variable for predicting forest type category. We produced two frameworks from these
 1171 variables, but the classification error associated with these frameworks could be considerable
 1172 (worse than a random assignment). Consequently, we explored one avenue of refinement
 1173 suggested by the analyses: coarsening of the forest type categories to three ecologically distinct
 1174 categories (DRY, MOIST, and COLD).

1175 When the forest type categories are coarsened to the three categories, the classification error
 1176 associated with the Phase I BRT Map decreases enough to be comparable to classifications based
 1177 on the elevation-based rules for the current three THT categories. Based on the 83 field sites, the

1178 classification error associated with both was about 30 percent (Tables 7 and 8). Overall, these
 1179 coarse categories also appear to resolve much of the confusion we see when using the fine
 1180 categories, especially around the overlap of the fine DRY and MOIST forest type categories we
 1181 examined in Phase I.

1182 **Table 7.** Confusion matrix shows the percentage error of the BRT Map predictions when
 1183 compared to the observed field site categories. The results show an overall slightly better
 1184 performance than the THT framework. However, the MOIST forest type category was predicted
 1185 with greater error than the THTs. Also, note the small sample size of the COLD group, the
 1186 decreased error was only a result of 1 data point.

		Predicted: BRT Map			Error
		DRY	MOIST	COLD	
Observed	DRY	37	10	0	21%
	MOIST	12	19	1	41%
	COLD	1	1	2	50%
	Total Error				30%

1187

1188 **Table 8.** Confusion matrix shows the percentage error of the Timber Habitat Type (THT)
 1189 framework when compared to the observed field site categories. ⁺The THT categories for
 1190 Ponderosa Pine, Mixed Conifer, and High Elevation were evaluated as DRY, MOIST, and
 1191 COLD types, respectively.

		Predicted: THT			Error
		DRY ⁺	MOIST ⁺	COLD ⁺	
Observed	DRY	31	16	0	34%
	MOIST	8	24	0	25%
	COLD	0	3	1	75%
	Total Error				33%

1192

1193 Despite this improvement, however, we recognized that the dependent variable (forest type
 1194 categories) used in the BRT Map was itself developed from an existing dataset, the 20yFHP
 1195 map, which has its own inherent, unknown error. Comparing the coarse types from the 83 field
 1196 sites to the coarse types mapped in the 20yFHP map (Table 9) gives an error of about 22%,
 1197 which is enough to confound modeling. This is not surprising because developing a model from
 1198 a pre-existing dataset with error (20yFHP map) usually results in amplification of the original
 1199 dataset's error. Indeed, when compared to both the THT and Phase 1 BRT Map (see tables
 1200 above), we see that, at the fine scale, the 20yFHP map outperforms both in most ILAP zones.

1201 This amplification of error can be overcome by calibrating the model with actual/observed field
 1202 data to develop a more accurate final product. But this would require considerably more data

1203 than possible under the scope of this study. Aside from the inherent error associated with the
 1204 dependent variables (forest type categories) modified from the 20yFHP map, there are also
 1205 inherent errors associated with the independent variables (e.g., physiographic attributes).

1206 **Table 9.** Confusion matrix shows the percentage error of the 20-year Forest health Plan mapped
 1207 coarse forest type categories when compared to observed field forest type categories. The
 1208 20yFHP map outperforms the THT regulatory zones overall and in each category.

		Predicted: 20yFHP map			Error
		DRY	MOIST	COLD	
Observed	DRY	38	8	1	19%
	MOIST	7	25	0	22%
	COLD	1	1	2	50%
	Total Error				22%

1209 **Discussion**

1210 We evaluated a total of three frameworks, one of which we developed: a Machine Learning map
 1211 (BRT Map) that was created after training on the dependent variables (forest type categories)
 1212 found in the 20yFHP map with a collection of ancillary datasets (independent variables) of site
 1213 factors, and later calibrated with field data. The other two frameworks we evaluated were: 1) the
 1214 20yFHP map, the base layer we used to develop our BRT map; and 2) the currently used Timber
 1215 Habitat Type (THT) elevation zones for forest type categories for comparison.

1216 Overall, we discovered that the 20yFHP map was the best available framework for predicting
 1217 meaningful riparian forest type categories within the study area ([Appendix III](#)). We define
 1218 “meaningful riparian forest type categories” as those types with species associations that give
 1219 similar responses when evaluated by function (e.g., LW recruitment potential and shade). We
 1220 also discovered that the evaluated functional responses were more distinct when the framework’s
 1221 forest type categories were collapsed from 6 categories (PP, DRY DF, MOIST MXD, DRY
 1222 MXD, WR, SF) to 3 categories (DRY, MOIST, COLD). However, our observation of the
 1223 convergence and divergence of each forest type category’s functional response (i.e., estimated
 1224 effective shade and LW recruitment potential at maturity) in the 6-category framework suggested
 1225 that the PP group remained distinct (i.e., divergent) from the other two “DRY” forest type
 1226 categories (DRY DF, DRY MXD; Figures 15 A and C, and 16 A). Ultimately, we interpret these
 1227 results as evidence that a 4-category framework (PP, DRY MXD, MOIST MXD, COLD) may be
 1228 more meaningful when considering function, especially differences in estimated effective shade.
 1229 Our interpretation of each framework’s performance is specifically discussed below.

1230 **The Boosted Regression Tree Map**

1231 The BRT Map was evaluated at two levels of forest type categories: 1) Fine, delineated into six
 1232 categories (PP, DRY DF, MOIST MXD, DRY MXD, WR, SF), and coarse, delineated into three
 1233 categories (DRY, MOIST, COLD). Evaluation of the fine-scale categories with 83 field sites
 1234 (collected in Phase II) revealed error rates considerably higher than predicted ([Appendix III](#)),

1235 ranging from 15% to 75% with an overall error rate of 52%. These error rates were reduced
1236 when evaluated by the coarse categories, ranging from 21% to 50%, with an overall error rate of
1237 30%. This was a slight improvement in performance over the THT framework, which showed
1238 error rates ranging from 25% to 75% with an overall error rate of 33%. This comparison utilized
1239 a crosswalk that equated forest type categories from the BRT Map with THT categories: DRY
1240 with PP (low elevation; THT), MOIST with Mixed Conifer (mid-elevation), and COLD with
1241 High Elevation.

1242 The benefit of the BRT Map is that it was produced using a method that can be calibrated and
1243 updated over time as new data becomes available, and is adept at capturing rapidly changing
1244 landscape features in forest type category. The BRT Map created for this report utilized tens of
1245 millions of data points (sourced in training and was then calibrated using 83 field data sites. We
1246 attempted to retrain and calibrate the model by increasing the weight of the 83 observed points
1247 (<0.01% of points) relative to the millions of geospatial data points. Calibration improved the
1248 model's performance (based on internal point prediction accuracy assessment); however, it could
1249 not be appropriately validated as it would require the collection of more field data, which was
1250 beyond the scope of our study.

1251 Considering its utility, the BRT Map at both fine and coarse scales provides a usable product for
1252 assessing riparian function. The forest groups are ecologically meaningful at both the fine and
1253 coarse scales, as substantiated by the FVS, LW, and Shade.xls modeling results. At a fine scale,
1254 the results of the riparian function modeling showed that the PP group and the SF groups
1255 maintained an average potential LW recruitment and effective shade over time, distinct from all
1256 other groups observed. Conversely, the DRY DF and DRY MXD groups converged over time
1257 for both riparian functions. Similarly, the WR group and the MOIST MXD group converged
1258 over time. Thus, a 4-category classification: PP, DRY MXD/DRY DF, MOIST MXD/WR, and
1259 SF may be a more accurate separation of forest type categories when considering ecological
1260 riparian function, based on our BRT Map results.

1261 The caveat of the BRT Map is that the machine learning process used to create the BRT Map
1262 was trained on modeled data, using the 20yFHP map forest groups as the dependent variable.
1263 This is not a traditional approach, and it is not recommended. The development of predictive
1264 species distribution models using tree-based learning (e.g., BRT) is best accomplished by
1265 training the model with large field verified or field collected historical datasets of species
1266 coverage that is then calibrated with more current or newly acquired species distribution data
1267 covering the study area (Liu et al. 2018). The model will then make predictions of species
1268 distributions across the area of interest that incorporates spatial and temporal variations.
1269 Unfortunately, no such datasets, historical or current, that contained riparian area specific species
1270 coverage data that spanned the study (FPA managed lands) could be found. During our Phase I
1271 exploration of the data, the 20yFHP map was the only geospatial dataset that provided total
1272 coverage of the study area and contained relevant information on important timber species and
1273 forest type categories. Thus, our modeling approach was exploratory in nature, and the BRT map
1274 produced was essentially a byproduct of our investigation of the 20yFHP. We saw this as an
1275 opportunity to explore its utility as an alternative framework. We attempted this modeling step,

1276 anticipating having the ability to conduct calibration and retraining with field data after the
1277 initiation of Phase II. However, as stated above, the field data sample size was proportionally
1278 minute compared to the geospatial training data (36,425,967 modeled points vs 83 field points).
1279 As a future direction, the model could be retrained with the field data and then calibrated with
1280 newly acquired, targeted field survey data. However, given the relatively large size of the study
1281 area along with its high variability in conditions, supplementation with high quality remotely
1282 sensed data would likely produce more accurate results (discussed further in the Future
1283 Directions section).

1284 **The 20yFHP map**

1285 Overall, the 20yFHP map was found to be the best-performing classification system for riparian
1286 forests along Type S and F streams we evaluated, based on our accuracy assessment using the 83
1287 field sites. For the fine-scale, six-category framework, error rates ranged from 21% to 75% with
1288 an overall error rate of 47%, an improvement over the BRT Map (error rate range: 15% to 75%;
1289 overall: 52%). The 20yFHP map's performance improved considerably when the fine-scale
1290 forest species groups (i.e., PP, DRY DF, DRY MXD, MOIST MXD, SF) collapsed into the
1291 coarse, three-category forest type categories (DRY, MOIST, COLD), with an error rates 19%
1292 (DRY), 22% (MOIST) and 50% (COLD) and an overall error rate of 22%. The 50% error rate,
1293 while high, was from the COLD group, which has very low representation (< 1%) in the study
1294 area compared to the other forest type categories, resulting in a low sample size (n = 4). Of all
1295 the frameworks, refinements, and available datasets assessed in this report - the current THT
1296 system, the fine and coarsened BRT Map, and the 20yFHP map (fine and coarse)—the coarse
1297 20yFHP map exhibited the lowest error rates within all forest type categories and overall. This
1298 includes two single-factor frameworks that we also developed from the 20yFHP map (see
1299 [Appendix IV](#)). The single-factor frameworks were an experimental refinement of the 20yFHP
1300 map dataset to maximize forest management utility; however, they resulted in equal or lower
1301 accuracy than the current THT and have thus been removed from the report.

1302 In addition to its performance during our evaluation, we recognize that the 20yFHP map is
1303 already in use as a management tool on WA State Forestlands managed under a different DNR
1304 HCP (1996) to “preserve and restore healthy forests in eastern Washington”. It was developed
1305 for conducting landscape evaluations, based on the best available science on the ecology and
1306 management of fire-dependent landscapes, as well as quantitative assessments of wildfire risks,
1307 treatment prioritization, and climate change impacts and adaptation strategies (WA DNR 2020).
1308 Thus, the purpose of the 20yFHP map aligns with the DNR's privately managed FPHCP (2005)
1309 objectives, as one of its goals is to improve forest health and development in eastern
1310 Washington.

1311 The 20yFHP map we evaluated and used for our framework development was developed and
1312 modified by WA DNR scientists using a combination of existing data sources, including local
1313 knowledge and photointerpretation. Furthermore, this project is currently operational and will
1314 continue to be updated and improved. We were, however, unable to find a record of any
1315 validation assessment. Thus, our interpretations of the 20yFHP map accuracy and utility are
1316 limited to the data collected for this study. A more robust evaluation of the accuracy of the

1317 20yFHP map, clipped to the stream level, with targeted, randomly selected field surveys of the
1318 represented forest groups, could have value.

1319 The main caveat to our study is the limited field sample size. We were able to gather high-quality
1320 field data at a total of 88 field sites representing approximately 4,400 feet of stream (0.83 stream
1321 miles) across the estimated 4,504 miles of stream within the study area. Further, because we
1322 needed to stratify our sampling by ecoregion, elevation, heatload, and precipitation to
1323 compensate for the full range of these conditions, each site represents a unique combination of
1324 these factors. Thus, we do not have replication for each combination of these important factors.
1325 However, it did provide replication within each forest type category, our dependent variable,
1326 especially when the categories were coarsened to three types. The sampling design used an
1327 orthogonal contrast of the most important predictor variables (elevation, precipitation, and
1328 heatload) to be used in our validation and calibration of the 20yFHP map. While each site is
1329 unique in its combined values of these three factors, it still inherently provided a sample size of
1330 each forest type category proportional to its relative frequency of occurrence in the study area.
1331 We also fall short of recognized sampling guidelines for classification accuracy assessments.
1332 Congalton and Green (2019) suggest collecting a minimum of 50 samples per map class for
1333 maps less than 1 million acres in size and fewer than 12 classes for assessing the accuracy of
1334 remotely sensed maps (the base of the available geospatial maps evaluated) to achieve a 95%
1335 confidence level. However, according to the national standard for spatial data accuracy
1336 (NSSDA), twenty points per class is recommended to achieve a positional accuracy estimation
1337 with 11% variability (López and Gordo, 2008). Using the three classes (DRY, MOIST, COLD),
1338 we obtained samples from 47 DRY, 32 MOIST, and 4 COLD categories.

1339 As with many studies, we were limited by the scope of the study, and unfortunately, we were
1340 unable to increase our sample size in time for the conclusion of this study. Regardless of these
1341 limitations, each alternative framework assessed, the predictive map generated with BRT, and
1342 the 20yFHP map itself both show similar or improved error rates compared to the current THT
1343 system for characterizing eastside riparian forests (Objective 2). The 20yFHP map showed the
1344 highest classification accuracy, especially when coarsened to three categories (DRY, MOIST,
1345 and COLD).

1346 **Future Directions**

1347 In parallel with improvements to field-based training data, integrating high-resolution remote
1348 sensing datasets offers exciting opportunities to refine riparian classification. The widespread
1349 availability of NAIP imagery and LiDAR-derived products enables finer-grained analyses of
1350 vegetation structure, surface water presence, and topographic variation. These datasets are
1351 particularly useful for detecting subtle riparian boundaries, capturing canopy height differences,
1352 and even classifying tree species (Rusnák et al. 2022; Tatum & Wallin 2021). As these
1353 technologies continue to advance, they provide a scalable approach for applying detailed
1354 classification techniques across large and heterogeneous landscapes, especially in regions with
1355 limited field access.

1356 Finally, if the 3-category or 6-category classification frameworks from the 20yFHP map (e.g.,
1357 “DRY,” “MOIST,” and “COLD”) are to guide harvest regulations, further examination of their
1358 baseline riparian functions and vulnerabilities to harvest will be necessary. The 20yFHP map
1359 categories were originally developed to manage resilience to fire and insect disturbances in
1360 upland ecosystems. Riparian systems in eastern Washington, however, often reflect complex
1361 interactions between local microclimate and upslope disturbances (Biswas and Mallik 2010;
1362 Ruzicka et al. 2014). This complexity can result in ecological idiosyncrasies; for example,
1363 riparian corridors serving as critical cold-water refuges may occur within upland “DRY” climate
1364 zones. To partially address differences in functional capacity owing to different landscape
1365 classification frameworks, we applied shade modeling using Shade.xls alongside potential wood
1366 recruitment modeling via Climate-FVS. Building on this work, it may be useful to characterize
1367 additional ecological endpoints, such as stream temperature and projected fish habitat under
1368 climate change, and evaluate their distribution within both the default THT framework and each
1369 alternative framework (Isaak et al. 2017; Fuller et al. 2022). This analysis could help managers
1370 assess whether a three-category or six-category classification better balances riparian functions
1371 with harvest practices.

1372 References:

- 1373 Bagdon, B. A., Nguyen, T. H., Vorster, A., Paustian, K., & Field, J. L. (2021). A model
1374 evaluation framework applied to the Forest Vegetation Simulator (FVS) in Colorado and
1375 Wyoming lodgepole pine forests. *Forest Ecology and Management*, 480, 118619.
- 1376 Barnes, B. V., Pregitzer, K. S., Spies, T. A., & Spooner, V. H. (1982). Ecological forest site
1377 classification. *Journal of Forestry*, 80(8), 493-498.
- 1378 Biswas, S. R., & Mallik, A. U. (2010). Disturbance effects on species diversity and functional
1379 diversity in riparian and upland plant communities. *Ecology*, 91(1), 28–35.
1380 <https://doi.org/10.1890/08-0887.1>
- 1381 Burcsu, T. K., Halofsky, J. S., Bisrat, S. A., Christopher, T. A., Creutzburg, M. K., Henderson,
1382 E. B., Hemstrom, M. A., Triepke, F. J., & Whitman, M. (2014). In J. E. Halofsky, M. K.
1383 Creutzburg, & M. A. Hemstrom (Eds.), *Integrating social, economic, and ecological values*
1384 *across large landscapes* (Gen. Tech. Rep. PNW-GTR-896, pp. 15–70). U.S. Department of
1385 Agriculture, Forest Service, Pacific Northwest Research Station.
- 1386 Ceder, K., Tepley, M., Ross, K., Anders, P. (2020) Eastside modeling Effectiveness Project
1387 (EMEP). Cooperative Monitoring Evaluation and Research Report CMER #2020.10.27.
1388 Washington State Forest Practices Adaptive Management Program. Washington Department of
1389 Natural Resources, Olympia, WA.
- 1390 Cooper, S. V., Neiman, K.E., & Roberts., D.W. (1991). Forest habitat types of northern Idaho: A
1391 second approximation. INT-GTR-236, U.S. Department of Agriculture, Forest Service,
1392 Intermountain Research Station, Ogden, UT.

- 1393 Congalton, R. G., & Green, K. (2019). Assessing the accuracy of remotely sensed data:
1394 principles and practices. CRC press.
- 1395 Crase, B., Liedloff, A. C., & Wintle, B. A. (2012). A new method for dealing with residual
1396 spatial autocorrelation in species distribution models. *Ecography*, 35(10), 879-888.
- 1397 Cristea, N., & Janisch, J., (2007). Modeling the effects of riparian buffer width on effective
1398 shade and stream temperature. Washington State Department of Ecology.
- 1399 Daubenmire, R. (1980). Mountain topography and vegetation patterns. *Northwest Science*, 54(2),
1400 146-152.
- 1401 Ducey, M. J., Jordan, G. J., Gove, J. H., & Valentine, H. T. (2002). A practical modification of
1402 horizontal line sampling for snag and cavity tree inventory. *Canadian Journal of Forest
1403 Research*, 32(7), 1217–1224.
- 1404 Elith, Jane, John R Leathwick, and Trevor Hastie. (2008) “A Working Guide to Boosted
1405 Regression Trees.” *Journal of Animal Ecology* 77.4: 802-813
- 1406 ETHEP. (2021). Eastside Timber and Habitat Evaluation Project Scoping Paper and Alternative
1407 Analysis. Cooperative Monitoring, Evaluation, and Research CMER 2021.03.23, Washington
1408 State Forest Practices Adaptive Management Program, Washington Department of Natural
1409 Resources, Olympia, WA.
- 1410 FPHCP. (2005). Forest Practices Habitat Conservation Plan. Washington Department of Natural
1411 Resources, Olympia, WA. [https://www.dnr.wa.gov/programs-and-services/forest-
1412 practices/forest-practices-habitat-conservation-plan](https://www.dnr.wa.gov/programs-and-services/forest-practices/forest-practices-habitat-conservation-plan).
- 1413 Franklin, J. F., & Dyrness, C. T. (1973). Natural vegetation of Oregon and Washington (Vol. 8).
1414 US Government Printing Office.
- 1415 Fuller, M. R., Leinenbach, P., Detenbeck, N. E., Labiosa, R., & Isaak, D. J. (2022). Riparian
1416 vegetation shade restoration and loss effects on recent and future stream temperatures.
1417 *Restoration Ecology*. Advance online publication. <https://doi.org/10.1111/rec.13626>Hanley, D.
1418 P., Baumgartner, D. M., & McCarter, J. B. (2005). Silviculture for Washington family forests.
- 1419 Hemingway, H., & Kimsey, M. (2020). A multipoint felled-tree validation of height–age
1420 modeled growth rates. *Forest Science*, 66(3), 275-283.
- 1421 Isaak DJ, Wenger SJ, Peterson EE, Ver Hoef JM, Nagel DE, Luce CH, et al. (2017) The
1422 NorWeST summer stream temperature model and scenarios for the western US: a crowd-sourced
1423 database and new geospatial tools foster a user community and predict broad climate warming of
1424 rivers and streams. *Water Resources Research* 53: 9181–9205.
1425 <https://doi.org/10.1002/2017WR020969>
- 1426 Keyser, C. E. (2008) Inland Empire (IE) Variant Overview – Forest Vegetation Simulator.
1427 Internal Rep. Fort Collins, CO: U. S. Department of Agriculture, Forest Service, Forest
1428 Management Service Center. 54pp.

- 1429 Keyser, C. E. & Dixon, G. E. (2008a) (revised April 7, 2015). Blue Mountains (BM) Variant
1430 Overview – Forest Vegetation Simulator (p. 56). Internal Rep. Fort Collins, CO: U. S.
1431 Department of Agriculture, Forest Service, Forest Management Service Center.
- 1432 Keyser, C. E. & Dixon, G. E. (2008b) (revised April 7, 2015). East Cascades (EC) Variant
1433 Overview – Forest Vegetation Simulator (p. 59). Internal Rep. Fort Collins, CO: U. S.
1434 Department of Agriculture, Forest Service, Forest Management Service Center.
- 1435 Kimsey Jr, M. J., Shaw, T. M., & Coleman, M. D. (2019). Site sensitive maximum stand density
1436 index models for mixed conifer stands across the Inland Northwest, USA. *Forest Ecology and*
1437 *Management*, 433, 396-404.
- 1438 Kovalchik, B. L., & Clausnitzer, R. R. (2004). Classification and management of aquatic,
1439 riparian, and wetland sites on the national forests of eastern Washington: series description. Gen.
1440 Tech. Rep. PNW-GTR-593. Portland, OR: US Department of Agriculture, Forest Service,
1441 Pacific Northwest Research Station. 354 p. In cooperation with: Pacific Northwest Region,
1442 Colville, Okanogan, and Wenatchee National Forests, 593.
- 1443 Laysner, E. F. (1974). Vegetative classification: its application to forestry in the northern Rocky
1444 Mountains. *Journal of Forestry*, 72(6), 354-357.
- 1445 Liu, Z., Peng, C., Work, T., Candau, J. N., DesRochers, A., & Kneeshaw, D. (2018). Application
1446 of machine-learning methods in forest ecology: recent progress and future challenges.
1447 *Environmental Reviews*, 26(4), 339-350.
- 1448 López, F. J., & Gordo, A. D. (2008). Variability of NSSDA estimations. *Journal of Surveying*
1449 *Engineering*, 134(2), 39-44.
- 1450 Mason, Bruce and Girard. MB & G 2006. Eastside Type F Riparian Assessment Project Phase 1
1451 Study Plan. Forest Practices Division. Washington Department of Natural Resources. Olympia
- 1452 Olea, R. A. (1984). Sampling design optimization for spatial functions. *Journal of the*
1453 *International Association for Mathematical Geology*, 16(4), 369-392.
- 1454 Pfister, R. D., & Arno, S. F. (1980). Classifying forest habitat types based on potential climax
1455 vegetation. *Forest Science*, 26(1), 52-70.
- 1456 Rusnák, M., Goga, T., Michaleje, L., Michalková, M. Š., Máčka, Z., Bertalan, L., & Kidová, A.
1457 (2022). Remote sensing of riparian ecosystems. *Remote Sensing*, 14(11), 2645.
1458 <https://doi.org/10.3390/rs14112645>
- 1459 Ruzicka, K. J., Jr., Puettmann, K. J., & Olson, D. H. (2014). Management of riparian buffers:
1460 Upslope thinning with downslope impacts. *Forest Science*, 60(5), 881–892.
1461 <https://doi.org/10.5849/forsci.13-107>
- 1462 Schuett-Hames, D. (2015). Characteristics of Riparian Management Zones Adjacent to Eastern
1463 Washington Fish-Bearing Streams Managed Under the Washington Forest Practices Habitat
1464 Conservation Plan. Cooperative Monitoring, Evaluation and Research Committee, Northwest
1465 Indian Fisheries Commission, Olympia, WA.

- 1466 Spei, B., Teply, M., Rubin, R., Kimsey, M., & Goebel, C. (2023). Eastside Timber Habitat
1467 Evaluation Project: Study design to evaluate frameworks for applying riparian harvest rules
1468 along Type S and Type F streams in Eastern Washington based on FPHCP objectives and
1469 performance targets. Washington State Department of Natural Resources.
1470 <https://www.dnr.wa.gov>
- 1471 Spies, T. A., & Barnes, B. V. (1985). A multifactor ecological classification of the northern
1472 hardwood and conifer ecosystems of Sylvania Recreation Area, Upper Peninsula, Michigan.
1473 *Canadian Journal of Forest Research*, 15(5), 949-960.
- 1474 Swann, D. E., Fried, J. S., & Gray, A. N. (2025). Evaluating Forest Vegetation Simulator (FVS)
1475 calibration options for predicting biomass accumulation across diverse Oregon landscapes.
1476 *Forest Ecology and Management*, 594, 122937.
- 1477 Tatum, J., & Wallin, D. (2021). Using discrete-point LiDAR to classify tree species in the
1478 riparian Pacific Northwest, USA. *Remote Sensing*, 13(14), 2647.
1479 <https://doi.org/10.3390/rs13142647>
- 1480 Teply, M., McGreer, D., & Ceder, K. (2014). Using simulation models to develop riparian buffer
1481 strip prescriptions. *Journal of Forestry*, 112(3), 302-311.
- 1482 WA DNR (1997). Final Habitat Conservation Plan. Board of Natural Resources, Washington
1483 Department of Natural Resources, Olympia, WA. (https://dnr.wa.gov/sites/default/files/2025-03/lm_hcp_plan_1997.pdf)
- 1485 WA DNR (2020). Forest health assessment and treatment framework (RCW 76.06.200),
1486 Washington State Department of Natural Resources, Olympia, WA.
- 1487 WA DNR. (2007). State of Washington Natural Heritage Plan. Washington Department of
1488 Natural Resources, Olympia, WA.
- 1489 WA DNR. (2001). Washington Forest Practices Rules: WAC 222-30-022. Washington State
1490 Department of Natural Resources, Olympia, WA.
- 1491 Washington State Department of Ecology. (2003). Shade.xls: A tool for estimating shade from
1492 riparian vegetation. <https://www.ecy.wa.gov/programs/eap/models/>
- 1493 Welty, J. J., Beechie, T., Sullivan, K., Hyink, D. M., Bilby, R. E., Andrus, C., & Pess, G. (2002).
1494 Riparian aquatic interaction simulator (RAIS): a model of riparian forest dynamics for the
1495 generation of large woody debris and shade. *Forest Ecology and Management*, 162(2-3), 299-
1496 318.
- 1497 Zar, J. H., & Zar, Jerrold H. (2014). *Biostatistical Analysis* (5th ed.). Noida: Pearson India.

Appendix I Supplemental Figures and Tables

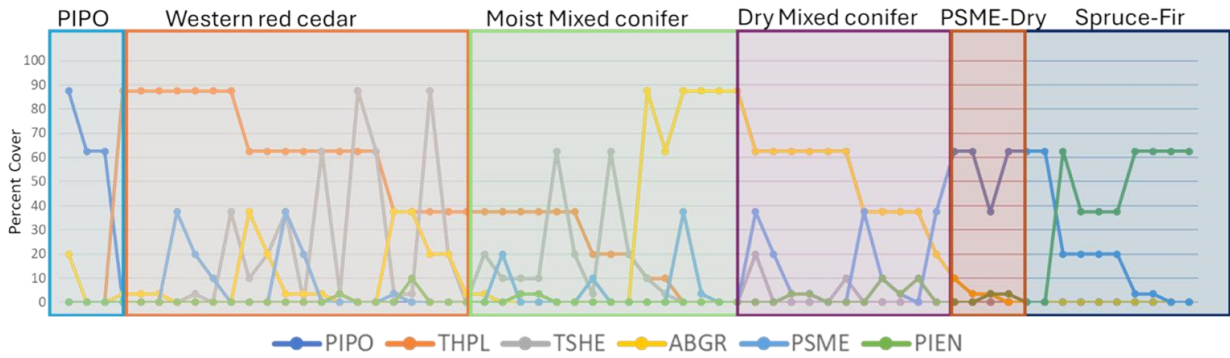


Figure S1. Visual ordination of vegetation cover data collected during field reconnaissance in the summer of 2023. Note that percent cover was based on the visual estimate of the percentage of plant canopy covering the sample plot. Thus, some plots with a multi-layered structure can have a total cover percentage of greater than 100%. Forest groups (colored boxes) were cross-referenced with those in the 20yFHP. The x-axis represents each site (63 total) sampled.

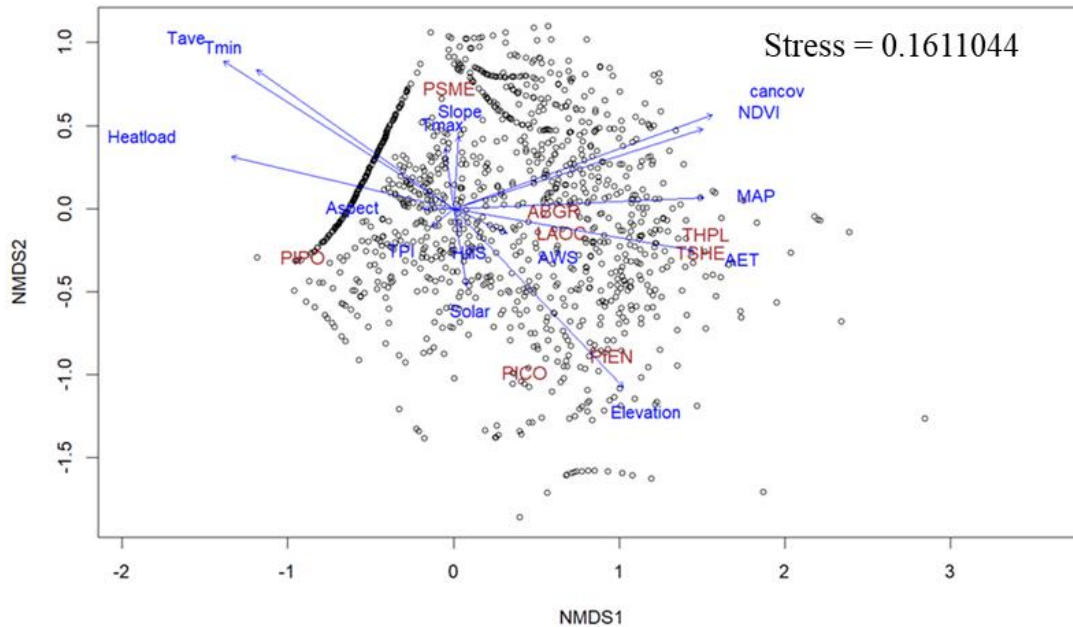


Figure S2. NMDS of 8,848 points extracted from the LEMMA dataset within the study area. The separation of species based on their relative frequency within each plot. The linear relationship of each independent factor with the distribution of each species.

The most significant factors correlating with the separations along the first axis (x: NMDS1) were mean annual precipitation (MAP; $r^2 = 0.99906$, $p < 0.001$) and heatload ($r^2 = -0.97366$, $p < 0.001$). Elevation, and all temperature factors were also significant ($p < 0.001$) and showed the strongest relationship with species distributions along the first and second axes (y: NMDS2). Not surprisingly, species expected to occur on moister sites (e.g., western redcedar, western hemlock) clustered to the right of the centroid along with increasing MAP, while drier species (e.g., PIPO) were distributed further to the left of the centroid away from MAP and with increasing temperature values. Species expected to occur in colder habitats (Engelmann spruce, lodgepole pine) are distributed in the direction of increasing elevation and away from all temperature factors.

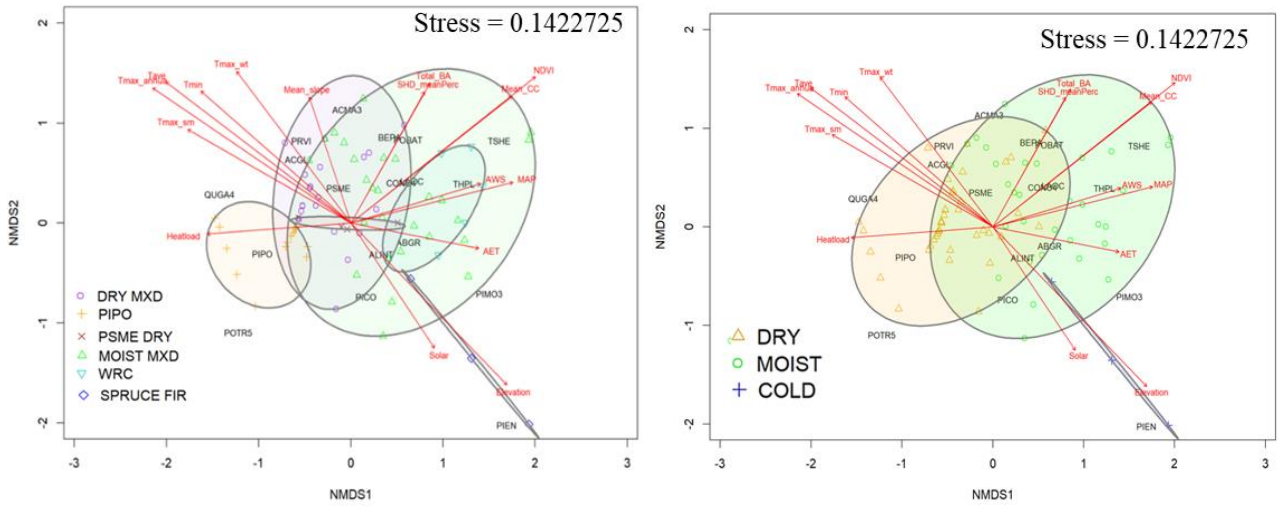
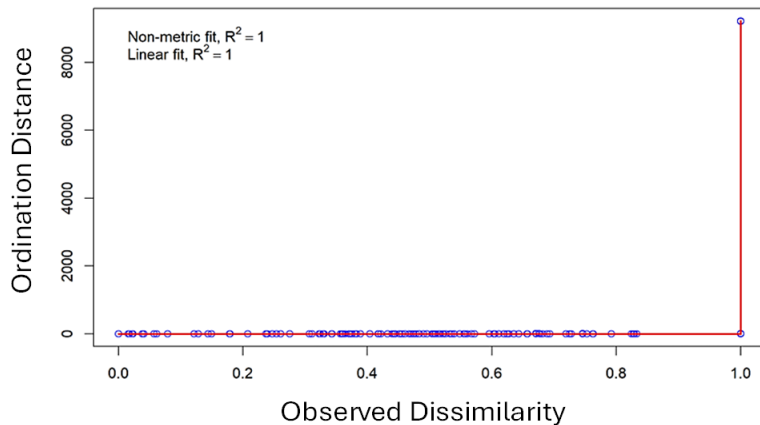


Figure S3, S4. NMDS ordination of species basal area/acre for the core zone (0-30') of 83 timber sites. Post hoc ellipses encompass full coverage of fine categories (S4) and coarse categories (S5) to show overlap.

Results from the NMDS ordination of the outer zone species matrix showed similar distributions, groupings, and site factor correlations as the ordination results for the full transect but with slightly higher overlap. For example, while the PIPO group in the fine categories, and the DRY type in the coarse categories still show distinct separation, a larger portion of the PIPO (fine) and DRY (coarse) sites fall within other categories (e.g., MOIST) than in the full transect ordinations.



	DCA 1	DCA 2	DCA 3	DCA 4
Eigenvalues	1.000	0.8792	0.7779	0.6659
Additive Eigenvalues	1.000	0.8786	0.7775	0.5766
Decorana values	1.000	0.9301	0.7594	0.4577
Axis lengths	1.003	4.5820	5.1385	2.8552

Figure S5. Stressplot for NMDS ordination attempt on species basal area/acre for the inner zone (0-30 ft) for 83 timber sites, and table showing results of detrended correspondence analysis with 26 segments. Rescaling of axes with 4 iterations. Total inertia (scaled Chi-square): 8.1298. DCA1 axis length <2.7 = linear ordination is reasonable.

Our attempt to apply NMDS ordination to the species matrix of the core zone failed to produce results. The stress output and stressplot showed near zero stress, indicating that the species distributions across plots were following a linear distribution as opposed to a unimodal distribution. To check for linearity of the species distributions within the core zone, we applied a detrended correspondence analysis (DCA), and to investigate the variance associated with the species distributions, we applied a redundancy analysis (RDA). Results of the DCA show that the species distributions indeed follow a linear distribution and that using a linear ordination approach (e.g., principal component analysis; PCA) is reasonable. The PCA analysis did produce some interpretable results. However, the RDA showed that the variance between species groups was excessively high (6405). Thus, we could not confidently interpret the results of the PCA of the core zone.

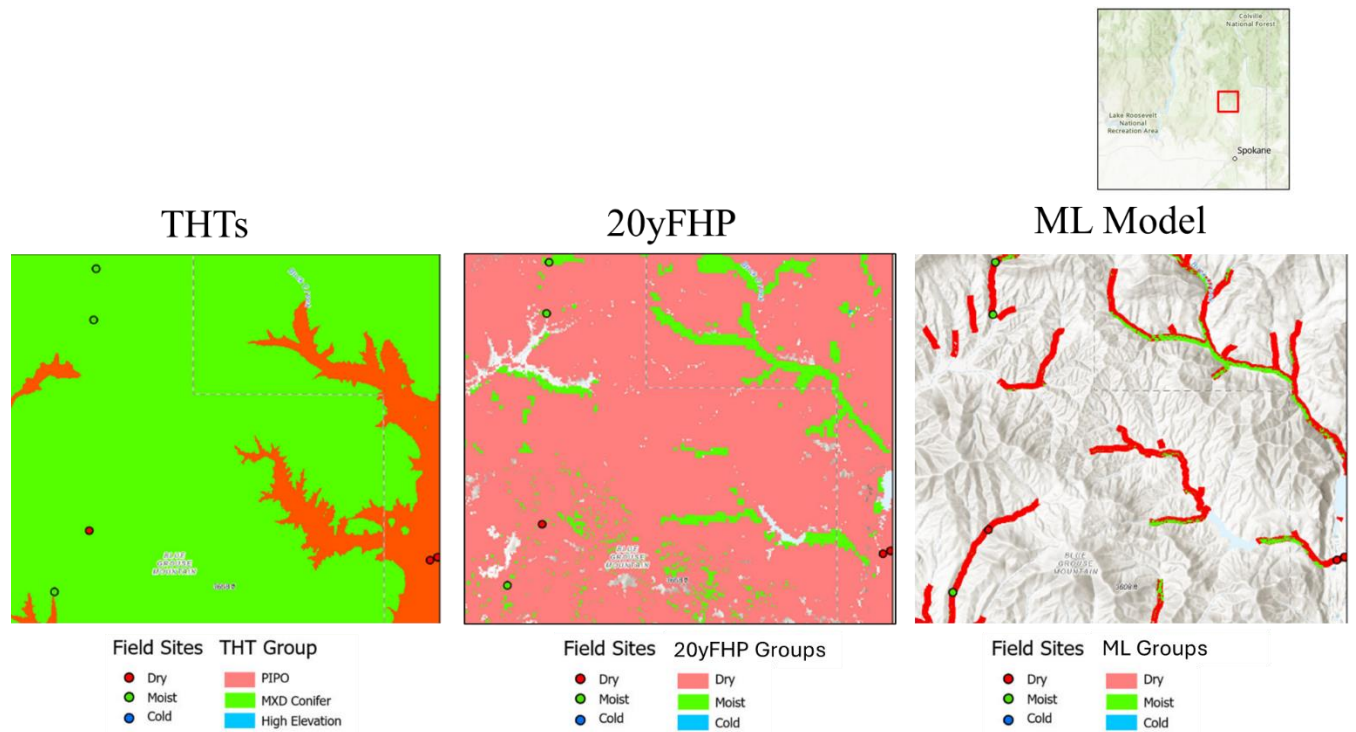


Figure S6. Zoomed in display of mapped regulatory zones of the THT for side-by-side comparison with forest types (coarse) mapped by the 20yFHP map, and the predictive forest type map (coarse) developed during the BRT assessment of the 20yFHP map forest types.

These figures show how the details of the 20yFHP map forest types are more devisive and follow streams and rivers identifying MOIST/DRY types. The BRT Map, developed from machine learning investigation of the 20yFHP map builds on the 20yFHP map and attempts to refine the classifications based on the input factors (independent variables) used to learn from the 20yFHP map forest groups and redefine them based on those predictions. The BRT Map shows an even finer resolution of forest type delineations along streams (note that aspect appears to influence typing more strongly than in the 20yFHP map). However, because the model learned from the 20yFHP map, the error already associated with the 20yFHP map has been folded in and compounded during the modeling process. We attempted to rectify the compounding of error by calibrating with field data, but the relatively small sample size across a large error had little impact.

Table S1 A-D. Results of Kruskal-Wallis analysis comparing the distributions of forest types across the spatial variations of mean annual precipitation (MAP), and elevation with post-hoc pairwise comparison (Dunn’s test) significance.

A. Blue Mountains	P-value	
	Elevation	MAP
Moist Mixed Conifer-Dry Douglas-fir	< 0.01	< 0.01
Ponderosa pine-Dry Douglas-fir	0.654	0.644
Ponderosa pine-Moist Mixed Conifer	< 0.01	< 0.01

MAP by Forest Type
Kruskal-Wallis chi-squared = 131.38, df = 2, p-value < 2.2e-16
Elevation by Forest Type
Elevation Kruskal-Wallis chi-squared = 23.076, df = 2, p-value = 9.75e-06

B. East Cascades	P-value	
	Elevation	MAP
Moist Mixed Conifer-Dry Mixed Conifer	< 0.01	< 0.01
Ponderosa pine-Dry Mixed Conifer	0.0244	< 0.01
Spruce Fir-Dry Mixed Conifer	< 0.01	< 0.01
Ponderosa pine-Moist Mixed Conifer	< 0.01	< 0.01
Spruce Fir-Moist Mixed Conifer	< 0.01	< 0.01
Spruce Fir-Ponderosa pine	< 0.01	< 0.01

MAP by Forest Type
Kruskal-Wallis chi-squared = 1056.1, df = 3, p-value < 2.2e-16
Elevation by Forest Type
Kruskal-Wallis chi-squared = 558.29, df = 3, p-value < 2.2e-16

C. Columbia Plateau	P-value	
	Elevation	MAP
Dry Mixed Conifer-Moist Mixed Conifer	< 0.01	< 0.01
Dry Mixed Conifer Ponderosa pine	< 0.01	0.343
Moist Mixed Conifer Ponderosa pine	< 0.01	< 0.01

MAP by Forest Type
Kruskal-Wallis chi-squared = 265.82, df = 2, p-value < 2.2e-16
Elevation by Forest Type
Kruskal-Wallis chi-squared = 138.93, df = 2, p-value < 2.2e-16

	P-value	
	Elevation	MAP
D. Northeast		
Dry Mixed Conifer - Moist Mixed Conifer	0.0174	< 0.01
Dry Mixed Conifer - Ponderosa pine	< 0.01	0.023
Dry Mixed Conifer - Spruce Fir	< 0.01	0.494
Dry Mixed Conifer - Western redcedar	0.0842	< 0.01
Moist Mixed Conifer - Ponderosa pine	< 0.01	< 0.01
Moist Mixed Conifer - Spruce Fir	< 0.01	< 0.01
Moist Mixed Conifer - Western redcedar	0.0823	< 0.01
Ponderosa pine - Spruce Fir	< 0.01	< 0.01
Ponderosa pine - Western redcedar	< 0.01	< 0.01
Spruce Fir - Western redcedar	< 0.01	< 0.01

MAP by Forest Type
Kruskal-Wallis chi-squared = 3060.9, df = 4, p-value < 2.2e-16
Elevation by Forest Type
Kruskal-Wallis chi-squared = 1552, df = 4, p-value < 2.2e-16

Appendix II Maps

Figures SM1-SM6. Maps showing forest type categories for six frameworks: (1,2) the 20-year Forest Health Plan (20yFHP map) 3-category, and 6-category (3) the Precipitation-based framework, (4) Elevation-based framework, (5) BRT predictive map, and (6) the Timber Habitat Types (THTs). Note the larger map insets show only the Northeast region of eastern Washington. The relatively small area of the stream buffer makes it virtually invisible when at the study area’s full extent.

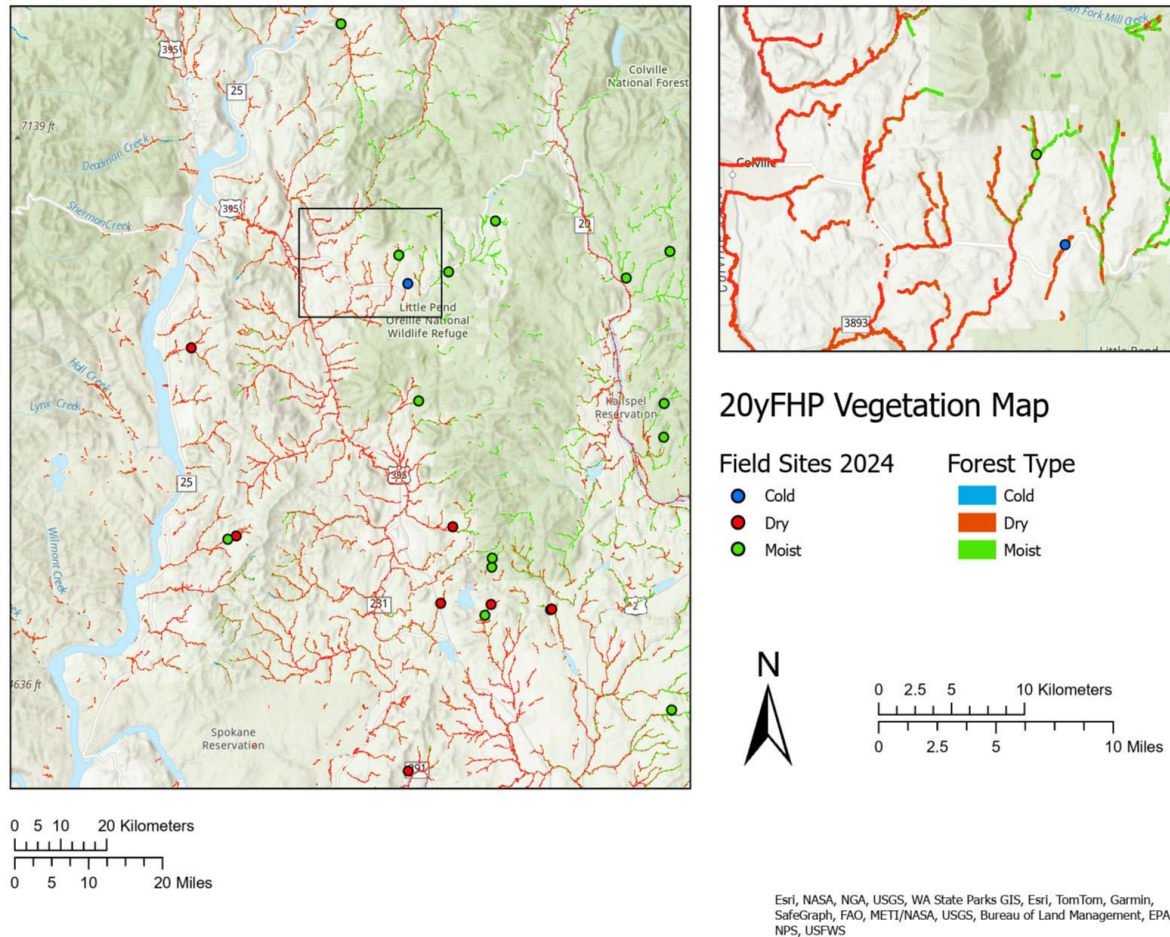


Figure SM1. Map of forest types defined by the 20-year Forest Health Plan (3-category) within 120 m of a Type F or Type S (fish-bearing) stream identified by the Washington State Department of Natural Resources Hydrology Layer. Field sites were identified as Cold, Dry, or Moist based on observed species composition, stand structure, and estimated fire return intervals (LANDFIRE dataset). The map shows the Northeastern area of Washington, centered on the Little Pend Oreille National Wildlife Refuge, to increase visibility of forest type variability.

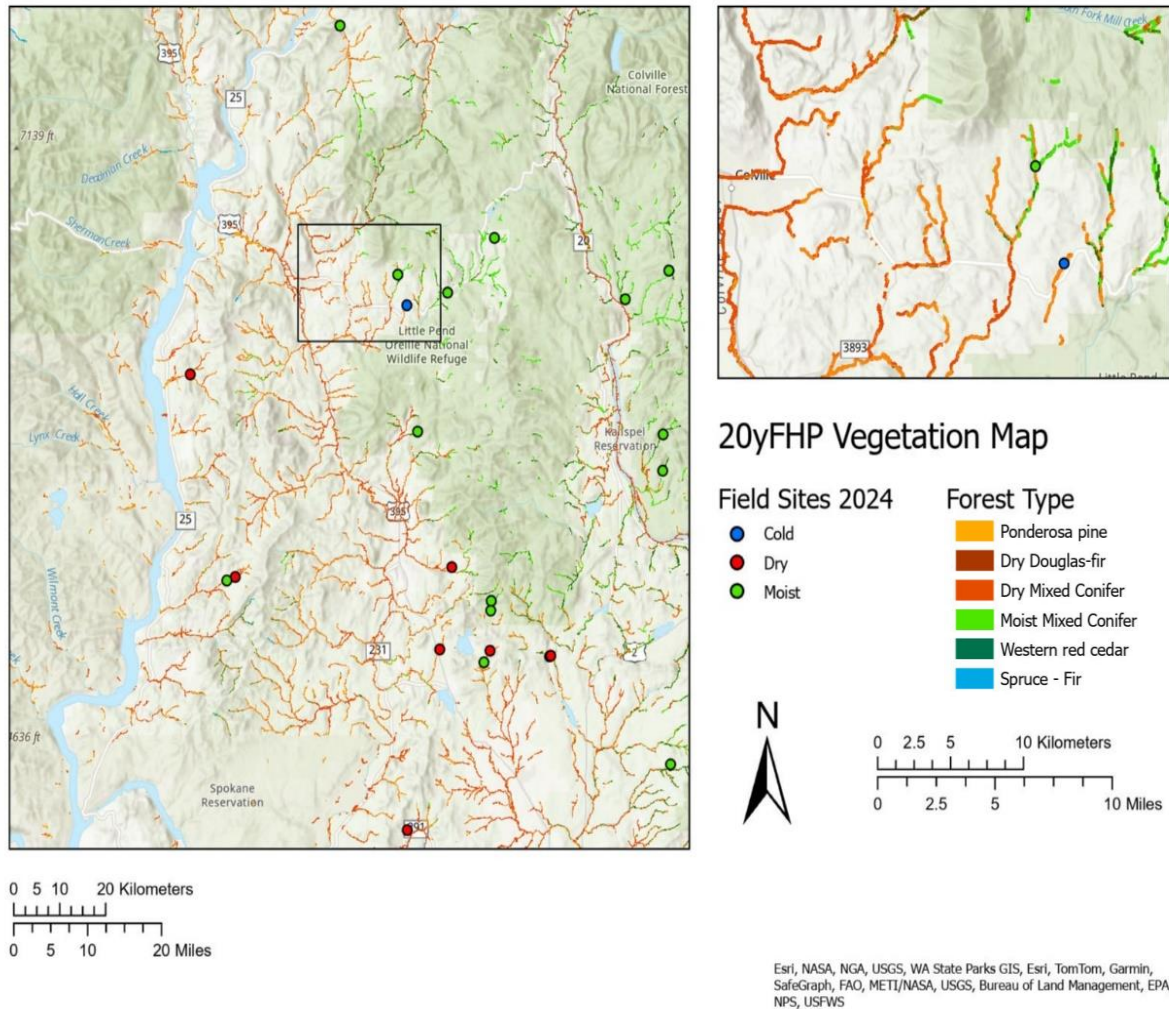


Figure SM2. Map of forest types defined by the 20-year Forest Health Plan (6-category) within 120 m of a Type F or Type S (fish-bearing) stream identified by the Washington State Department of Natural Resources Hydrology Layer. Field sites were identified as Cold, Dry, or Moist based on observed species composition, stand structure, and estimated fire return intervals (LANDFIRE dataset). The map shows the Northeastern area of Washington, centered on the Little Pend Oreille National Wildlife Refuge, to increase visibility of forest type variability.

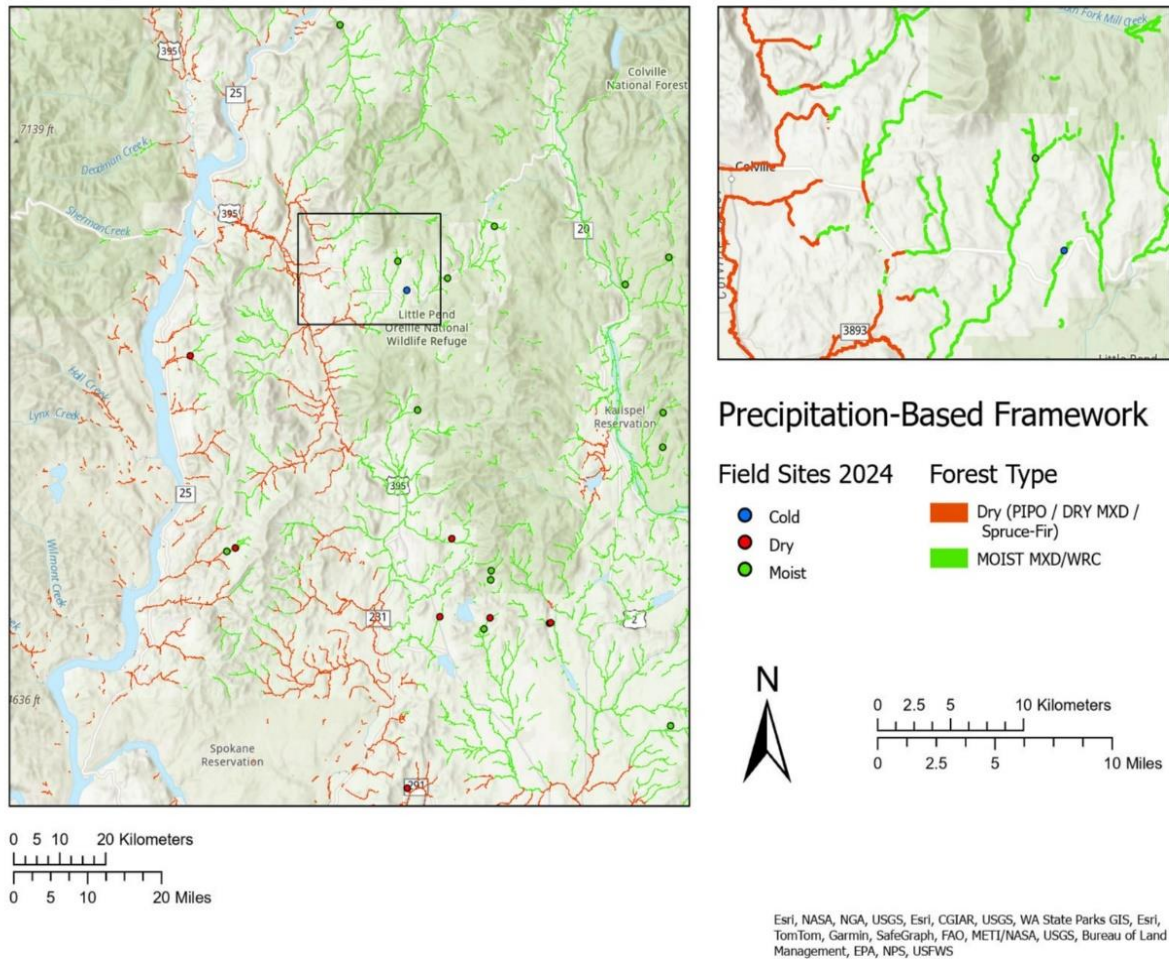


Figure SM3. Map of forest types defined by the Precipitation-based framework developed during Phase I, Step 2, within 120 m of a Type F or Type S (fish-bearing) stream identified by the Washington State Department of Natural Resources Hydrology Layer. Field sites were identified as Cold, Dry, or Moist based on observed species composition, stand structure, and estimated fire return intervals (LANDFIRE dataset). The map shows the Northeastern area of Washington, centered on the Little Pend Oreille National Wildlife Refuge, to increase visibility of forest type variability.

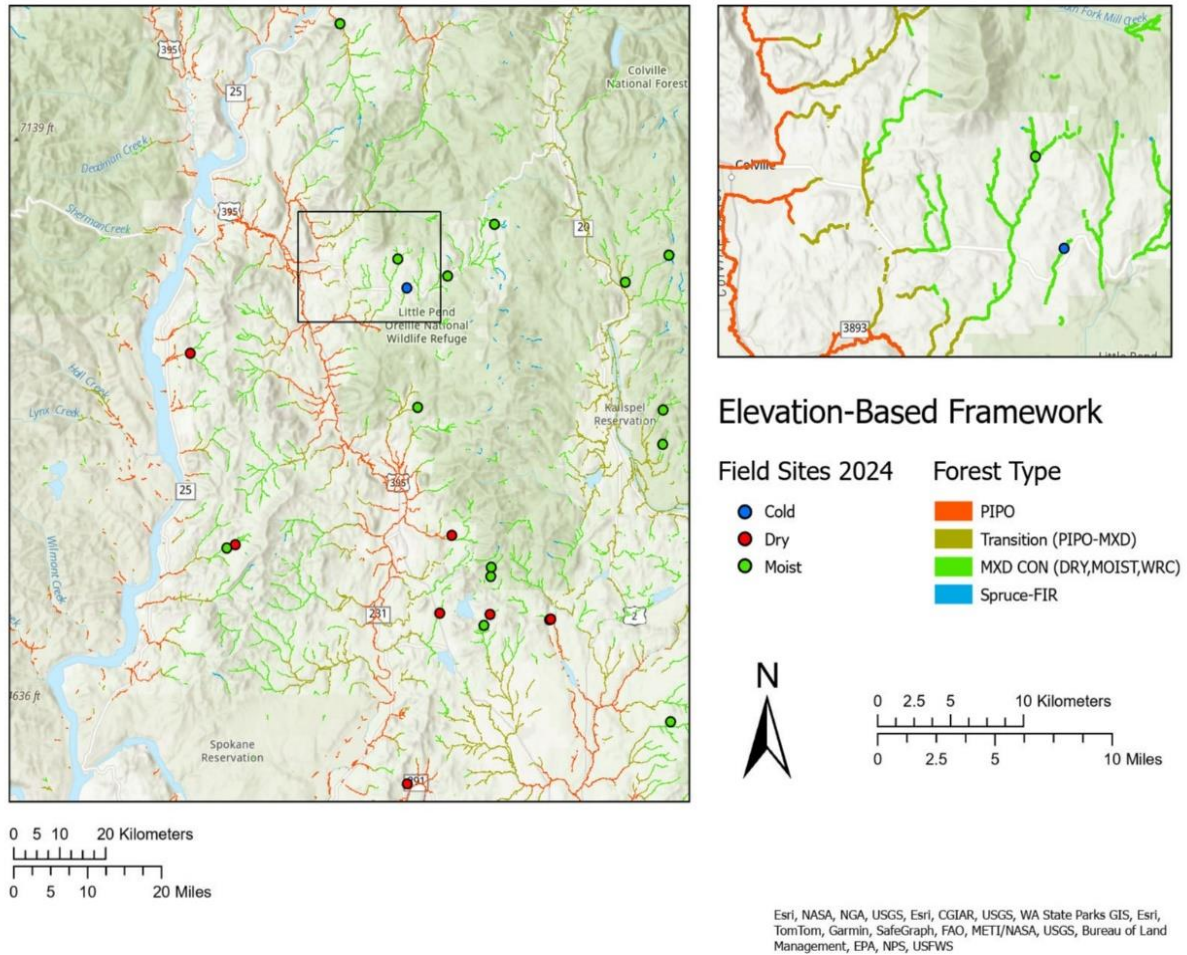


Figure SM4. Map of forest types defined by the Elevation-based framework, developed during Phase I, Step 2, within 120 m of a Type F or Type S (fish-bearing) stream identified by the Washington State Department of Natural Resources Hydrology Layer. Field sites were identified as Cold, Dry, or Moist based on observed species composition, stand structure, and estimated fire return intervals (LANDFIRE dataset). The map shows the Northeastern area of Washington, centered on the Little Pend Oreille National Wildlife Refuge, to increase visibility of forest type variability.

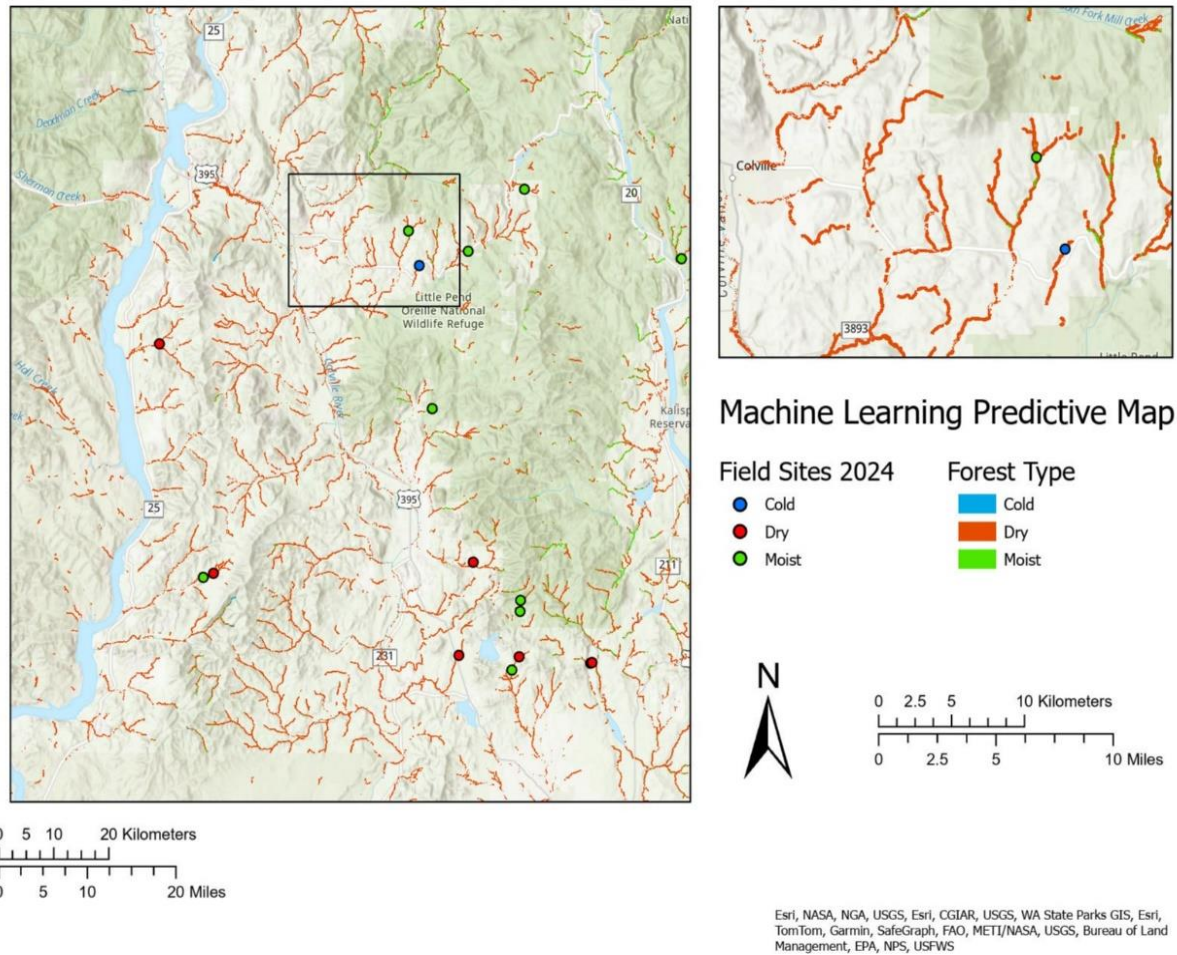


Figure SM5. Map of forest types defined by the Machine Learning predictive map developed during Phase I, Step 2, within 120 m of a Type F or Type S (fish-bearing) stream identified by the Washington State Department of Natural Resources Hydrology Layer. Field sites were identified as Cold, Dry, or Moist based on observed species composition, stand structure, and estimated fire return intervals (LANDFIRE dataset). The map shows the Northeastern area of Washington, centered on the Little Pend Oreille National Wildlife Refuge, to increase visibility of forest type variability.

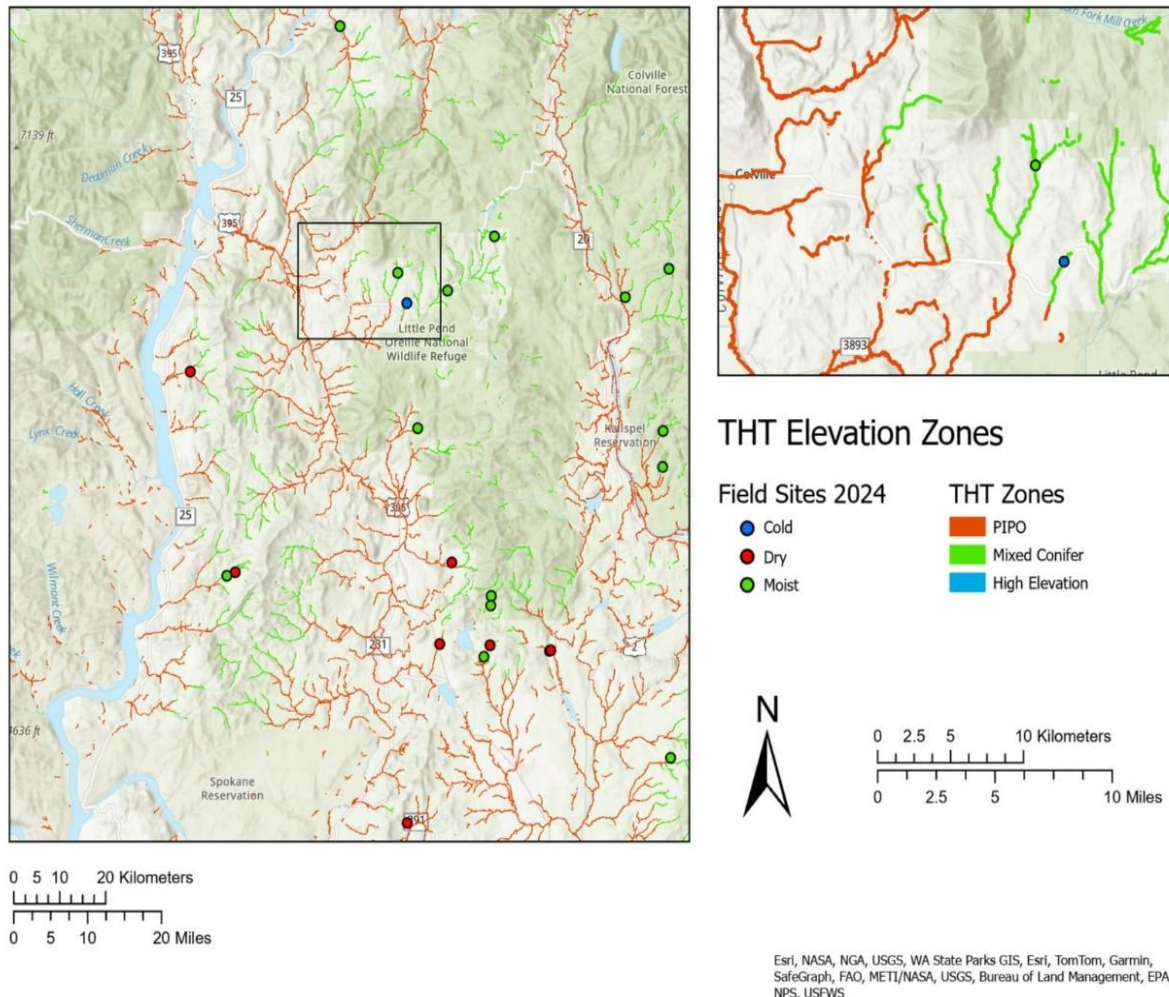


Figure SM6. Map of forest types defined by the Timber Habitat Type (THT) framework within 120 m of a Type F or Type S (fish-bearing) stream identified by the Washington State Department of Natural Resources Hydrology Layer. Field sites were identified as Cold, Dry, or Moist based on observed species composition, stand structure, and estimated fire return intervals (LANDFIRE dataset). The map shows the Northeastern area of Washington, centered on the Little Pend Oreille National Wildlife Refuge, to increase visibility of forest type variability.

Appendix III Confusion matrices

Table S1. Confusion matrices for accuracy assessments of observed riparian forest types from field data (PI method) vs. riparian forest types predicted by 4 frameworks: (1) the Timber Habitat Type (**THT**) framework, (2) the 20-year Forest Health Plan (**20yFHP map**), (3) model framework developed from 20yFHP map and calibrated with field data (**BRT**). Confusion matrices were developed for each ILAP zone to estimate performance. ^Five sites were removed from The Blue Mountains region due to non-conifer dominance. +DRY = PP, DRY MXD; MOIST = MOIST MXD, western redcedar; COLD = SF. *DRY = 0-2500 ft elevation, MOIST = 2501 – 5000 ft elevation, COLD = 5001+ ft elevation.

Blue Mountains

		Predicted: THT			Error
		DRY*	MOIST*	COLD*	
Observed	DRY+	3	4	--	57%
	MOIST+	0	5	--	0%
	COLD+	--	--	--	--
	Total				33%

		Predicted: 20yFHP map			Error
		DRY	MOIST	COLD	
Observed	DRY+	3	4	--	57%
	MOIST+	0	5	--	0%
	COLD+	--	--	--	--
	Total				33%

		Predicted: BRT			Error
		DRY	MOIST	COLD	
Observed	DRY+	1	6	--	86%
	MOIST+	1	4	--	20%
	COLD+	--	--	--	--
	Total				58%

Columbia Plateau

Predicted: **THT**

Observed		DRY*	MOIST*	COLD*	Error
	DRY+	11	4	--	27%
	MOIST+	2	0	--	100%
	COLD+	--	--	--	--
	Total				35%

Predicted: **20yFHP map**

Observed		DRY*	MOIST*	COLD*	Error
	DRY+	11	4	--	27%
	MOIST+	0	2	--	0%
	COLD+	--	--	--	--
	Total				24%

Predicted: **BRT**

Observed		DRY*	MOIST*	COLD*	Accuracy
	DRY+	12	3	--	20%
	MOIST+	0	2	--	0%
	COLD+	--	--	--	--
	Total				18%

East Cascades

Predicted: **THT**

Observed		DRY*	MOIST*	COLD*	Error
	DRY+	6	3	0	33%
	MOIST+	3	5	0	37%
	COLD+	0	1	0	100%
	Total				39%

Predicted: **20yFHP map**

Observed		DRY*	MOIST*	COLD*	Error
	DRY+	9	0	0	0%
	MOIST+	3	5	0	37%
	COLD+	0	1	0	100%
	Total				22%

Predicted: **BRT**

Observed		DRY*	MOIST*	COLD*	Error
	DRY+	8	1	0	11%
	MOIST+	3	5	0	37%
	COLD+	0	1	0	100%
	Total				28%

Northeast: Okanogan/Canadian Rockies

Predicted: **THT**

Observe		DRY*	MOIST*	COLD*	Error
	DRY+	11	5	0	31%
MOIST+	3	14	0	28%	
COLD+	0	2	1	66%	
Total				28%	

Predicted: **20yFHP map**

Observe		DRY*	MOIST*	COLD*	Accuracy
	DRY+	15	0	1	6%
MOIST+	4	13	0	24%	
COLD+	1	0	2	33%	
Total				17%	

Predicted: **BRT**

Observe		DRY*	MOIST*	COLD*	Error
	DRY+	16	0	0	0%
MOIST+	8	8	1	53%	
COLD+	1	0	2	33%	
Total				28%	

Appendix IV: Single-factor frameworks

Alternative Framework Development

In the interest of utility for forest managers, frameworks that categorize the study area based on a single factor are most easily applied. The THT is a single-factor framework based on elevation. The following is a report of our attempt to develop two different alternative frameworks that are informed by a single factor (one for precipitation, and one for elevation). These were developed by manipulating the forest type categories in the 20yFHP (identified as the most useful dataset in Phase I, Step1) into different groupings (collapsing) based on their relationships with precipitation or elevation. We expect there to be a reduction in accuracy compared to the 20yFHP, but with the trade off of increasing utility (i.e. usefulness by forest managers). The scoping document, SAGE, and CMER have not provided us with a minimum threshold of acceptable error. We instead compare the results of this experiment to the error values observed from the same field data for the THT framework.

After the most important factors for predicting forest type categories were identified in the BRT (Table 5),

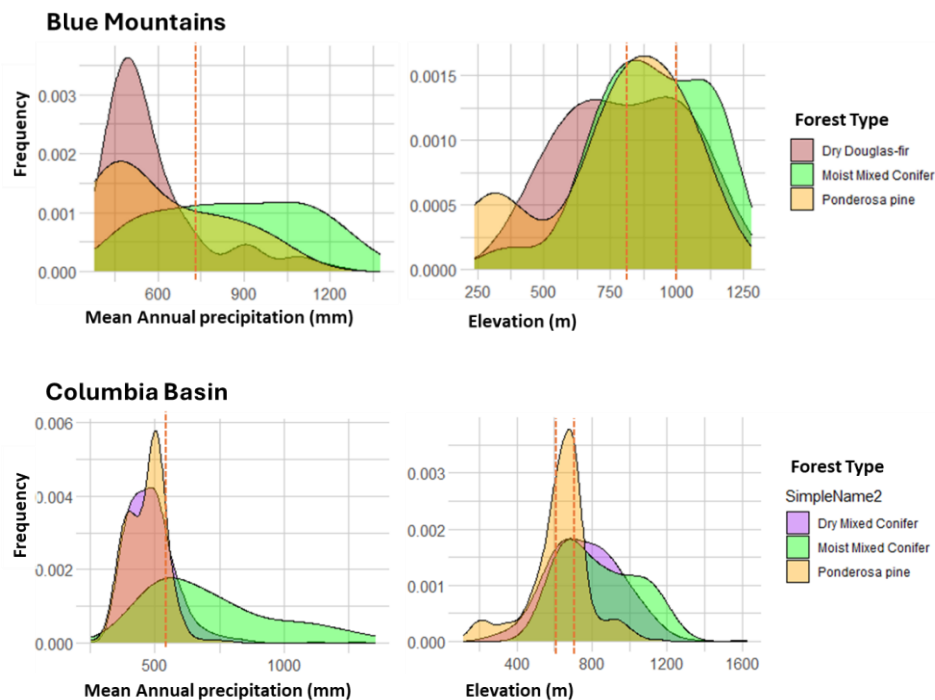
We used histogram analysis to estimate under what conditions (e.g., elevation, annual precipitation) each forest type category was most commonly found. That is, thresholds, or break points, above and below which forest type categories were distributed. Within each ILAP zone, we visually inspected the distribution of forest type categories across either precipitation or elevation gradients to identify the values where one or more forest type categories transition to a different forest type category. For example, as the mean annual precipitation increases on the x-axis, forest type categories that favor drier types (e.g., dry Douglas-fir, ponderosa pine) become less frequent and moister types more frequent (e.g., moist mixed conifer, western redcedar). The resulting breaks constituted the first two alternative frameworks to the Timber Habitat Type (THT) framework: one for elevation and one for precipitation.

To test for differences in forest type distributions based on individual environmental factors for use in the single-factor frameworks, we used either an Analysis of Variance (ANOVA) if key assumptions were satisfied (e.g., normality, equality of variances) or the Kruskal-Wallis rank sum test (KW) if key assumptions were not met. We then applied a Tukey's test for pairwise comparison. We extracted the values for mean annual precipitation (MAP) and elevation for each point in the study area based on their designated forest type category. The comparison of mean values for MAP and elevation (ANOVA, KW) was used to explore differences in forest type category distributions based on these factors. We checked for homogeneity of variances using a Levene's test and distribution normality using a Shapiro-Wilkes test.

We tested the null hypotheses that the means of precipitation and elevation for each forest group, stratified by ILAP zone, were equal. Results that showed a significant difference in forest

distributions based on their values for MAP or elevation reinforced our confidence in separations made from visual inspection of the histograms (Figure 7). All analysis and figures were conducted and constructed using R 4.2.0. This analysis gave us empirical evidence and objective reasoning for splitting or combining categories. In order to evaluate the significance of separation among forest type categories, we chose a minimum 65% probability (i.e., more likely to be statistically different than a 1:1 probability) of predicting forest type categories for each predictor variable before combining categories (Zar & Zar, 2014).

Given the foregoing, several independent variables consistently showed strong relationships with the distribution of forest type categories throughout the study area: ILAP zone, mean annual precipitation, and elevation. From this finding, we developed alternative frameworks, delineating the forest type categories of the 20yFHP map based on meaningful thresholds, or breaks, above and below which forest type categories tended to associate themselves (Figure 7). We used the ILAP zone as the first level of delineation because it was ranked as the variable with the highest importance in the machine learning approach (Table 5). For each ILAP zone, we then determined thresholds—one for mean annual precipitation and one for elevation—above and below which forest type categories tended to associate themselves. We attempted to separate the forest groups based on temperature thresholds as well, but the distributions all peaked in a narrow range of temperatures (1-2 degrees Celsius), making it difficult to separate groups with confidence. The resulting two alternative classification frameworks (one for elevation and one for precipitation) from this analysis are shown in Figures 8 and 9. The expected error of each category was created based on the percentage of points that fell within the ranges defined by the histogram analysis.



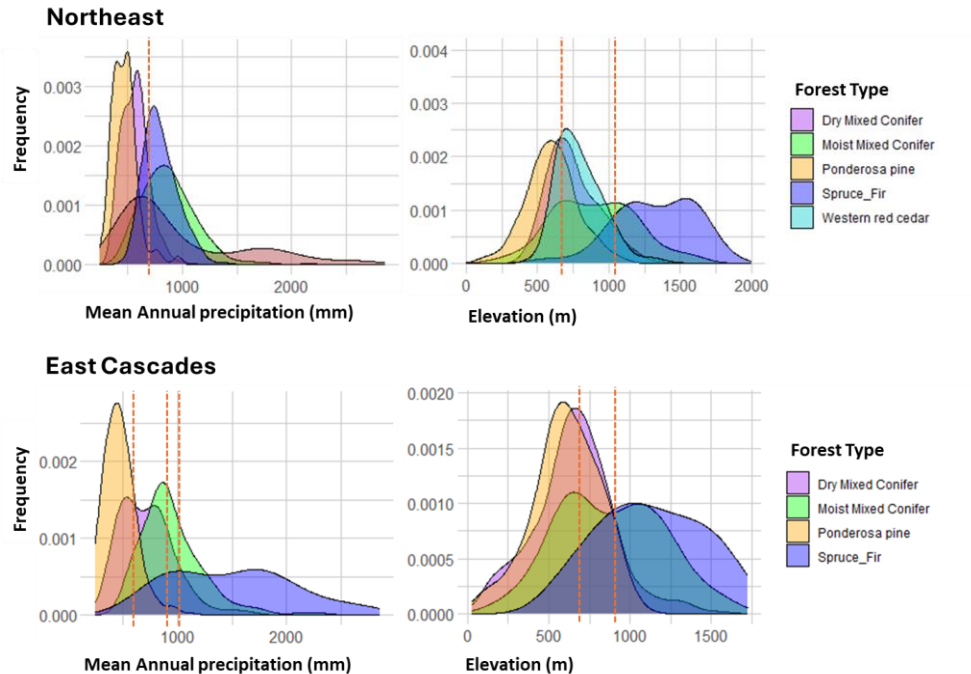


Figure S7. Frequency distributions of each 20yFHP map forest type category by mean annual precipitation (mm) and elevation (m) for each ILAP zone (Blue Mountains, Columbia Basin, East Cascades, and Northeast). From here, breakpoints for the distribution of forest type categories along elevation and precipitation gradients were developed based on visual inspection of the histograms. Red dashed lines indicate values that separate forest groups. Note: the x- and y-axis scales are not standardized across figures to increase visibility of the forest type category distributions within each ecoregion.

<u>Expected Covertypes Based on Precipitation Gradient</u>	
A. <u>Blue Mountains</u>	
a. <u>Mean annual precipitation</u>	
i.	< 745 mmDry Douglas-fir, Ponderosa Pine (20.7%)
ii.	>745 mmMoist Mixed Conifer (34.7%)
B. <u>East Cascades</u>	
a. <u>Mean annual precipitation</u>	
i.	< 600 mmPonderosa Pine (15.0%)
ii.	500 – 1000 mmDry Mixed Conifer (32.5%)
iii.	>800 mmMoist Mixed Conifer (27.1%)
iv.	>1000Spruce/Fir (24.7%)
C. <u>Columbia Basin</u>	
a. <u>Mean annual precipitation</u>	
i.	<550 mm.....Dry Mixed Conifer; Ponderosa Pine (15.2%)
ii.	>550 mm.....Moist Mixed Conifer (32.5%)
D. <u>Northeast (Okanogan and Canadian Rocky Mountains)</u>	
a. <u>Mean annual precipitation</u>	
i.	< 700 mm.....Spruce-Fir; Ponderosa Pine; Dry Mixed Conifer (19.3%)
ii.	>700 mm.....Western Red Cedar; Moist Mixed Conifer (24.2%)

Figure S8. Preliminary framework for predicting forest type categories based on their expected distributions along a precipitation gradient within each ILAP zone. The value shown in

parentheses represents the estimated expected error for each group. Expected error was calculated as the percentage of points of each group that fell outside of the chosen threshold.

<u>Expected Covertypes Based on Elevational Gradient</u>	
A. <u>Blue Mountains</u>	
a. <u>Elevation</u>	
i.	< 1000 m.....Dry Douglas-fir; Ponderosa Pine (24.7%)
ii.	>800Moist Mixed Conifer (31.5%)
B. <u>East Cascades</u>	
a. <u>Elevation</u>	
i.	< 800 mPonderosa Pine, Dry Mixed Conifer (24.3%)
ii.	> 700 m.....Moist Mixed (31.1%)
iii.	>900 m.....Spruce/Fir (27.6%)
C. <u>Columbia Basin</u>	
a. <u>Elevation</u>	
i.	<725 mPonderosa Pine (16.4%)
ii.	>600 mDry/Moist Mixed Conifer (15.6%)
D. <u>Northeast (Okanogan and Canadian Rocky Mountains)</u>	
a. <u>Elevation</u>	
i.	< 700 m.....Ponderosa Pine (27.0%)
ii.	600 -1100 mDry/Moist Mixed Conifer; Western redcedar (28.0 %)
iii.	> 1050 m.....Spruce/Fir (15.2%)

Figure S9. Preliminary framework for predicting forest type categories based on their expected distributions along an elevation gradient within each ILAP zone. The value shown in parentheses represents the estimated expected error for each group. Expected error was calculated as the percentage of points of each group that fell outside of the chosen threshold.

Results

			Predicted by Mean Annual Precipitation			
			PP/DRY DF	MOIST MXD	% Error	Rate
Blue Mountains						
Observed	< 745 mm	PP/ DRY DF	2	5	71	5/7
	> 745 mm	MOIST MXD	3	2	60	3/5
	Total		5	7	52.9	8/12

			Predicted by Mean Annual Precipitation				%Error	Rate
			PP	DRY MXD	MOIST MXD	SF		
East Cascades								
Observed	< 600 mm	PP	3	0	0	0	0/3	
	500 - 1000 mm	DRY MXD	4	7	8	63.2	12/19	
	> 800 mm	MOIST MXD	0	1	2	50	2/4	
	>1000 mm	SF	0	0	3	75	3/4	
	Total		7	8	13	2	56.7	17/30

			Predicted by Mean Annual Precipitation			
			PP/DRY MXD	MOIST MXD	Error	Rate
Columbia Plateau						
Observed	< 550 mm	PP/ DRY MXD	11	4	29	5/16
	> 550 mm	MOIST MXD	0	2	0	0/1
	Total		11	6	29.4	5/17

			Predicted by Mean Annual Precipitation			
			SF/ PIPO/ DRY MXD	WR/ MOIST MXD	%Error	Rate
Northeast						
Observed	<700 mm	SF/PP/DRY MXD	18	1	5	1/19
	>700 mm	WR/ MOIST MXD	4	13	24	4/17
	Total		22	14	13.9	5/36

Figure S10. Error matrices describing the percent error and error rate for each predicted forest type category by precipitation within each ILAP zone as defined and delineated in the Precipitation framework (Figure 8). The error rate and percentage are calculated based on the accuracy of each field site forest type category (observed) when compared to the forest type category predicted by the preliminary framework (predicted).

			Predicted by Elevation			
			PP/DRY DF	MOIST MXD	% Error	Rate
Blue Mountains						
Observed	< 1000 m	PP/ DRY DF	10	3	23	3/13
	> 745 m	MOIST MXD	0	5	0	0/5
	Total		10	8	16.7	3/18

			Predicted by Elevation			
			PP/DRY MXD	MOIST MXD/SF	% Error	Rate
East Cascades						
Observed	< 800 m	PP/ DRY MXD	12	7	40	7/19
	> 700 m	MOIST MXD/ SF	0	2	0	0/2
	Total		12	9	33.3	7/21

			Predicted by Elevation			
			PP	DRY MXD/MOIST MXD	% Error	Rate
Columbia Plateau						
Observed	< 725 m	PP	6	3	33.3	3/9
	> 600 m	DRY MXD/ MOIST MXD	4	9	31	4/13
	Total		10	12	31.8	7/22

			Predicted by Elevation				
			PP	DRY MXD/MOIST MXD/WR	SF	% Error	Rate
Northeast							
Observed	< 700 m	PP	5	5	0	50	5/10
	600 - 1100 m	DRY MXD/ MOIST MXD	5	23	2	23	7/30
	> 1050 m	SF	0	1	2	33.3	1/3
	Total		10	29	4	30.2	13/43

Figure S11. Error matrices describing the percent error and error rate for each predicted forest type category by elevation within each ILAP zone as defined and delineated in the preliminary framework (Figure 9). The error rate and percentage are calculated based on the accuracy of each field site forest type category (observed) when compared to the forest type category predicted by the preliminary framework (predicted).

Conclusions: The precipitation- and elevation-based frameworks

The precipitation- and elevation-based frameworks were both developed directly from the 20yFHP map. Our exploratory analysis of the 20yFHP map using BRT yielded results indicating that ecoregion (by ILAP zone), moisture, and temperature factors were the strongest predictors of vegetation groups. We corroborated these results with several other independent investigations (e.g., ordination) of the relationships between species coverage and site factors sourced from different datasets (e.g., reconnaissance field data and the LEMMA dataset; see [Appendix II](#) for results).

The elevation-based framework performed better than the precipitation-based framework in all ecoregions (by ILAP zones) except the Northeast (30.2% versus 13.9% error rate). In general, the elevation-based framework also performed as well or better than the THTs, depending on the ecoregion. The THT framework yielded an overall error rate of 33% when evaluated using our data collected from 83 field sites. The elevation-based framework exhibited overall error rates ranging from 16.7% to 33.3%, depending on the ecoregion. Thus, our elevation- and precipitation-based frameworks did not perform as well as predicted and do not show evidence of improvement over the THTs.

The potential utility of elevation- and precipitation-based frameworks varies across different ecoregions. During their development, the species groupings based on histogram analysis caused aggregations in some categories that had varied riparian function. For example, the SF category (COLD) aggregated with the MOIST MXD (MOIST) category in the East Cascades. This grouping of forest type categories is likely less ecologically meaningful than the THT categories or the coarse categories of the BRT Map, as evidenced by the results of riparian function modeling; further supported by documented disturbance regimes, forest development and regeneration patterns of COLD forest species groups (e.g., Engelmann spruce, subalpine fir, lodgepole pine) versus MOIST forest species groups (e.g., western hemlock, grand fir, western larch) (Hanley, 2005). Thus, we cannot recommend these frameworks as improved alternatives to the current THT.

These single variable frameworks (precipitation or elevation), however, have some potential for improvement if the source from which they were developed were improved. Considering they were each designed based on the relationship of forest type categories in the 20yFHP map, and derived from a single factor (i.e., precipitation or elevation), their performance will likely never exceed that of the source (i.e., the 20yFHP map). However, considering utility, a framework that defines treatment by as few factors as possible would be the most useful. Our objective of producing a simple framework (single variable approach) with improved performance over the THTs was unsuccessful, however, our process of data exploration, forest type classification, and framework development has yielded meaningful results that inform managers of the relationships between forest type categories and riparian function. Indeed, this work has led to the consideration of other existing alternatives to applying forest harvest rules (e.g., the 20yFHP map).